F. Schwab

NATIONAL RADIO ASTRONOMY OBSERVATORY

High-Resolution Imaging Spectroscopy at Terahertz Frequencies

Part I: Investigation and Technical Plan

A Proposal to the National Aeronautics and Space Administration under A.O. No. OSSA 3–88

National Radio Astronomy Observatory

November 1988

— Concept Study —

High-Resolution Imaging Spectroscopy at Terahertz Frequencies

Part I: Investigation and Technical Plan

A Proposal to the National Aeronautics and Space Administration under A.O. No. OSSA 3–88

National Radio Astronomy Observatory

November 1988

Dr. Robert L. Brown
Associate Director, NRAO
Principal Investigator
(804–296–0222)

Dr. Paul A. Van den Bout
Director, NRAO

Mr. James L. Desmond
Associate Director for Administration
(804–296–0315)

The National Radio Astronomy Observatory (NRAO) is operated by Associated Universities, Inc., under Contract No. NSF AST 84–03744 with the National Science Foundation.

TABLE OF CONTENTS

Names and Addresses of Principal and Co- Investigators v

1 INVESTIGATION AND TECHNICAL PLAN 1

1.1 **Summary** 1

1.2 **Objective and Significant Aspects** 2

1.2.1 The Distribution of Galactic UV Radiation 2

1.2.2 Temperature of the UV Sources 3

1.2.3 Chemical and Isotopic Enrichment in Interstellar Clouds 4

1.2.4 Propagation of Ultraviolet Radiation in Molecular Clouds and Its Effect on Star Formation 4

1.2.5 The Density Structure of Molecular Clouds 7

1.2.6 Galactic UV Radiation in Perspective 8

1.3 **Concept of the Investigation** 9

1.3.1 Spectral Lines to be Observed 9

1.3.2 Targets to be Observed 10

1.3.3 Angular Resolution to be Achieved 10

1.3.4 Related Investigations 11

1.4 **Procedure for the Investigation** 12

1.4.1 Coherent Interferometry and Aperture Synthesis 12

1.4.2 Spatial Frequency Coverage and Point Source Response Provided by a Space Station Interferometer 12

1.4.3 Observing Procedures and Techniques 17

1.4.4 Summary: Requirements of the Investigation and Goals of the Concept Proposal 19

2 INSTRUMENTATION 21

2.1 **Instrument Description** 22

2.1.1 Antennas 22

2.1.2 Pointing 22

2.1.3 IF, Delay, and Correlator Subsystems 22

2.1.4 Low-Noise Receivers 23

2.1.4.1 Critical Components of the Receivers 23

2.1.4.2 Proposed Study of Receiver Components 25

2.2 **Instrument Integration** 27

2.3 **Ground Operations** 27

2.4 **Flight Operations** 28

3 DATA REDUCTION AND ANALYSIS 29

4 Orbiter Crew and/or Payload Specialist Training Requirement 29

Appendix A: Receiver Considerations 31

A.1 **Receiver Specifications** 31

A.2 **Mixers** 31

A.2.1 Schottky vs. SIS Mixers 31

A.2.2 Harmonic Mixers vs. Fundamental Mixers 32

A.2.3 Mixer Configurations 32

A.3 **SIS Junctions** 33

Appendix B: Abstracts of Papers Referenced in Receiver Discussion 35

Appendix C: Positions of Galactic H II Regions/Molecular Cloud Complexes 37

Principal Investigator:

Dr. Robert L. Brown
National Radio Astronomy Observatory
Edgemont Road
Charlottesville, VA 22903–2475
telephone: 804–296–0222

Co-Investigator:
(Electronics)

Dr. Anthony R. Kerr
National Radio Astronomy Observatory
2015 Ivy Road
Charlottesville, VA 22903–1797
telephone: 804–296–0363

Co-Investigator:
(System Design)

Dr. A. Richard Thompson
National Radio Astronomy Observatory
2015 Ivy Road
Charlottesville, VA 22903–1797
telephone: 804–296–0285

Co-Investigator:
(Imaging and Data Handling)

Mr. Frederic R. Schwab
National Radio Astronomy Observatory
Edgemont Road
Charlottesville, VA 22903–2475
telephone: 804–296–0331

1. Investigation and Technical Plan

1.1. Summary

The goal of this mission is to determine the origin and propagation of ultraviolet radiation in the Galaxy by studying the excitation of atomic carbon and oxygen at submillimeter wavelengths. Obscured by the Galactic disk, ultraviolet (UV) radiation from most of the Galaxy is invisible at the earth. However, we can infer its presence from its effect on interstellar material. We intend to obtain spectroscopic images at high angular resolution of those submillimeter lines of C, O, and C^+ to which the Galactic disk is transparent and which are critical diagnostics of UV excitation.

In the vicinity of the Sun, 8.5 kiloparsecs from the center of the Galaxy, the energy density of UV radiation, at wavelengths $91 < \lambda < 300$ nm, is nearly equal to that of visible light or infrared radiation. But the influence of the UV radiation on the interstellar medium is disproportionately large: the UV ionizes all elements with ionization potentials less than one Rydberg, and it heats the gas via collisions between the resultant photoelectrons and the atomic and ionic gas. Further, because the ultraviolet radiation has its origin in early-type stars, it serves to delineate regions of active star formation. We can study such regions in the solar neighborhood with UV detectors stationed above the atmosphere. However, the UV opacity of the Galactic disk is large, and therefore we cannot directly observe UV light which arises at distances greater than a few hundred parsecs from the Sun: we have little knowledge of the UV energy density, its origin, propagation, and effect throughout most of the Galaxy.

We propose to bridge these gaps in our understanding by use of spectroscopic observations from an imaging interferometer attached to the space station. We will investigate secondary effects of the UV radiation in sufficient detail to permit us to infer the nature of the UV emission and its propagation throughout the Galaxy. The unique capabilities of the space station provide an ideal environment for operation of an interferometer which will provide high-resolution images of the submillimeter lines of C, O, and C^+. Observed with arcsecond angular resolution, images of the distribution of these species in relation to their source of excitation will reveal:

- The distribution of sources of ultraviolet radiation in the Galaxy;
- The effective temperature of the UV radiation as a function of galactocentric radius;
- The chemical and isotopic enhancement of atomic carbon and oxygen with galactic radius;
- The propagation of UV radiation in molecular clouds and its stimulative, or inhibitive, effect on star formation within clouds;
- The density structure, clumpiness or fragmentation, of molecular clouds throughout the Galaxy.

In the sections that follow we describe a Space Station Attached Payload that allows us to achieve these results. The plan is evolutionary: as technology matures and is incorporated into the instrument the scientific yield increases. At

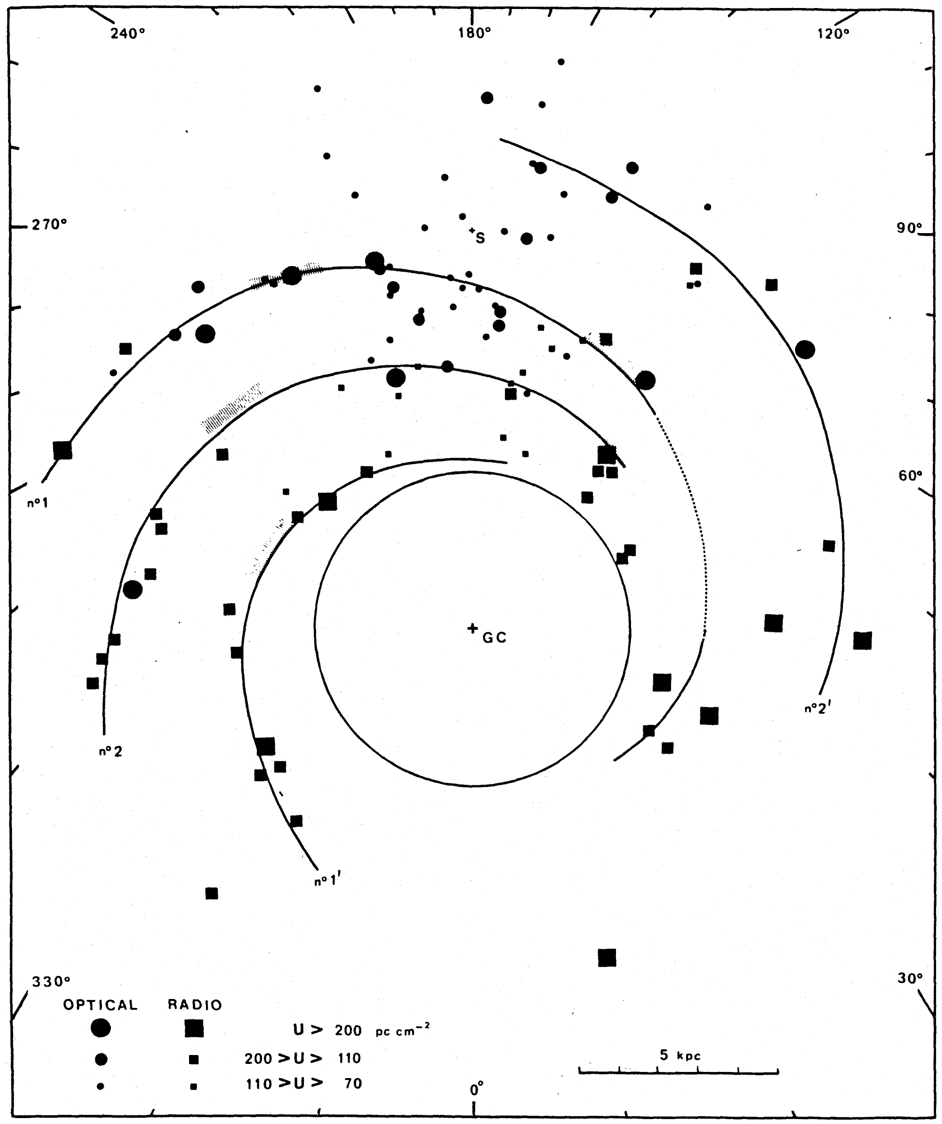

Figure 1. Spiral model of our Galaxy showing the locations of high-excitation H II regions. The solid lines indicate a proposed spiral pattern. U (pc cm^{-2}) is the H II region excitation parameter. [From Y. M. Georgelin and Y. P. Georgelin, "The spiral structure of our galaxy determined from H II regions", *Astron. Astrophys.*, **49** (1976) 57.]

all phases the instrument provides unique scientific insight that is complementary to ground-based capabilities and to orbiting instruments such as SIRTF and LDR.

1.2. Objective and Significant Aspects

1.2.1. The Distribution of Galactic UV Radiation. The single unmistakable manifestation of a stellar source of ultraviolet radiation is a region of atomic hydrogen ionized by the radiation $\lambda < 91$ nm of the hot star. From observations of their radio and infrared (IR) emission such H II regions are found throughout the Galaxy, preferentially in the Galactic plane and preferentially interior to the solar circle. Measurements of the velocities of nebular, or circumnebular, radio

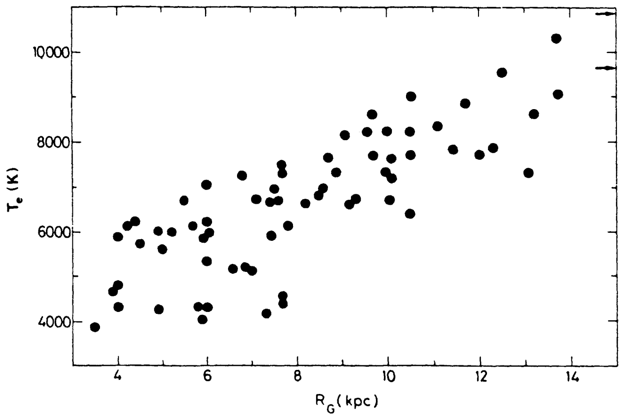

Figure 2. H II region electron temperature, as a function of galactocentric radius. [From P. A. Shaver, R. X. McGee, L. M. Newton, A. C. Danks, and S. R. Pottasch, "The galactic abundance gradient", *Mon. Not. Roy. Astr. Soc.*, **204** (1983) 53.]

spectral lines together with a kinematic model of the Galaxy allows positions within the Galaxy to be established for each H II region. A recent determination of the Galactic distribution of more than 100 H II regions is shown in Figure 1.

Each of these H II regions is a copious source of UV emission longward of 91 nm, with energies of 10^{36}–10^{38} ergs s^{-1}, which freely escapes the region of ionized hydrogen and is absorbed by gas and dust in its vicinity. It is this radiation that we wish to understand. Fortunately, because massive stars which excite H II regions have lifetimes of only 10^7 years or so, while their peculiar velocities relative to their surroundings are rarely greater than 10 km s^{-1}, they become displaced by no more than approximately 100 pc from their placental molecular cloud. The stellar UV at $\lambda > 91$ nm is therefore deposited in that molecular cloud; we can study its effects and infer its properties by means of observations of the spectral lines of the most abundant elements, O, C, and C^+. As noted below, these observations need to be made from a space platform. Additional scientific perspective will be added by ground-based molecular line and radio continuum observations as well as by the extensive IRAS database and subsequent SIRTF observations.

1.2.2. Temperature of the UV Sources. The effective blackbody temperature of stellar sources of UV radiation can be computed accurately using numerical models of stellar atmospheres. The emergent stellar intensity, at all wavelengths, depends in these models on the chemical abundance adopted for the star. Using solar abundances as characteristic of all stars near the sun, one can compute the emergent intensity in the Lyman continuum, for example, and compare that with the value inferred from observations of stars which excite H II regions.[1] Such models for well-studied stars, such as θ^1C Ori which excites the Orion nebula, agree well with the observations.

[1] R. L. Kurucz, E. Peytremann, and E. H. Avrett, *Blanketed Model Atmospheres for Early-Type Stars*, Smithsonian Institution, Washington, D. C., 1974.

On the other hand, we have no assurance that the models are applicable to stars that excite distant, and optically obscured, H II regions. To the extent that the chemical composition of the stellar atmospheres of the UV sources differs from the solar composition, the stellar UV luminosity will differ from the models.[2] Specifically, as the abundance of heavy elements (O, C, N, Ne, Si, S, Fe, Mg) increases relative to the solar values, the effective temperature of the exciting star decreases, the average energy of the nebular photoelectrons also decreases and hence the heating rate in the H II region is lowered. The temperature of the H II region excited by such a star will be cooler than that excited by the same star having solar abundances.

Radio observations show a systematic decrease in the temperature of H II regions with galactocentric radius, as illustrated in Figure 2. Nebulae near the Galactic center are systematically cooler. Whether this temperature gradient represents an increase in heavy element abundance in the UV source that excites the H II region or an increase in the abundances in the nebular gas—or both—awaits the [C I], [O I], and [C II] observations noted below.

1.2.3. Chemical and Isotopic Enrichment in Interstellar Clouds. Since their discovery several decades ago, metallicity gradients across the disks of spiral galaxies have been studied with keen interest. Grand-design spirals such as M33 and M101 have steep O/H gradients which increase toward the nuclear region, while barred galaxies show little increase and irregulars none.[3] In the Milky Way, O/H is largest at the Galactic center, and it decreases with distance from the center as $10^{-0.07}$ kpc^{-1}. Data illustrating this effect are shown in Figure 3.

Galactic abundance gradients play an important role in discriminating between nucleosynthesis models involving primary and secondary species. Primary elements, C and O, have H or He as their direct progenitors, whereas secondary species, such as ^{13}C and ^{17}O, are products of subsequent nucleosynthesis processes. The ratio of the abundances of any two primary elements, for example the ratio C/O, should thus be a constant, whereas the abundance of a secondary element should increase as the abundance of its primary progenitor, e.g., ^{13}C/C. Thus these two ratios together provide a complete picture of the efficacy of nucleosynthesis as a function of position in the Galaxy. The space station interferometric images of [O I], [C I], and [^{13}C I] obtained in this mission will directly address these questions.

1.2.4. Propagation of Ultraviolet Radiation in Molecular Clouds and Its Effect on Star Formation. The stellar ultraviolet radiation longward of the Lyman limit, $\lambda > 91$ nm, freely escapes the H II region which the star excites and is absorbed by the gas and dust in molecular material found in close proximity to early-type stars. The subsequent transfer of this radiation through the molecular cloud has a profound impact on the chemical, thermal, and kinetic state of the cloud. Observations of these "dissociation regions," such as we propose below, thus allow us to investigate in detail the chemistry, heating, and

[2] B. Balick and C. Sneden, "The ionization structure of H II regions: the effects of stellar metal opacity", *Astrophys. J.*, **208** (1976) 336.

[3] B. E. J. Pagel and M. G. Edmunds, "Abundances in stellar populations and the interstellar medium in galaxies", *Ann. Rev. Astron. Astrophys.*, **19** (1981) 77.

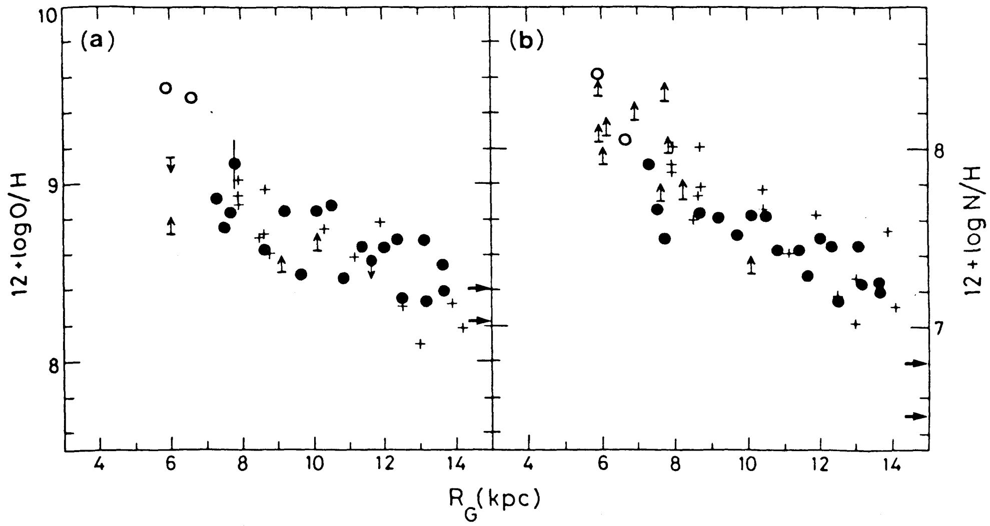

Figure 3. Abundance of oxygen *(left panel)* and nitrogen *(right panel)* relative to hydrogen, as a function of galactocentric radius. [From Shaver *et al.* 1983, *op. cit.*]

disruption of molecular clouds by stellar ultraviolet radiation and to infer the properties of the stellar UV itself.

In their seminal work on dissociation regions, Tielens and Hollenbach[4] note that the transfer of UV radiation involves:

- Photodissociation of H_2 via absorption of the UV radiation in the Lyman–Werner bands;
- Photodissociation of CO also, by absorption of the continuum UV radiation in discrete lines leading to electronically excited CO which may dissociate upon fluorescence;
- Photoionization of the abundant atomic species C, Si, S, Mg, and Fe with ionization potentials less than one Rydberg;
- Direct absorption of the UV by dust grains;
- Photoionization of dust grains.

The magnitude of each of these effects is strongly dependent on the UV penetration depth in the molecular cloud. Figure 4 schematically illustrates the structure of a homogeneous dissociation region.

At the surface of the cloud that is exposed to the unattenuated UV radiation, H_2 is dissociated; CO is also dissociated and the resultant carbon atoms are ionized. The gas is heated by dust grain photoelectrons. However, the major part of the UV opacity is not provided by these atomic processes but rather is a result of direct absorption by dust grains. Further into the cloud, at a column depth corresponding to a visual extinction A_v of 3–5 magnitudes, C^+ will radiatively recombine and both H_2 and CO will survive undissociated owing to the self- (and mutual-) shielding provided by the high UV opacity in the H_2 and CO electronic and vibrational lines. The variation of chemical composition within the dissociation region outlined here is shown as a function of visual

[4]A. G. G. M. Tielens and D. Hollenbach, "Photodissociation regions. I. Basic model", *Astrophys. J.*, **291** (1985) 722.

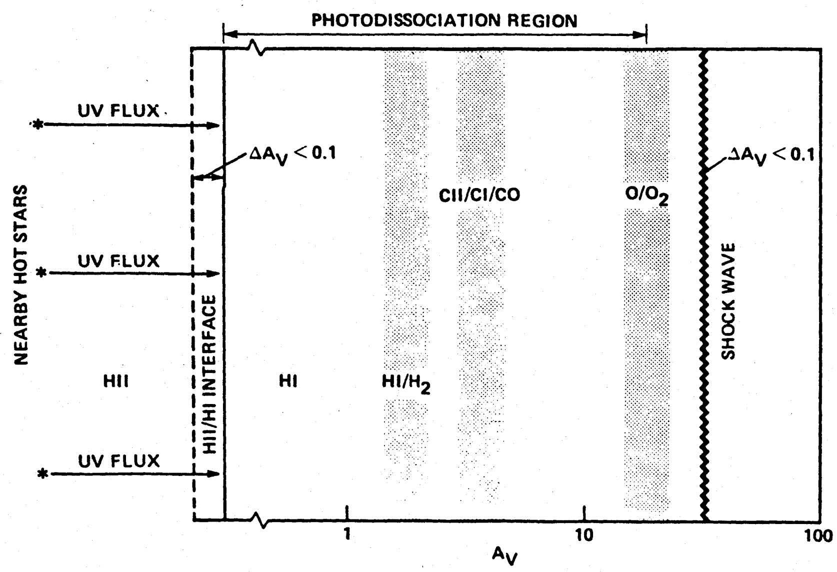

Figure 4. Schematic diagram of a dissociation region. [From Tielens and Hollenbach 1985, *op. cit.*]

extinction in Figure 5.

As is evident in this presentation, if we are to understand the nature of such dissociation regions we require detailed images of H_2, H, CO, C, O, and C^+. A comparison of such images with the physical understanding provided by calculations such as illustrated in Figure 5 will allow us to investigate both the stellar UV properties and the chemical abundances and dust properties of the molecular clouds. Below we propose to image C, C^+, and O using a low-noise heterodyne interferometer attached to the space station. High resolution images of atomic hydrogen and CO can be obtained from ground-based telescopes, while molecular hydrogen, in its vibrationally excited state $H_2{}^*$, will be imaged by SIRTF. Together these observations will provide a complete picture of the physics of dissociation regions throughout the Galaxy.

Finally, it is important to note that the high ionization rate provided by dissociation regions will stimulate cloud fragmentation, gravitational collapse of the fragments, and it will catalyze a rapid phase of massive star formation. Pudritz and Silk[5] demonstrate that when magnetic support of molecular clouds is taken into proper account during the compression or collapse phase of a cloud—initiated, for example by the shock wave associated with the dissociation region (Fig. 4)—the density structure of the cloud will become filamentary. Embedded in the filaments are dense clumps, rotating and flattened or disk-like, which shed angular momentum (and hence continue their collapse to become true protostars) by accretion-driven magnetic torques. The expected density structure in the cloud is as illustrated in Figure 6.

The high ionization rate in dissociation regions, and in the molecular cloud adjacent to the dissociation regions, will increase the accretion rate and hence

[5]R. E. Pudritz and J. Silk, "Ionization-regulated star formation in magnetized molecular clouds", *Astrophys. J.*, **316** (1987) 213.

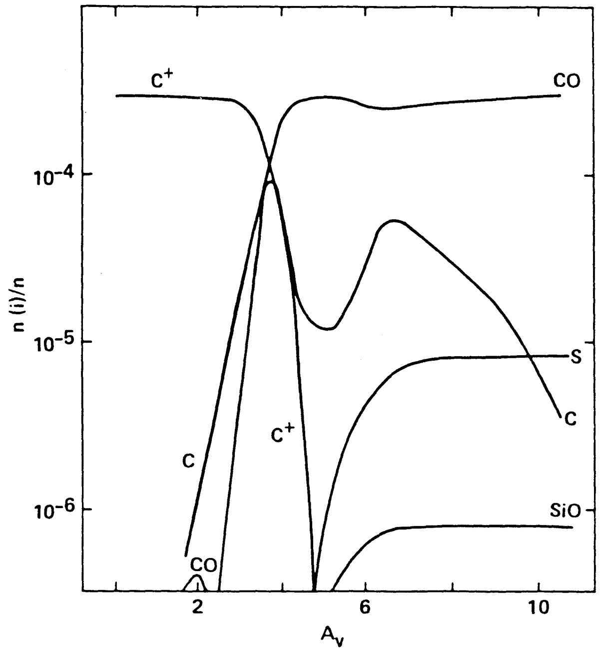

Figure 5. Fractional abundance of atomic and molecular species plotted as a function of visual extinction into a homogeneous molecular cloud. [From Tielens and Hollenbach 1985, *op. cit.*]

favor the continued formation of massive stars once the first such star forms. This, too, is subject to observational verification provided that observations at high angular resolution are possible.

1.2.5. The Density Structure of Molecular Clouds. We noted above that the density structure in molecular clouds will be filamentary and clumpy in those clouds in which the magnetic field is dynamically significant. Myers and Goodman[6] present a convincing observational argument that indeed magnetic pressure equals or exceeds kinetic and thermal pressure in all clouds except for the low mass molecular cores which have presumably shed their fields and angular momentum as described by Pudritz and Silk.[7] We know clouds are clumpy.[8] But if they are clumpy then the analysis of the propagation of UV radiation illustrated in Figures 4 and 5 is incomplete. The ultraviolet radiation will penetrate the cloud to a great depth around and between the dense molecular clumps and filaments. Dissociated CO and ionized atomic carbon may then be found throughout the interior of a molecular cloud adjacent to a source of UV radiation, not simply in a thin transition region as in Figure 4. The comprehensive CO and C^+ observations by Stutzki *et al.*[9] of the dissociation region adjacent

[6] P. C. Myers and A. A. Goodman, "Magnetic molecular clouds: indirect evidence for magnetic support and ambipolar diffusion", *Astrophys. J.*, **329** (1988) 392.
[7] Pudritz and Silk 1987, *op. cit.*
[8] N. J. Evans II, L. G. Mundy, J. H. Davis, and P. A. Vanden Bout, "Submillimeter spectral line observations in very dense regions", *Astrophys. J.*, **312** (1987) 344.
[9] J. Stutzki, G. J. Stacey, R. Genzel, A. I. Harris, D. T. Jaffe, and J. B. Lugten, "Submillimeter and far-infrared line observations of M17 SW: A clumpy molecular cloud penetrated by ultraviolet radiation", *Astrophys. J.*, **332** (1988) 379.

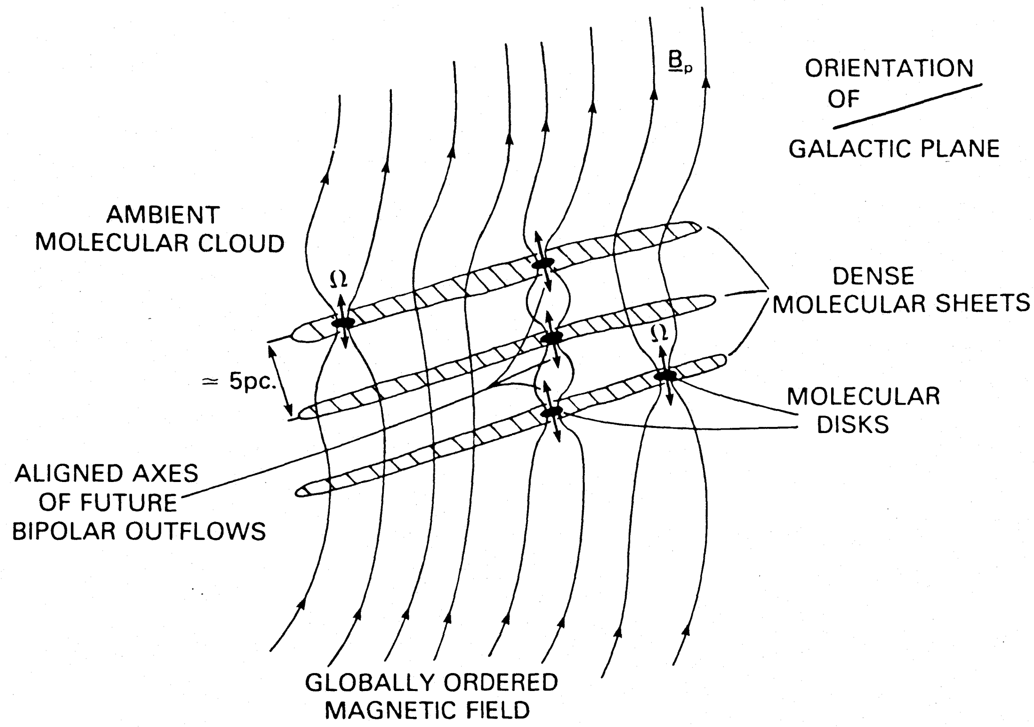

Figure 6. Global magnetic and density structure of a model molecular cloud. The gas condenses into sheet-like layers in which dense, cold molecular cores are embedded. [From Pudritz and Silk 1987, *op. cit.*]

to M17 demonstrate that this is indeed the reality. Figure 7, reproduced from Stutzki *et al.* is revealing: CO and C^+ regions are not layered adjacent to the H II region but rather these species are seen together throughout the molecular cloud.

In detail, molecular CO and ionized atomic carbon will not be spatially co-located, for the reasons noted in 1.2.4. Nevertheless, they appear to be so in Figure 7 because the angular structure separating CO regions from C^+ regions in the molecular cloud is small compared to the telescope beam (45″) used for the observations. To understand this prototypical clumpy dissociation region/molecular cloud, and by inference all such regions throughout the Galaxy, requires that we obtain observations of the important constituents, CO, O, C, and C^+, at significantly higher angular resolution than is presently available. An imaging heterodyne interferometer attached to the space station will provide images with the required resolution.

1.2.6. Galactic UV Radiation in Perspective. Proper understanding of the origin and propagation of UV radiation in the Galaxy must be based upon observations of the effects of that radiation on its surroundings, since the primary UV itself from most of the Galaxy does not reach the earth. The observed effects, in turn, provide us with insight into the extent of nucleosynthesis in the Galaxy, the galactic abundance gradient, interstellar chemistry, and the structure of molecular clouds. These inter-related fields require a large body of observational

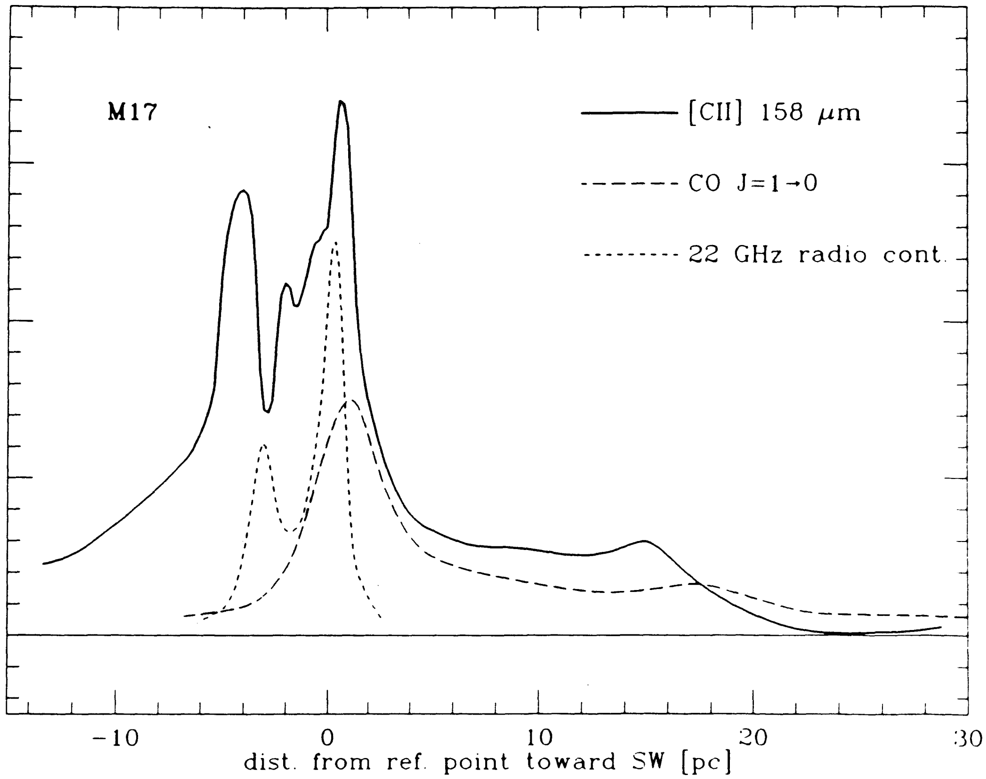

Figure 7. Comparison of the large-scale [C II] emission region with the distribution of molecular CO emission and the extent of the H II region M17. [From Stutzki *et al.* 1988, *op. cit.*]

data for us to be able to disentangle and understand them. High-resolution spectroscopic imaging, as available from a heterodyne interferometer attached to the space station, is a crucial component of the data that are required.

1.3. Concept of the Investigation

1.3.1. Spectral Lines to be Observed. The propagation of UV radiation through interstellar molecular clouds has as its principal effects the dissociation of H_2 and CO, the ionization of atomic carbon and the heating of dust grains. The chemical species which need to be observed if we are to understand these processes are H_2, CO, H, C, O, and O^+. Fortunately, all can be observed at high angular resolution. Molecular hydrogen can be observed in its excited state $H_2{}^*$ either from the ground or, in the future, from SIRTF. Atomic hydrogen and CO may be imaged using ground-based synthesis telescopes. Fine structure lines of atomic carbon, ionized carbon, and atomic oxygen occur in the submillimeter and far infrared, and high resolution observations of these species are the specific subject of this investigation. However, a complete understanding requires observations of all the species noted above.

By means of a heterodyne interferometer attached to the space station, we propose to image the (forbidden) ground state fine-structure lines of C, O, and C^+. The investigation will be conducted in two phases. First, the interferometer will be equipped with low-noise SIS receivers for simultaneous observations of both of the ground state [C I] lines. Phase II of the investigation is paced by development of low-noise receivers for frequencies in excess of 1 THz. These receivers will then augment the Phase I instrumentation on the interferometer, and the ground state lines of C^+ and O will be observed.

Table 1. Lines to be Observed

	Species	Transition	Frequency (GHz)
Phase I	[C I]	$^3P_1 - {}^3P_0$	492.1612
		$^3P_2 - {}^3P_1$	809.3432
Phase II	[C II]	$^2P_{3/2} - {}^2P_{1/2}$	1900.54
	[O I]	$^3P_0 - {}^3P_1$	2060.06

Note that the isotopic spectral line of ^{13}C will appear in the same spectra with the [C I] and [C II] main lines and will also be imaged.

In Phase I, simultaneous measurement of both transitions of C I is important: the two lines together provide a complete characterization of the 3-level ground state of atomic carbon and hence of the physical conditions in the region of excitation. We can determine the optical depth independently of excitation or abundance effects. Looking at the extremes, if the [C I] emission region is hot and the [C I] lines optically thin then the 2–1 line will be twice as bright as the 1–0 line, whereas if the gas is cool and the lines optically thick then [C I] 2–1 will be half as bright as 1–0. Spatial variations in these ratios are expected, and will be revealed by the space station attached interferometer.

1.3.2. Targets to be Observed. Observations will be needed of a large sample of molecular clouds found in close proximity to Galactic H II regions. Since one of the primary goals of the mission is to investigate Galactic abundance gradients and spatial inhomogeneity of Galactic chemical abundances, the targets must be distributed throughout the Galactic disk. Appendix C is a tabulation of the positions of more than 450 Galactic H II regions/molecular cloud complexes of known velocities. The objects to be observed will be selected from this list based on high resolution images of their H I, CO, and radio continuum emission which we are compiling from ground-based observations.

1.3.3. Angular Resolution to be Achieved. We have noted above that fine-scale spatial structure, filamentation, clumping and granularity, in molecular clouds is both expected from theoretical considerations[10] and observed[11]. The precise character of the cloud structure has a profound effect on the propagation of UV radiation in the clouds, and indeed it is one of the principal questions we intend to address with this mission.

Adopting $n = 10^5$ cm^{-3} as the density characteristic of clumps in molecular clouds[12] together with the UV penetration depth, A_v = 5–10 magnitudes,[13] we

[10] Pudritz and Silk 1987, *op. cit.*; R. C. Fleck, "The mechanical equilibrium of interstellar clouds: scaling relations for gas density, line width, and magnetic field strength", *Astrophys. J.*, **328** (1988) 299.
[11] Evans *et al.* 1987, *op. cit.*; Stutzki *et al.* 1988, *op. cit.*
[12] Evans *et al.* 1987, *op. cit.*
[13] Tielens and Hollenbach 1985, *op. cit.*

infer that the typical dimension of a clump is $\sim (0.03\text{–}0.06)/N$ pc, where N is the average number of clumps through the dissociation region of the cloud. Even for $N = 1$ we require an instrument capable of resolving structure in the cloud on a size scale of 0.1 pc or smaller. The table below illustrates the angular resolution needed to resolve 0.1 pc structure in clouds located at the indicated distances from the sun. Higher resolution is desirable.

Table 2.

Distance	Resolution
1 kpc	20″
5 kpc	4″
10 kpc	2″
20 kpc	1″

1.3.4. Related Investigations. Submillimeter spectroscopy, even heterodyne spectroscopy using GaAs Schottky diode mixers and optically-pumped laser local oscillator sources, is an active area of research which has led to the detection of all the lines noted in Table 1. From observations made with high-precision, single-dish radio antennas or optical telescopes, we know that all these lines are luminous in molecular clouds associated with H II regions—the line "radiation" temperature exceeds 10 K in the regions studied and the brightness temperature is many times higher[14]—as expected on the basis of theoretical models.[15]

Both of the Phase I atomic carbon, fine-structure [C I] lines have been observed from telescopes on Mauna Kea.[16] Although such ground-based observations are possible, the atmospheric transmission at these frequencies at the best, dry site in the world rarely exceeds 30 percent, and the transmission at that locale is unstable. The variation in atmospheric transmission makes calibration uncertain; since the excitation of the region is inferred from the ratio of the intensity of the two [C I] lines, the physics is in error if the calibration is in error. There is no simple way to minimize these problems on the ground.

The Phase II lines have also been detected using the same type of Schottky receiver flown at 40,000 feet on the KAO.[17] Observations at the frequencies of these lines, of course, are not at all possible from the ground.

The on-going ground-based and KAO observations provide important insight into the large-scale distribution of [C I], [O I], and [C II] and into the relative luminosity in each of these lines. But because the observations are made with telescopes of modest aperture, the angular resolution obtained, 25″–60″, is

[14] J. Keene, "C I, C II, and CO as tracers of gas phase carbon", Caltech preprint, 1987; to appear in a SETI conference publication, *Carbon in the Galaxy: Studies from Earth and Space.*

[15] E.g., Tielens and Hollenbach 1985, *op. cit.*

[16] T. G. Phillips and P. J. Huggins, "Abundance of atomic carbon (C I) in dense interstellar clouds", *Astrophys. J.*, **251** (1981) 533; D. T. Jaffe, A. I. Harris, M. Silber, R. Genzel, and A. L. Betz, "Detection of the 370 micron $^3P_2-{}^3P_1$ fine-structure line of [C I]", *Astrophys. J.*, **290** (1985) L59.

[17] M. K. Crawford, J. B. Lugten, W. Fitelson, R. Genzel, and G. Melnick, "Observations of far-infrared line profiles in the Orion–KL region", *Astrophys. J.*, **303** (1986) L57; Stutzki *et al.* 1988, *op. cit.*

coarse compared to what is needed for the investigation noted here (*cf.* Table 2). No interferometric observations have been made of any of the lines. Scientific insight at high angular resolution awaits access to a coherent interferometer above the atmosphere on a stable platform. The space station is an ideal environment.

1.4. Procedure for the Investigation

1.4.1. Coherent Interferometry and Aperture Synthesis. Since the angular resolution of a telescope varies in direct proportion to the observing wavelength and in inverse proportion to the diameter of the aperture, one can obtain better resolution either by observing at shorter wavelengths or by using larger telescopes. Both have limits. In the former case, if our wavelength of interest is predefined (e.g., the lines in Table 1) and we seek higher resolution, then we must use a larger telescope. But it need not be a single telescope. Instead we may simulate the high resolution imaging capability of a single large telescope by using two or more small telescopes to coherently sample the electric field at discrete locations within an aperture that corresponds to the large telescope. This equivalent large telescope is referred to as the "synthetic aperture." An image of the sky is then formed by Fourier transforming the correlations among the sampled data.[18]

The fidelity of an interferometric image is directly related to the completeness with which the interferometer samples the range of spatial frequencies represented by the synthetic aperture. Radio synthesis telescopes such as the Very Large Array make use of a large number of antennas to increase the number of correlations and hence enhance the spatial frequency coverage. In addition, by tracking in hour-angle, the relative orientation of the vector separation between pairs of antennas and the vector to the source changes with the earth's rotation. This too aids in filling in coverage of the synthetic aperture plane. A similar technique can be exploited by a synthesis interferometer attached to the orbiting space station.

1.4.2. Spatial Frequency Coverage and Point Source Response Provided by a Space Station Interferometer. First, consider the geometry of a two-element interferometer whose baseline vector $\mathbf{b}$ is assumed to lie parallel to the transverse boom of the space station, and thus parallel also to the Y-axis of the Space Station Body Coordinate System.[19] Let $\mathbf{r}$ denote the position vector of the space station in geocentric Cartesian coordinates,[20] and $\dot{\mathbf{r}}$ the tangential velocity vector. Then, since the transverse boom is oriented perpendicularly to $\mathbf{r}$ and to the direction of motion $\dot{\mathbf{r}}$, the baseline vector $\mathbf{b}$ lies in the direction of the angular momentum vector $\mathbf{L} = \mathbf{r} \times \dot{\mathbf{r}}$. In terms of the Keplerian orbital elements $\{a, e, i, \omega, \Omega, M\}$, $\mathbf{L}$ is given by $\mathbf{L} = L \begin{pmatrix} \sin i \sin \Omega \\ -\sin i \cos \Omega \\ \cos i \end{pmatrix}$, where $L^2 = G\mathfrak{M}_\oplus a(1 - e^2)$ and $G\mathfrak{M}_\oplus$ is the geocentric gravitational constant.

[18] The theory and techniques of aperture synthesis are described in the book by A. R. Thompson, J. M. Moran, and G. W. Swenson, Jr., *Interferometry and Synthesis in Radio Astronomy*, John Wiley & Sons, New York, 1986.

[19] Defined in NASA Publication JSC 30219, *Space Station Reference Coordinate Systems*.

[20] E.g., the standard Aries Mean of 2000 Coordinate System of NASA Publication JSC 30219.

For observations of a radio source at right ascension α and declination δ, a unit vector oriented in the direction of the source (in geocentric coordinates) is given by $\mathbf{s}(\alpha,\delta) = \begin{pmatrix} \cos\delta\cos\alpha \\ \cos\delta\sin\alpha \\ \sin\delta \end{pmatrix}$. Now if one calculates the coordinates (u, v, w) of the baseline vector in a new coordinate system in which the w-axis points in the $\mathbf{s}(\alpha,\delta)$-direction and in which the common plane of the u- and v-axes is perpendicular to $\mathbf{s}(\alpha,\delta)$, with the u-axis going East and the v-axis North, one has that

$$\begin{pmatrix} u \\ v \\ w \end{pmatrix} = |\mathbf{b}| \begin{pmatrix} -\sin i\cos(\Omega-\alpha) \\ -\sin\delta\sin i\sin(\Omega-\alpha)+\cos\delta\cos i \\ \cos\delta\sin i\sin(\Omega-\alpha)+\sin\delta\cos i \end{pmatrix}.$$

Of particular interest is that locus of points in the u-v plane which is traced out by the baseline vector as the orbital plane of the space station precesses in longitude. For the space station, the rate of the regression of the nodes is approximately 7° of longitude per day. Over a time interval equal to the period of revolution of the nodes (this internodal period is approximately 50 days, or 360/7), the baseline vector traces out a closed elliptical curve in the u-v plane. Its equation is

$$u^2 + \frac{(v-|\mathbf{b}|\cos\delta\cos i)^2}{\sin^2\delta} = |\mathbf{b}|^2\sin^2 i\,. \tag{1}$$

An example of such an ellipse, for $\delta = 45°$ and $i = 28.5°$, is shown in the top portion of Figure 8. Also shown, for a reason explained below, is a geometrically similar ellipse centered on the opposite side of the u-axis.

Now consider the problem of estimating the intensity I of the spatially incoherent celestial radio emission over all of a region in the neighborhood of right ascension α_0 and declination δ_0. Let $\mathbf{s}_0 \equiv \mathbf{s}(\alpha_0,\delta_0)$ and let (l, m) denote the direction cosines of $\mathbf{s}(\alpha,\delta)$, with respect to the u- and v-axes determined by $\mathbf{s}_0$. After correlation and calibration of the data obtained with the instrument, the interferometric data are samples at spatial frequencies (u, v) of the Fourier transform V of the sky brightness I, where now I is regarded as a function of l and m.[21] In radio astronomy, V is called the *visibility function* of I. The samples $V(u,v)$ are obtained at spatial frequencies (u,v) along an ellipse, as defined by Equation 1. If one is interested in mapping out the Stokes parameter defining the total intensity of the radio emission, then I is real-valued, and so V is Hermitian (i.e., $V(-u,-v)$ is just the complex conjugate of $V(u,v)$); and that is why we find a pair of ellipses in Figure 8. Instead of a simple two-element interferometer, one might consider a multi-element interferometer, comprising three or more elements (the more elements, of course, the better the u-v coverage and the better the imaging fidelity and speed).

For a three-element, three-baseline instrument the u-v coverage would consist of three pairs of ellipses, as shown for various declinations in Figure 9. A potentially attractive option for a space station interferometer might be a three-element instrument comprising two fixed elements and one movable element.

[21] See, for example, Thompson, Moran, and Swenson, *op. cit.*, Chapter 4.

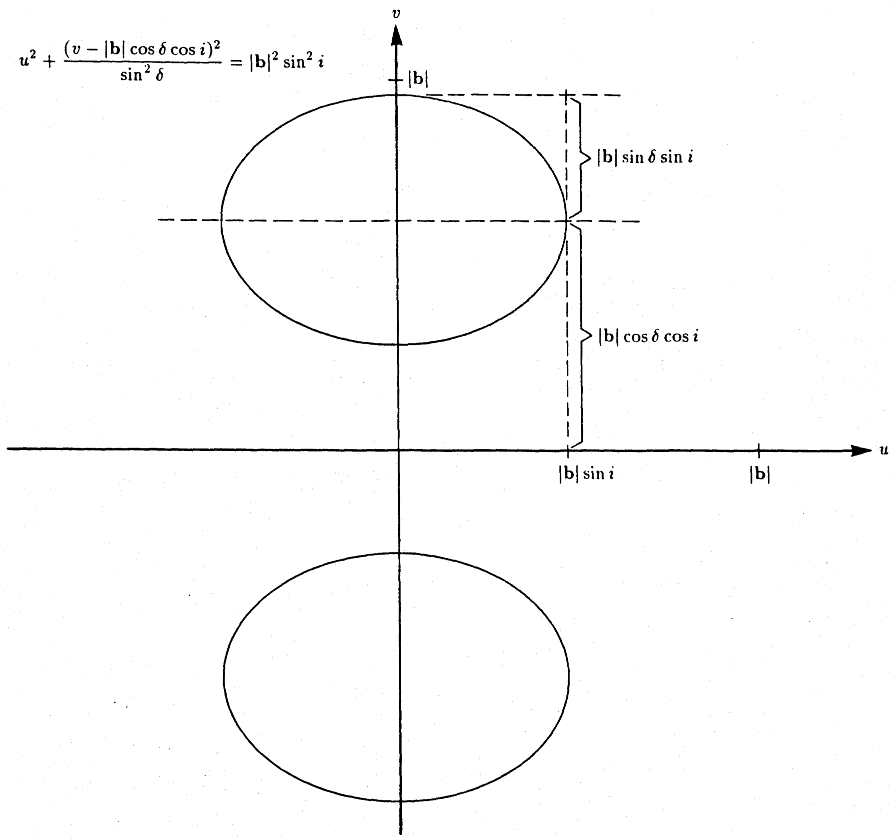

Figure 8. The u-v coverage provided by a single-baseline (i.e., a two-element) space station interferometer. In this example, $\delta = 45°$ and $i = 28.5°$. Over a time interval equal to the internodal period of the longitudinal precession of the satellite orbit the tip of the baseline vector traces out an ellipse in the u-v plane.

The movable element would be re-positioned only infrequently—most likely at time intervals no shorter than the internodal period of the orbit.

The most straightforward means of obtaining a radio interferometric image is by inverse Fourier transformation of the data, weighting each data sample $V(u_s, v_s)$ by a unit mass $\delta(u - u_s, v - v_s)$ (here δ is the Dirac δ-function). Ignoring noise in the observations, the image one obtains is the convolution of the actual sky brightness I with the (suitably normalized) inverse Fourier transform of the u-v measurement distribution S. S is a distribution with unit mass at the position of each data sample but zero elsewhere; its inverse Fourier transform B is the *point source response*, or the *synthesized beam* in radio astronomical terminology. Assuming continuous observations over a full internodal period, the point source response of a space station interferometer can be easily evaluated in closed form. For N collinear baselines $\mathbf{b}_1, \ldots, \mathbf{b}_N$, the point source response B, normalized to unit peak amplitude, is given by

$$B(l, m) = \frac{\sum_{n=1}^{N} |\mathbf{b}_n| \, J_0\left(2\pi |\mathbf{b}_n| \sin i \sqrt{l^2 + m^2 \sin^2\delta}\right) \cos(2\pi m |\mathbf{b}_n| \cos\delta \cos i)}{\sum_{n=1}^{N} |\mathbf{b}_n|}, \tag{2}$$

where J_0 denotes the first-kind Bessel function of 0 order. One could not, in reality, observe a cosmic source over a full internodal period because any given

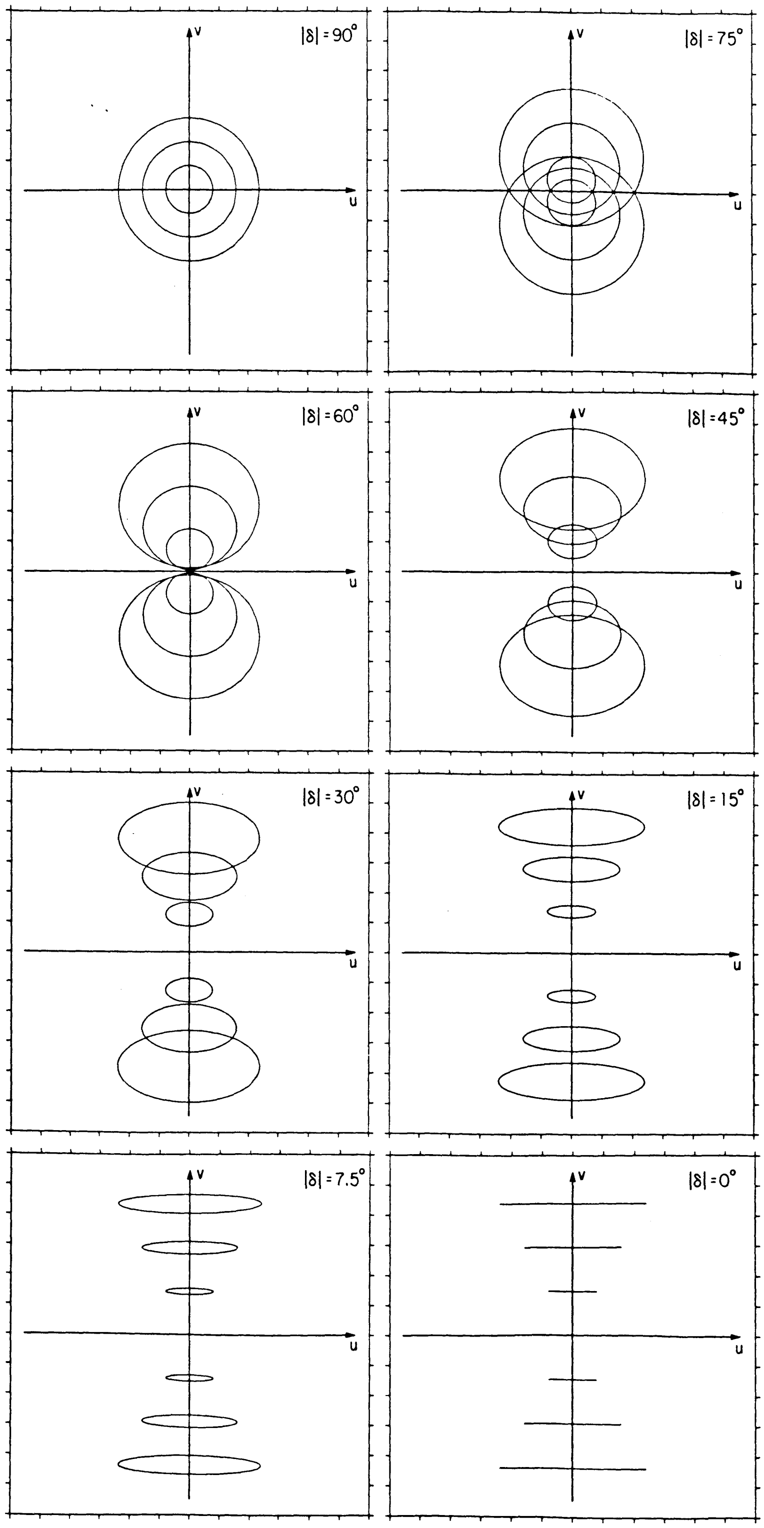

Figure 9. The u-v coverage attainable with a three-element space station interferometer, for various declinations. The baseline lengths are in the ratio 3 : 2 : 1, and the orbital inclination $i = 28.5°$.

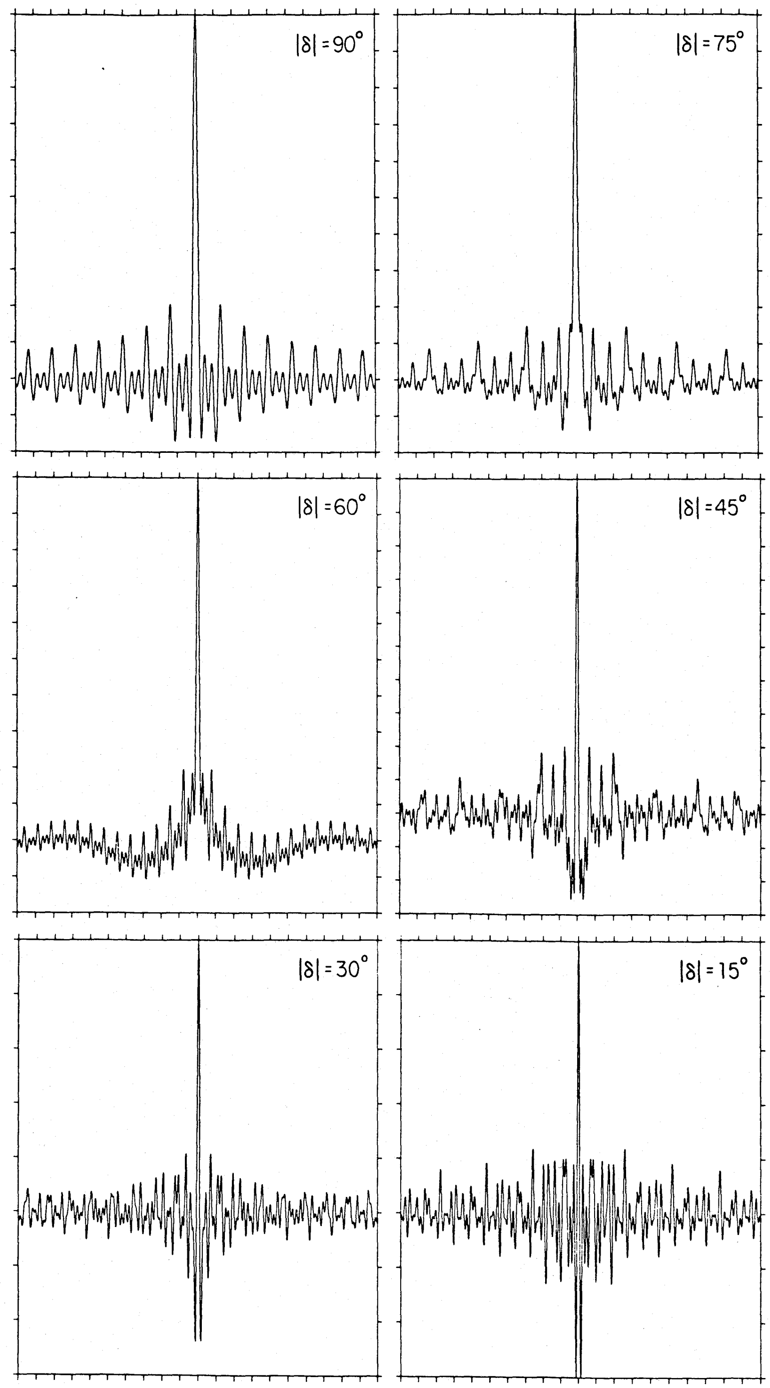

Figure 10. The angular resolution attainable with a three-element space station interferometer at various declinations δ, illustrated by taking one-dimensional cuts (with $l = 0$) through the point spread function B—i.e., plots of $B(0, m)$ are shown. Here the baseline lengths are in the ratio 3 : 2 : 1 with a maximum baseline of 30 meters, and the orbital inclination $i = 28.5°$. For an observing frequency of 492 GHz the spacing of horizontal-axis tick marks is $10''$. The amplitude scale is linear, and the mean oscillation is about zero amplitude. $B(l, 0)$ is independent of δ; i.e., $B(l, 0)$, at all declinations, is identical to $B(0, m)$ at $\delta = 90°$.

region of the sky would be in view for only a fraction (typically near one-half) of each orbital period. Nevertheless, Equation 2 is a generally adequate approximation to the point source response that would result from repeated observations of a source over a full internodal period (observations during every orbit or every few orbits, say). The point source response of a three-element space station interferometer is shown, for sources at various declinations, in Figure 10.

There are several advantages to using more than two antennas in an imaging array. The ability to sample the visibility function over a wide u-v range is directly related to the number of different baselines available. A number N_a of antennas allows as many as $N_a(N_a - 1)/2$ simultaneous baselines. Thus the speed at which the u-v plane is covered is approximately proportional to N_a^2. Also, for a given observing time, the sensitivity is proportional to N_a. Finally, with three or more antennas it is possible to form observables of the form $\phi_{123} = \phi_{12} + \phi_{23} + \phi_{31}$, where ϕ_{mn} is the phase difference between the signals received in antennas m and n. The "closure phase" ϕ_{123} is easily shown to be independent of instrumental phase responses, and to depend only on the phases of V for the baselines involved. For terrestrial arrays, use of the closure phase allows the separation of atmospheric phase effects. For an array in space, the closure phase terms would be very helpful in calibrating systematic phase variations, which may be difficult to control because of the temperature variations in space. Thus there are strong arguments for using at least three antennas. Minimization of complexity and power consumption imposes an upper limit of not many more antennas than three.

1.4.3. Observing Procedures and Techniques. The observations required for this investigation are defined by the pioneering single antenna observations and the UV propagation models noted above. The principal constraints are the following:

- In dissociation regions found at the interface between H II regions and molecular clouds, all the lines in Table 1 have an optical depth on the order of unity;[22]
- The kinetic temperature of the line emission region is 50–300 K;[23]
- The observed antenna temperatures of the lines are 10 K or greater as seen by a single dish;
- The emission region is highly clumped—the filling factor is 0.1 or less—the line brightness temperature of optically thick clumps will approach the kinetic temperature;
- The line emission extends over regions of the cloud of one to several parsecs in size.[24]

These constraints imply that our interferometer observations must achieve the following:

- An image size of one-half to several arcminutes;
- Angular resolution of order one arcsecond (see Section 1.3.3);
- Brightness sensitivity less than 10 K.

[22]Keene 1987, *op. cit.*
[23]Tielens and Hollenbach 1985, *op. cit.*
[24]Stutzki *et al.* 1988, *op. cit.*

The half power beam width of a single antenna of diameter D (meters) is $\sim 74(\nu/1000\ \mathrm{GHz})^{-1} D^{-1}$ arcseconds. Thus unless D is a small fraction of one meter, which is unacceptable as noted below, we require several interferometer pointings to image a single field. Usually, the final image will be a "mosaic" of several overlapping fields, each of which is observed separately.

The achieved angular resolution depends on the spatial separation of the two antennas: i.e., on the length $B = |\mathbf{b}|$ of the baseline. Table 3 shows the angular resolution of the interferometer, at each of the frequencies of interest, for baseline lengths in the range 5–50 meters. Baseline lengths on the order of 30 meters appear to be well suited to this investigation.

The brightness sensitivity of the interferometer depends on the number of antennas in the array, their diameter, and the baseline. Specifically, the r.m.s. brightness fluctuation in a spectroscopic image of frequency resolution $\Delta\nu$ after an observing time Δt is[25]

$$\Delta T_b = \frac{2}{\Gamma\gamma\epsilon_q\epsilon_a\pi}\left(\frac{B}{D}\right)^2 \frac{T_{\mathrm{sys}}}{\sqrt{N_b\Delta\nu\,\Delta t}}\ \mathrm{K}\,,$$

where N_b is the number of baselines. If we assume $N_b = 3$ and adopt the following parameters,

$\Gamma \approx 1$	a spatial smoothing parameter,
$\gamma \approx 1$	a factor dependent on the precise weighting scheme used in imaging,
$\epsilon_q = 0.88$	the correlator quantization efficiency (assuming a 4-level correlator with sampling at the Nyquist rate),
$\epsilon_a = 0.50$	the antenna aperture efficiency,
$\Delta\nu = 2.5$ MHz	to attain a resolution of $\sim$ 1 km/s at the observing frequencies,

then

$$\Delta T_b = 5.3 \times 10^{-4}\left(\frac{B}{D}\right)^2 \frac{T_{\mathrm{sys}}}{\sqrt{\Delta t}}\ \mathrm{K}\,.$$

Three baselines can mean either three antennas used simultaneously, or two antennas reconfigured once during the observation.

The sensitivity, ΔT_b, will be improved (lowered) as $(B/D)^2$ is decreased; D should not be very small compared to the value of $B \approx 30$ meters, needed to provide the necessary angular resolution. If we adopt $D = 2$ meters, then

$$\Delta T_b = \frac{0.12 T_{\mathrm{sys}}}{\sqrt{\Delta t}}\ \mathrm{K}\,.$$

We would like ΔT_b no larger than 2 K, in which case the observing time needed on each field of the mosaic image is

$$\Delta t \approx 39\left(\frac{T_{\mathrm{sys}}}{1000\ \mathrm{K}}\right)^2\ \text{minutes}\,.$$

[25] R. M. Hjellming, "The concept of the NRAO millimeter array", in *Science with a Millimeter Array*, A. Wootten and F. R. Schwab, Eds., NRAO, Green Bank, 1988.

Table 3. Interferometer Resolution (arcseconds)

	— Species Transition Frequency —			
B (meters)	492 GHz	809 GHz	1900 GHz	2060 GHz
5	12.6	7.7	3.3	3.0
10	6.3	3.8	1.6	1.5
15	4.2	2.6	1.1	1.0
20	3.1	1.9	0.81	0.75
30	2.1	1.3	0.54	0.50
40	1.6	0.96	0.41	0.38
50	1.3	0.76	0.33	0.30

In order to image a $3' \times 3'$ field, for example, at the Phase I frequencies will require 20–30 individual antenna pointings and a total integration time of 15–20 hours if $T_{sys} = 1000$ K. Here we can see that the investigation would not be tractable from the ground. The receiver temperature of current Schottky technology, degraded by the effect of the atmosphere,[26] would lead to a system temperature $T_{sys} > 10,000$ K. *A low-noise system, $T_{sys} \approx 1000$ K, is crucial for these observations.* Demonstrating the feasibility of such a low-noise receiver is the central task of this concept proposal.

High fidelity imaging requires good coverage of the synthetic aperture plane. This means that the total integration time needed for each field (from the sensitivity calculation above) should be accumulated over the full internodal period of the space station orbit. We expect to make brief observations of each field every few days. Determining how to optimize the data taking so as to maximize the image fidelity is the second major goal of the concept proposal.

1.4.4. Summary: Requirements of the Investigation and Goals of the Concept Proposal.

Scientific Requirements:

- To understand the origin and propagation of Galactic ultraviolet radiation we need to investigate secondary effects of that radiation throughout the Galaxy;
- Spectroscopic observations of [C I], [O I], and [C II] lines allow us to explore the breadth of the phenomenon and discriminate between competing interpretations;
- High angular resolution is needed to describe properly the structure of the line-emitting regions.

Technical Goals:

- The observations first require low-noise receivers which will allow us to achieve $T_{sys} < 1000$ K at 492 and 809 GHz. Our principal goal is to demonstrate the feasibility of such receivers at the Phase I frequencies;
- High fidelity spectroscopic imaging will require data to be taken over the full internodal period of the space station orbit. The

[26] Jaffe and Harris 1985, *op. cit.*

secondary goal of the proposal is to define a data-taking technique, given the constraints of the space station orbit, that provides for images of the highest fidelity.

Technical Evolution:

- As the technology of low-noise heterodyne receivers matures at still higher frequencies, we plan to complement the Phase I receivers with Phase II instrumentation and extend the observational program. Design of the Phase II instrumentation is outside the scope of the present concept proposal.
- An imaging interferometric array is an instrument that could grow as the space station expands, allowing for longer antenna spacings that will provide even higher-resolution images. The possibility might also exist of increasing the number of antennas, thereby enhancing the sensitivity and speed of imaging. Thus although the present study is scientifically complete as outlined within this proposal, it also provides a necessary first step toward a possibly larger and more general-purpose imaging array. Such an array could be used for a wide range of remote sensing problems, including planetary and extragalactic astronomy.

2. Instrumentation

Below we describe a two (or more) element heterodyne interferometer attached to the space station and designed to accomplish our scientific objectives. We refer to this instrument by an acronym derived from its application, *HISAT*—High-Resolution Imaging Spectroscopy at Terahertz Frequencies. A schematic diagram illustrating the essential components of such an interferometer is shown in Figure 11. The essential HISAT specifications are summarized in Table 4 and described further in the sections below.

Table 4. HISAT Instrumentation

Antennas:	2 (or more), each of 2 meter diameter, with surface accuracy ≤ 10 μm r.m.s.
Pointing:	3 arcseconds r.m.s.
Frequencies:	492 and 809 GHz (during Phase I)
Receivers:	Low noise, $T_{\mathrm{sys}} < 1000$ K
Correlator:	Analog/digital with bandwidth ≥ 250 MHz
Baselines:	5–30 meters, reconfigurable

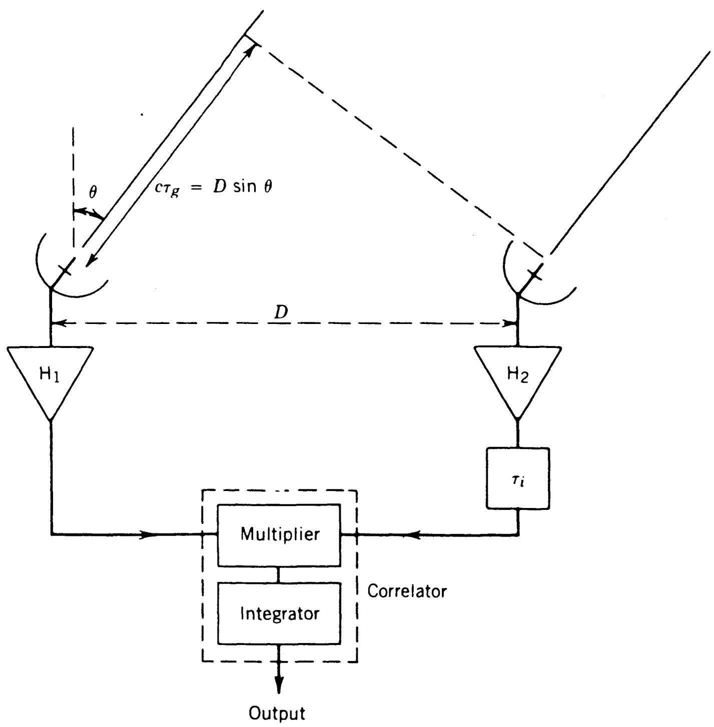

Figure 11. Sketch of an elementary interferometer. The two receivers are identified as H_1 and H_2. τ_g is the geometric time delay and τ_i the instrumental delay. Here the separation of the two antennas, the baseline, is denoted by D.

2.1. Instrument Description

2.1.1. Antennas. Two-meter diameter antennas with a surface accuracy of $\lambda/15$, or approximately 10 μm r.m.s. at the shortest Phase II wavelength, are available from industry. We also require good thermal stability from the antennas: they should be constructed of materials with a small thermal coefficient. The University of Arizona/Max-Planck-Institut 10-meter telescope is to be fabricated from carbon-fiber surface panels which meet our specifications and can be purchased commercially.

2.1.2. Pointing. A pointing accuracy of $3''$ r.m.s. can be achieved with a star tracker and servo mount which we will provide. The light-weight antennas and instrument package may not require such a high capacity structure as the PPS.

2.1.3. IF, Delay, and Correlator Subsystem. The received signals will be converted to an intermediate frequency (IF) of a few gigahertz at the antennas and transmitted by cable to a processing unit for conversion to baseband and digital sampling. Four IF signals, each of bandwidth 250 MHz, come from each antenna. This bandwidth provides a velocity coverage of 150 km sec^{-1} at 492 GHz and 100 km sec^{-1} at 809 GHz. Before sampling, each IF signal will be divided into a number of narrow-bandwidth baseband channels, say 5 channels of 50 MHz bandwidth, or 16 channels of 16 MHz bandwidth. The wider bandwidths require higher clock rates for the digital sampling and may require a higher-power type of logic circuitry. A careful design study is required to minimize power consumption and overall volume of the electronics.

Since an incoming wavefront from a radio source will not, in general, reach all three antennas simultaneously, signals from two of the antennas must be delayed to compensate for this effect. With an overall baseline length of 30 m, the maximum delay required is 100 ns. This can most accurately be implemented digitally, after the signals have been sampled.

The correlator forms the cross products of the signals from the three antennas. These cross products are averaged for time intervals of typically 0.1 to 1 second, and provide the visibility data V introduced in Section 1.4.2. Since there are three antenna-pair combinations, two polarizations, and two frequencies, a total of 12 complex numbers are read out for each averaging interval. These data can be transmitted directly to earth or stored on the space station for periodic data-dumping. The use of a correlator on board the station thus reduces the downlink rate to a very modest level.

The spectral variation of the visibility across the 250 MHz-wide signal band can be measured by performing each cross correlation with a range of time offsets between the signals, or by performing a real-time fast Fourier transform on each signal bit-stream before the cross products are formed. The latter method, which has been developed only in the last few years[27] has particular advantages with large numbers of antennas. Experience at NRAO includes both types of correlators. Our study will address the question of which type to use.

[27] Y. Chikada, M. Ishiguro, H. Hirabayashi, M. Morimoto, K.-I. Morita, K. Miyazawa, K. Nagane, K. Murata, A. Tojo, S. Inoue, T. Kanzawa, and H. Iwashita, "A digital FFT spectrocorrelator for radio astronomy", in *Indirect Imaging*, J. A. Roberts, Ed., Cambridge Univ. Press, Cambridge, 1984, pp. 387–404.

2.1.4. Low-Noise Receivers.

2.1.4.1. Critical Components of the Receiver. The scientific requirement for $T_{\rm sys} \leq 1000$ K SSB is the most demanding technical specification of the HISAT project. The major part of the investigation will focus on heterodyne receivers for the proposed interferometer and particularly on the mixers, which to a very large degree govern the overall system noise temperature. Almost all coherent receivers used for submillimeter radio astronomy are based on GaAs Schottky-diode mixers. These have sensitivities about an order of magnitude worse than needed for the HISAT interferometer. In the last few years mixers using superconducting tunnel diodes (*S*uperconductor–*I*nsulator–*S*uperconductor junctions) have been established as the most sensitive at millimeter wavelengths, with mixer noise temperatures comparable to the photon noise temperature $h\nu/k \approx 5$ K at 100 GHz.[28] At submillimeter wavelengths a lack of suitable SIS junctions and fabrication facilities has greatly delayed SIS mixer development. So far, the few attempts to use SIS mixers in the submillimeter region have given results comparable with the best Schottky diode mixers. It has recently been shown,[29] however, that a well optimized SIS receiver should be capable of near quantum-limited performance up to almost twice the *gap frequency* (1.5–2.2 THz for the junctions we propose using). Figure 12 indicates the overall receiver noise temperature achievable in theory by an SIS receiver with junctions of different quality. At 800 GHz, our desired receiver noise temperature (1000 K SSB) requires an improvement by a factor of ~ 4 over the best reported SIS receiver to date, but that is still a factor of 25 greater than the photon noise. We are therefore confident that, by using high quality SIS junctions and newly developed radiation coupling and tuning structures, it should be possible to achieve the necessary sensitivity for the proposed instrument.

Appendix A lists the required receiver specifications and discusses, in more detail, the options in designing the mixers and SIS junctions.

The generation of local oscillator power for the receivers is the next major consideration. In the past, with Schottky diode mixers requiring ~ 1 mW of LO power, FIR lasers were the only acceptable LO sources above ~ 400 GHz. For SIS mixers, however, the required LO power can be less than 1 μW. Experimental solid state sources have already been demonstrated with sufficient power at 800 GHz.[30,31] High power InP Gunn oscillators now being developed by industry give substantial power at frequencies above 100 GHz, and work on

[28] S.-K. Pan, A. R. Kerr, M. J. Feldman, A. Kleinsasser, J. Stasiak, R. L. Sandstrom, and W. J. Gallagher, "An 85–116 GHz SIS receiver using inductively shunted edge-junctions", *IEEE Trans. Microwave Theory Tech.*, **MTT-37** (Mar. 1989), to appear (see abstract in Appendix B).

[29] M. J. Feldman, "Theoretical considerations for THz SIS mixers", *Int. J. Infrared & Millimeter Waves*, **8** (1987), 1287–1292.

[30] A. V. Räisänen, "State-of-the-art and prospects of frequency multipliers at millimeter- and submillimeter-waves", *IEEE Workshop on Solid State Sources at Millimeter and Submillimeter Wavelengths*, Ulm, W. Germany, 29–30 Sept. 1987.

[31] H. Rothermel, T. G. Phillips, and J. Keene, "A Solid-state frequency source for submillimeter astronomy", presented in the *Open Symposium of Millimeter Techniques in Telecommunications, Remote Sensing, and Radio Astronomy*, XXII$^{\rm nd}$ General Assembly of URSI, Tel Aviv, 24 Aug.–2 Sept. 1987.

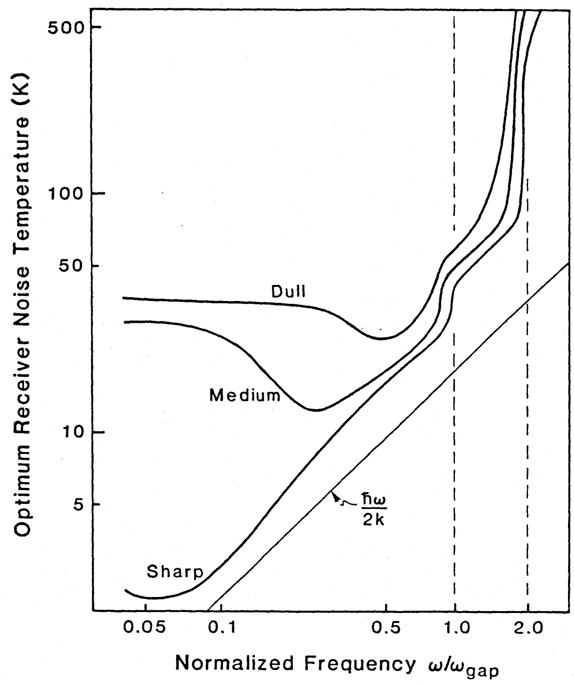

Figure 12. Optimum receiver noise temperature as a function of frequency for poor, medium, and high quality SIS junctions. Also shown is the quantum noise limit for SSB receivers, $\hbar\omega/2k$, which is half the photon temperature. Notice that, for high quality junctions, the receiver noise temperature is near the quantum limit up to almost $2\nu_{\mathrm{gap}}$. A conservative IF amplifier noise temperature of 10 K was assumed in computing these results. [From Feldman 1987, *op. cit.*]

varactor multipliers is progressing rapidly in industry and at universities. We anticipate that, within the three-year period of this proposal, it will be possible to obtain the necessary LO's commercially.

Low-noise IF amplifiers have been developed at the NRAO in recent years[32] and are in wide use in radio astronomy. These use commercial transistors (HEMT's) and in the 1–2 GHz range routinely give IF noise temperatures < 2 K over a 500 MHz bandwidth. It is clear, therefore, that the IF amplifier will not contribute appreciably to the system noise temperature of the interferometer.

The receiver optics must be designed to couple efficiently between the main reflector and the various mixers, and should include the following components:

(i) calibration loads and a beam-switch,
(ii) a polarization splitter,
(iii) diplexers to separate the 492 and 809 GHz bands,
(iv) filters to remove the unwanted image frequency bands, and
(v) diplexers to introduce the LO power to the mixers with minimum signal and LO loss.

The last three of these functions can be implemented using Martin–Puplett polarization-rotating interferometers[33] in front of the mixer—an approach now

[32] M. W. Pospieszalski, S. Weinreb, R. D. Norrod, and R. Harris, "FET's and HEMT's at cryogenic temperatures: their properties and use in low-noise amplifiers", *IEEE Trans. Microwave Theory Tech.*, **MTT-36** (1988) 552–560.

[33] D. H. Martin and E. Puplett, "Polarised interferometric spectrometry for the millimeter and

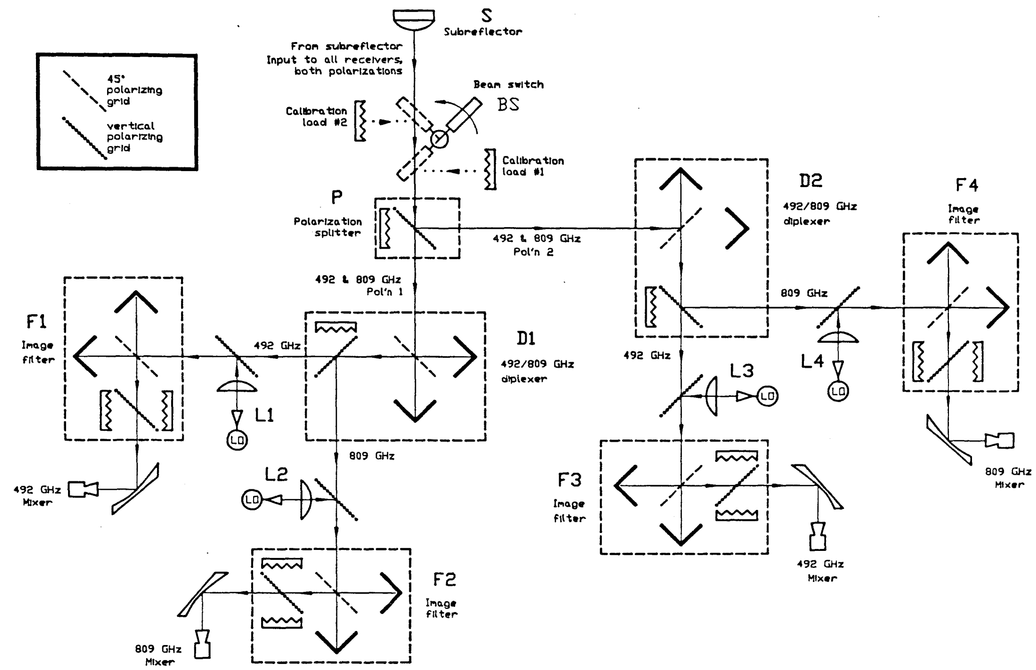

Figure 13. Schematic diagram showing one possible optics configuration for the receiver package on one element of the interferometer. The package contains receivers for both polarizations at 492 and 809 GHz. The incoming beam is split at polarization splitter P into two separate beams. Diplexers D1 and D2 separate the beams into 492 and 809 GHz channels. LO power is injected with polarization opposite that of the signal by polarizing grids at L1–L4. The image filters F1–F4 dump the image power into loads while transmitting the signal power (unattenuated) and the LO power (with 3 dB loss) into the mixers. The diplexers and image filters are based on the Martin–Puplett polarization rotating interferometer. The beam switch BS allows precise calibration of the receivers using thermal loads at two reference temperatures.

widely used in millimeter wavelength astronomy. Figure 13 shows a possible configuration for a receiver package which allows dual-polarization observations at 492 and 809 GHz, with image rejection. All elements of the interferometer have identical receiver packages.

2.1.4.2. Proposed Study of Receiver Components. Based on the discussion of receivers above and in Appendix A, we conclude that receivers with sufficient sensitivity for the HISAT interferometer should be practical following the development of suitable SIS mixers. We therefore propose a three-year study aimed at evaluating the various mixer configurations and SIS junction technologies, demonstrating the feasibility of one or more SIS mixer designs, and finally constructing a prototype receiver for the HISAT interferometer. Work will proceed in parallel on the mixer circuit configuration and on compatible SIS junction technologies.

The work on SIS technology will be carried out in close collaboration with

---

submillimeter spectrum", *Infrared Physics*, **10** (1969) 105–109.

Profs. R. J. Mattauch and M. J. Feldman of the University of Virginia Electrical Engineering Department. The UVa group has already developed processes for two types of SIS junction which appear very attractive for the proposed submillimeter receivers—Nb/Al–Al_2O_3/Nb trilayer junctions, and NbN/Ox/PbBi edge junctions.

The trilayer process appears to be the prime choice for millimeter wave mixers. The UVa trilayer junctions have the highest quality parameter V_m ever reported.[34] Furthermore, the trilayer process is well suited to incorporation of the integral tuning structures essential for submillimeter operation. So far, this type of junction has not been used at submillimeter wavelengths. The UVa edge junctions have the highest quality (V_m) and energy gap of any edge junctions reported.[35] Together with the inherent advantages of edge junctions for submillimeter operations (see Appendix A), this makes the UVa edge junction a strong contender for our application. The feasibility of extending the edge-junction process to include additional circuit elements will be investigated as part of this study.[36]

The approach to be taken in our investigation is as follows:

Mixer Circuit Configuration —

- Study mixer circuit designs for fundamental and harmonic SIS mixers.
- Build models of chosen mixer configurations, scaled to operate in the microwave region. These will enable accurate measurements to be made of the radiation patterns and embedding impedances as functions of frequency. (The use of large-scale models in designing SIS mixers has proven extremely beneficial in our earlier work on millimeter-wave SIS mixers.[37])
- Fabricate prototype mixers for 492 and 809 GHz, and test.

SIS Junction Technology —

- Investigate SIS harmonic mixers using Tucker's quantum mixer theory[38]. Determine noise temperature, conversion loss, and required LO power.
- Develop suitable tuning circuits for the tri-layer junctions.

---

[34]A. W. Lichtenberger, C. P. McClay, R. J. Mattauch, M. J. Feldman, S.-K. Pan, and A. R. Kerr, "Fabrication of Nb/Al–Al_2O_3/Nb junctions with extremely low leakage currents", *IEEE Trans. Magnetics*, to appear (see abstract in Appendix B).

[35]A. W. Lichtenberger, M. J. Feldman, and R. J. Mattauch, "The effects of ion gun beam voltage on the electrical characteristics of NbCN/PbBi edge junctions", *IEEE Trans. Magnetics*, to appear (see abstract in Appendix B).

[36]Concern that the PbBi counter-electrode may adversely affect the reliability of these junctions is allayed by experience at NBS with their widely used voltage standards which have $\sim 10,000$ Nb/Ox/Pb-alloy junctions in series. Although junctions employing Pb-alloy *base* electrodes have generally poor stability and reliability, those with Pb-alloy *counter*-electrodes over a refractory base electrode appear extremely good in these respects.

[37]M. J. Feldman, S.-K. Pan, A. R. Kerr, and A. Davidson, "SIS mixer analysis using a scale model", *IEEE Trans. Magnetics*, **MAG-19** (1983) 494–497.

[38]J. R. Tucker and M. J. Feldman, "Quantum detection at millimeter wavelength", *Rev. Mod. Phys.*, **57** (1985) 1055–1113.

- Study the feasibility of integrating tuning elements with the edge-junction process.
- Fabricate trial tri-layer and edge junctions with integrated tuning circuits.
- Design and fabricate junctions for prototype mixers.

These two parallel efforts—the mixer design study and the SIS technology study—will, clearly, be highly interactive. At submillimeter wavelengths the multi-mode part of the mixer (i.e., the radiation collecting elements) and the single-mode elements (SIS junction and tuning elements) are no longer separable as they are at microwave and millimeter wavelengths. The choice of SIS junction technology and mixer circuit configuration must therefore be regarded as two parts of the same problem; the choice of a particular substrate thickness, convenient for junction fabrication, may result in an impossible radiation collecting structure, for example.

2.2. Instrument Integration

For a concept investigation such as this, many of the physical instrument parameters are not well established. Nevertheless, in Table 5 estimates are made of the essential parameters for each of the important sub-assemblies. The HISAT interferometer does not generate contaminants, nor is it sensitive to EMI or gaseous effluents.

Table 5.

	Antenna (per antenna)	Receivers (each)	Correlator
Volume (m^3)	3	1	1
Weight (kg)	150	50	150
Power (watts)	150	50	1000
Thermal requirements	none*	$20 \pm 5°$ C	$20 \pm 5°$ C
Telemetry	—	—	100 kbits/sec
Data processing	—	—	internal

*Except that a solar shielding membrane is required.

Preceding launch, we would expect to test the payload components by temporarily installing and operating the interferometer at a high altitude site such as a location near the summit of Mauna Kea, Hawaii. Such testing will help to assure the instrument integrity and to validate the data quality.

2.3. Ground Operations

We anticipate the following ground operations support requirements for the HISAT interferometer:

- Target acquisition is a continuing task for ground operations. We expect to acquire approximately two targets per orbit. Observing schedules will be sent to the instrument package on a daily basis.
- The accumulated and averaged visibility data from the correlator are telemetered to the ground, where they are recorded on magnetic tape.

2.4. Flight Operations

The HISAT interferometer requires the following flight operations support:

- At initial deployment, the HISAT antennas should be mounted on top of the space station truss with as large an unobstructed viewing angle as possible, particularly above and in the direction of flight.
- The movable antennas, if any, will be re-located by the EVA flight crew at time intervals of 50–60 days or longer.
- Although the HISAT interferometer operates continuously there is no need for on-board critical monitoring of real-time instrumental performance.
- The helium dewars in which the cryogenic receivers are mounted must be refilled every 60 days. This will require EVA support. It requires access to a reservoir of liquid helium on the space station.

3. Data Reduction and Analysis

The output of the HISAT correlator is visibility data which have been pre-averaged (and pre-"fringed") over sufficiently long time intervals that the telemetry rate to the ground is modest. At the ground operations center these data are translated to a standard "export" tape format, for subsequent calibration and imaging using the NRAO Astronomical Image Processing System (AIPS) software, described below.

The most computationally intensive data reduction needs of HISAT are mosaicing (i.e., making up a composite image from data taken at different antenna pointings) and deconvolution of the point source response. Sophisticated state-of-the-art algorithms for both needs are already incorporated in AIPS. To be done properly, mosaicing and deconvolution must be done as a joint operation—this capability, too, already exists. Some specially adapted software for calibration of visibility data is required; this we will incorporate in AIPS.

AIPS is a machine-portable interactive software package for calibration, construction, display, and analysis of astronomical images made from interferometric data via Fourier synthesis methods. Design and development of the package began in Charlottesville in 1978; it presently contains over 600,000 lines of code and about 200 distinct applications "tasks," representing approximately 30 man-years of effort since 1978. AIPS is particularly appropriate for the HISAT interferometer because of its facility for handling many relevant coordinate geometries precisely, and its emphasis on display and analysis of the data in reciprocal Fourier domains.

AIPS has been the principal tool for display and analysis of both two- and three-dimensional images (i.e., continuum "maps" and spectral line "cubes") from NRAO's Very Large Array (VLA) since early in 1981. It contains facilities for display and editing of data in the aperture, or u-v, plane; for image construction by Fourier inversion; for deconvolution of the point source response by CLEAN and by maximum entropy methods; for image combination, filtering, and parameter estimation; and for a wide variety of TV and graphical displays. It records all user-generated operations and parameters that affect the quality of the derived images, as "history" files that are appended to the data sets and can be exported with them from AIPS in the IAU-standard FITS (Flexible Image Transport System) format. FITS copies of all HISAT images will be provided to the National Space Science Data Center in a timely manner.

For data reduction, HISAT computing needs, in hardware, are expected to be modest in comparison with those of the NRAO's VLA and VLBA operations.

4. Orbiter Crew and/or Payload Specialist Training Requirement

The crew and/or payload specialist would need to be trained for the task of transferring liquid Helium into the receiver dewars. If the interferometer has a movable element, or more than one, the crew would need to be trained in reconfiguring the interferometer baseline.

Appendix A: Receiver Considerations

A.1. Receiver Specifications

Frequencies:	492 and 809 GHz
Noise temperature:	$T_{\rm rcvr} \leq 1000$ K SSB
Instantaneous bandwidth:	250 MHz

A.2. Mixers

A.2.1. Schottky vs. SIS Mixers. Only the SIS mixer has the potential sensitivity to meet the requirements of the present proposal. The scope for improvement of the Schottky-diode mixer is limited to better diode design and more efficient coupling structures—probably no more than a factor of two in noise temperature. The high conversion loss of the Schottky mixer greatly increases the contribution of the IF amplifier to the overall system noise. It has recently been shown[39] that SIS receivers should be capable of near quantum-limited performance in the frequency range of interest. The planar thin-film mixer circuits now under development in our laboratory will enable us to integrate impedance matching circuits with the junctions, and also to integrate the junctions into the radiation collecting structures, thereby obtaining low conversion loss. (Conversion *gain*, while possible, should generally be avoided in the interest of wide dynamic range). Table A–1 compares Schottky and SIS mixers.

Table A–1.

Schottky Mixer	SIS Mixer
At 800 GHz, best $T_{\rm rcvr} \approx 5400$ K SSB.	At 800 GHz, best $T_{\rm rcvr} \approx 3700$ K SSB; potentially quantum limited (~ 40 K).
Needs contact whisker; subject to degradation with time and temperature.	Planar thin-film structure—stable with time and temperature.
Conversion loss $L \approx 15$–20 dB.	Potential gain; but prefer to design for $L \approx 0$ dB.
LO power ≈ 1 mW.	LO power ≈ 0.2 μW.

Interference from the Josephson effect is observed in short millimeter and submillimeter SIS mixers. Various stratagems for avoiding this problem are discussed by Tucker and Feldman[40], and these will substantially affect the design of both our mixer circuit and SIS junctions.

---

[39] M. J. Feldman, "Theoretical considerations for THz SIS mixers", *Int. J. Infrared & Millimeter Waves*, **8** (1987) 1287–1292.

[40] J. R. Tucker and M. J. Feldman, "Quantum detection at millimeter wavelength", *Rev. Mod. Phys.*, **57** (1985) 1055–1113.

A.2.2. Harmonic Mixers vs. Fundamental Mixers. The harmonic mixer has two main attractions: (i) The local oscillator is at a lower frequency where power is much more easily generated, and (ii) in the more sophisticated harmonic mixer designs, the LO and signal ports are physically separate, removing the need for an LO diplexer ahead of the mixer.

Because of the relatively high LO power requirements of Schottky-diode mixers, Schottky harmonic mixers may be feasible at frequencies beyond the range of Schottky fundamental mixers. It was for this reason that harmonic mixers were chosen for the $\sim$ 500 GHz receivers on the Eos Microwave Limb Sounder now being proposed by JPL. Sufficient LO power was available near 250 GHz from a solid-state Gunn oscillator/varactor multiplier chain.

With SIS mixers, however, it is much easier to obtain sufficient LO power, and the choice between fundamental and harmonic mixers rests mainly on performance considerations and the feasibility of designing the generally more complex harmonic mixer. Very little work, theoretical or experimental, has been done on SIS harmonic mixers. Factors needing study are: (i) LO power requirements of SIS harmonic mixers, (ii) the design of an integrated tuning circuit for an SIS harmonic mixer (as required for high performance fundamental SIS mixers[41]), and (iii) the effects of Josephson noise on harmonic mixers; it is possible, for example, that Josephson noise will be less of a limitation in harmonic mixers than in fundamental mixers.

A.2.3. Mixer Configurations. At millimeter wavelengths the best mixers have employed waveguide mounts with scalar feed horns to obtain well controlled embedding impedance for the junctions and high beam efficiency. In the submillimeter range, conventional waveguide mixers become impractical because of the small dimensions involved, and open-structures—quasi-optical mixers—are attractive. The most widely used quasi-optical mixer is the corner-cube Schottky-diode mixer[42]. Several designs which should be considered for submillimeter SIS mixers are given in Table A–2, together with their polarization characteristics and a comment on whether they are suitable for operation as harmonic mixers.

For harmonic mixer applications, the *corner cube mixer* has the possibility of angle-diplexing the signal and LO beams. However, the long-wire antenna needs to be integrated with the SIS circuit, and the introduction of a dielectric substrate into a corner cube antenna is expected to have detrimental effects (e.g., surface wave modes) which can be avoided with other mixer configurations.

The *log-spiral antenna* is intrinsically broadband, and therefore suitable for harmonic or fundamental mixers. The need for a very thin dielectric substrate probably rules out the cavity-backed log spiral. The proper design of the lens for the lens mounted log-spiral antenna has proven elusive so far.

The *planar log-periodic antenna* appears to have no substantial advantage over the log-spiral, but is more difficult to design.

---

[41] A. R. Kerr, S.-K. Pan, and M. J. Feldman, "Integrated tuning elements for SIS mixers", *Int. J. Infrared & Millimeter Waves*, **9** (1988) 203–212.

[42] H. P. Röser, E. J. Durwen, R. Wattenbach, and G. V. Schultz, "Investigation of heterodyne receiver with open structure mixer at 324 GHz and 693 GHz", *Int. J. Infrared & Millimeter Waves*, **5** (1984) 301–314.

Table A–2.

Type of Mixer	Polarization	Harmonic/Fundamental
Quasi-Optical:		
Corner cube	linear	f or h?
Log-spiral on cavity	circular	f or h
Log-spiral on lens	circular	f or h
Planar log-periodic on cavity	linear	f or h
Planar log-periodic on lens	linear	f or h
Waveguide-backed planar array	linear	f
Waveguide:		
Rectangular waveguide	linear	f
Circular waveguide	linear	f

The *waveguide-backed planar mixer* is a new concept which we believe will be easy to fabricate and does not require a substrate lens.

Conventional *waveguide mixers* as used at millimeter wavelengths are impractical in the submillimeter region primarily because the dielectric substrates become too small to fabricate. However, a new concept may enable us to fabricate a waveguide SIS mixer without a dielectric substrate. At 1 THz a fundamental-mode waveguide is approximately 0.005 inches $\times$ 0.010 inches, a size which can be made using electroforming techniques.

A.3. SIS Junctions

Many of the early SIS mixers used lead-alloy junctions. These are adversely affected by moisture or elevated temperatures, they change with time, and are extremely sensitive to electrical overload such as excess LO power or static discharge. We believe they are not suitable for space applications, where reliability is crucial.

More recently, all-refractory junctions using a Nb/Al–Al_2O_3/Nb tri-layer structure have been developed. These have much better electrical characteristics than Pb-alloy junctions, are stable, can be heated to 200° C in soldering or bonding, and are relatively immune to electrical overload. Such junctions have been extensively used at NRAO in receivers for the 80–120 GHz band.

Edge-junctions, as opposed to parallel-plate junctions, are potentially attractive for submillimeter work because of the relative ease of fabricating very small-area junctions and because they lend themselves better to suppression of Josephson interference noise. Nb/Ox/PbInAu edge-junctions have recently given outstanding results at 100 GHz,[43] and initial experiments with NbN/Ox/Pb-alloy edge junctions have given encouraging results.[44]

[43]S.-K. Pan, A. R. Kerr, M. J. Feldman, A. Kleinsasser, J. Stasiak, R. L. Sandstrom, and W. J. Gallagher, "An 85–116 GHz SIS receiver using inductively shunted edge-junctions", *IEEE Trans. Microwave Theory Tech.*, **MTT-37** (Mar. 1989), to appear (see abstract in Appendix B).

[44]A. W. Lichtenberger, M. J. Feldman, and R. J. Mattauch, "The effects of ion gun beam volt-

For their higher energy gap, all-NbN junctions seem very desirable. Progress on these has been slow, however, despite extensive research in the US and Japan.

Table A–3 summarizes the characteristics of the types of SIS junction presently in use which might be considered for our concept study. T_c is the critical temperature—it is desirable to operate SIS mixers at $\lesssim T_c/2$. The quantity $2\nu_{\text{gap}}$ is roughly the upper frequency limit for near quantum-limited receiver sensitivity.[45] C_s is the specific capacitance of the junction (compare to the figure of about 2 fF/μm^2 for Schottky diodes).

Table A–3.

Material	T_c	$2\nu_{\text{gap}}$	C_s	Comments
PbBi/Ox/PbInAu	7 K	1.3 THz	42 fF/μm^2	Unstable
Nb/Ox/PbInAu	7 K	1.3 THz	167 fF/μm^2	Edge-jns
Nb/Al–Al_2O_3/Nb	9 K	1.5 THz	40 fF/μm^2	Tri-layer
NbN/Ox/PbBi	8.4 K	2.2 THz	100 fF/μm^2	Edge-jns
NbN/MgO/NbN	15 K	2.4 THz	? 80 fF/μm^2	Tri-layer

Two factors bearing on the choice of junctions for submillimeter SIS mixers are:

(i) The relatively high values of C_s, which make it essential to integrate tuning circuits with the junctions.[46] Fabrication of additional circuit elements may not be practical for all types of junction.

(ii) Depending on ν_{gap}, means may be needed to suppress Josephson interference noise. Some types of junction are better suited to this, depending on approach (e.g., edge junctions may allow suppression of Josephson noise by magnetic fields weak enough not to affect the superconductivity of the thin-film electrodes).

age on the electrical characteristics of NbCN/PbBi edge junctions", *IEEE Trans. Magnetics*, to appear (see abstract in Appendix B).

[45] M. J. Feldman 1987, *op. cit.*

[46] Kerr *et al.* 1988, *op. cit.*

Appendix B:
Abstracts of Papers Referenced in Receiver Discussion

Three papers which were referenced in Section 2.1 and in Appendix A have not yet appeared in publication. Abstracts of these papers are given below.

A. W. Lichtenberger, M. J. Feldman, and R. J. Mattauch, "The effects of ion gun beam voltage on the electrical characteristics of NbCN/PbBi edge junctions", *IEEE Trans. Magnetics*, to appear.

Abstract. We have succeeded in fabricating high-quality submicron NbCN edge junctions using a technique which is commonly employed to make Nb edge junctions. A modified commercial ion gun was used to cut an edge in SiO_2/NbCN films partially covered with photoresist. An insulating barrier was then formed on the exposed edge by reactive ion beam oxidation, and a counterelectrode of PbBi was deposited. The electrical quality of the resulting junctions was found to be strongly influenced by the ion beam acceleration voltages used to cut the edge and to oxidize it. For low ion beam voltages, the junction quality parameter was as high as $V_m = 55$ mV (measured at 3 mV), but higher ion beam voltages yielded strikingly poorer quality junctions. In light of the small coherence length of NbN ($\xi \approx 3$ nm), the dependence of the electrical characteristics on ion beam voltage is presumably due to mechanical damage of the NbCN surface. In contrast, for similar ion beam voltages, no such dependence was found for Nb ($\xi \approx 30$ nm) edge junctions.

A. W. Lichtenberger, C. P. McClay, R. J. Mattauch, M. J. Feldman, S.-K. Pan, and A. R. Kerr, "Fabrication of Nb/Al–Al_2O_3/Nb junctions with extremely low leakage currents", *IEEE Trans. Magnetics*, to appear.

Abstract. Nb/Al–Al_2O_3/Nb trilayer films are deposited using DC magnetron sputtering guns in a UHV system which is capable of 5×10^{-10} Torr. SIS junctions as small as $3.2 \times 3.2\ \mu m^2$ are isolated from the trilayer by standard photolithography. The junctions typically have $V_m = 70$–90 mV at 4.2 K, while at 2.0 K V_m is as large as 1 *Volt.* The sub-gap leakage current is compared to the predictions of the BCS theory. The specific capacitance is preliminarily measured to be 45 ± 5 fF/μm^2.

S.-K. Pan, A. R. Kerr, M. J. Feldman, A. Kleinsasser, J. Stasiak, R. L. Sandstrom, and W. J. Gallagher, "An 85–116 GHz SIS receiver using inductively shunted edge-junctions", *IEEE Trans. Microwave Theory Tech.*, **MTT-37** (Mar. 1989), to appear.

Abstract. For the most part, SIS receivers have failed by a wide margin to achieve the sensitivity promised by theory. One of the main reasons for this is the difficulty of providing appropriate embedding impedances at the signal and image frequencies as well as the higher harmonic sidebands. We describe an SIS mixer with a broadband integrated tuning structure. The mixer is tunable from 85–116 GHz, and at 114 GHz has a noise temperature ≤ 5.6 K DSB and unity DSB conversion gain. The mixer noise temperature is less than or comparable to the photon noise temperature $hf/k \approx 5.5$ K. Referred to the mixer input flange, the receiver noise temperature is ≤ 9.5 K DSB when operated with an L-band HEMT IF amplifier. Saturation measurements have been made using CW and broadband noise sources.

Appendix C: Positions of Galactic H II Regions/ Molecular Cloud Complexes

l	b	α (1950)	δ (1950)
350°.129	0°.088	17h16m06s.5	-37°06'28"
350.335	0.107	17 16 37.6	-36 55 44
350.524	0.960	17 13 42.7	-36 16 48
350.813	-0.019	17 18 30.9	-36 36 37
350.996	-0.577	17 21 19.3	-36 46 40
351.063	0.662	17 16 27.8	-36 00 50
351.192	0.708	17 16 38.7	-35 52 55
351.201	0.483	17 17 34.8	-36 00 15
351.358	0.666	17 17 17.2	-35 46 14
351.467	-0.462	17 22 10.7	-36 19 28
351.590	0.183	17 19 53.7	-35 51 26
351.601	-0.348	17 22 05.3	-36 08 59
351.613	-1.270	17 25 54.8	-36 39 26
351.662	0.518	17 18 44.6	-35 36 24
352.398	-0.057	17 23 07.2	-35 19 39
352.611	-0.172	17 24 10.4	-35 12 57
352.836	1.273	17 18 59.9	-34 12 43
353.035	0.748	17 21 38.2	-34 20 50
353.083	0.358	17 23 19.8	-34 31 40
353.136	0.660	17 22 15.9	-34 18 49
353.186	0.887	17 21 29.8	-34 08 38
353.381	-0.114	17 26 02.3	-34 32 43
353.398	-0.391	17 27 12.2	-34 41 06
353.557	-0.014	17 26 06.7	-34 20 36
354.200	-0.054	17 27 59.8	-33 49 51
354.486	0.085	17 28 12.0	-33 30 56
354.664	0.470	17 27 08.3	-33 09 15
354.665	0.247	17 28 01.7	-33 16 37
355.242	0.096	17 30 08.9	-32 52 43
355.700	-0.010	17 31 45.7	-32 33 12
356.235	0.642	17 30 33.9	-31 44 56
356.307	-0.210	17 34 07.1	-32 09 10
356.650	0.129	17 33 39.1	-31 40 51
357.988	-0.159	17 38 09.1	-30 42 27
2.303	0.243	17 46 56.6	-26 49 31
2.611	0.135	17 48 04.2	-26 37 03
2.901	-0.006	17 49 16.7	-26 26 29
3.262	0.019	17 50 00.5	-26 07 08
3.270	-0.101	17 50 29.2	-26 10 24
3.342	-0.079	17 50 34.0	-26 06 01

l	b	α (1950)	δ (1950)
3°.655	-0°.111	17h51m24s.0	-25°50'52"
4.412	0.118	17 52 14.2	-25 04 47
4.568	-0.118	17 53 29.1	-25 03 55
5.049	0.254	17 53 08.9	-24 27 43
5.193	-0.284	17 55 30.5	-24 36 35
5.479	-0.241	17 55 58.7	-24 20 28
5.899	-0.427	17 57 36.5	-24 04 16
5.956	-1.265	18 00 55.3	-24 26 21
5.973	-1.178	18 00 37.6	-24 22 53
6.083	-0.117	17 56 50.3	-23 45 24
6.148	-0.635	17 58 56.5	-23 57 34
6.165	-1.168	18 01 00.3	-24 12 35
6.220	-0.096	17 57 03.6	-23 37 39
6.225	-0.569	17 58 51.6	-23 51 35
6.398	-0.474	17 58 52.6	-23 39 45
6.553	-0.095	17 57 47.0	-23 20 20
6.565	-0.297	17 58 34.3	-23 25 46
6.667	-0.247	17 58 36.3	-23 18 58
6.930	-2.130	18 06 19.5	-24 01 00
6.979	-0.250	17 59 17.6	-23 02 50
7.299	-0.116	17 59 28.9	-22 42 11
7.387	0.668	17 56 43.9	-22 14 05
7.472	0.060	17 59 11.6	-22 27 55
8.006	-0.156	18 01 09.1	-22 06 33
8.137	0.228	17 59 59.6	-21 48 18
8.310	-0.090	18 01 33.2	-21 48 45
8.362	-0.303	18 02 27.7	-21 52 21
8.438	-0.331	18 02 43.7	-21 49 13
8.533	-0.288	18 02 46.1	-21 42 59
8.666	-0.351	18 03 17.2	-21 37 55
8.865	-0.323	18 03 36.2	-21 26 41
9.615	0.198	18 03 14.6	-20 32 08
9.717	-0.832	18 07 17.9	-20 57 05
9.982	-0.752	18 07 33.1	-20 40 51
10.073	-0.412	18 06 28.4	-20 26 08
10.159	-0.349	18 06 25.0	-20 19 48
10.190	-0.426	18 06 46.1	-20 20 26
10.190	-0.426	18 06 46.1	-20 20 26
10.266	0.075	18 05 03.9	-20 01 45
10.314	-0.262	18 06 25.0	-20 09 08

l	b	α (1950)	δ(1950)
10°.314	-0°.262	18ʰ06ᵐ25ˢ.0	-20°09'08"
10.315	-0.150	18 06 00.1	-20 05 47
10.458	0.024	18 05 39.3	-19 53 12
10.617	-0.384	18 07 30.0	-19 56 50
10.664	-0.467	18 07 54.3	-19 56 47
10.689	0.031	18 06 06.5	-19 40 54
10.876	0.085	18 06 17.8	-19 29 32
10.966	0.009	18 06 45.9	-19 27 03
11.197	-1.128	18 11 27.8	-19 48 02
11.207	0.088	18 06 58.3	-19 12 07
11.707	-1.722	18 14 43.0	-19 38 18
11.898	0.747	18 05 58.1	-18 16 38
11.936	-0.616	18 11 04.4	-18 54 22
11.944	-0.037	18 08 56.9	-18 37 08
11.987	-0.245	18 09 48.3	-18 40 56
12.204	-0.116	18 09 46.3	-18 25 47
12.204	-0.116	18 09 46.3	-18 25 47
12.431	-0.042	18 09 57.8	-18 11 43
12.445	-1.113	18 13 56.9	-18 41 57
12.446	-0.619	18 12 07.3	-18 27 39
12.745	-0.153	18 11 00.6	-17 58 27
12.762	0.370	18 09 07.3	-17 42 22
12.807	-0.204	18 11 19.5	-17 56 40
12.909	-0.277	18 11 48.0	-17 53 25
13.186	0.045	18 11 10.6	-17 29 33
13.208	-0.144	18 11 54.9	-17 33 51
13.381	0.071	18 11 28.5	-17 18 33
13.535	-0.186	18 12 43.8	-17 17 52
13.826	-0.758	18 15 25.1	-17 19 01
13.875	0.282	18 11 41.9	-16 46 28
13.886	-0.017	18 12 49.0	-16 54 32
13.998	-0.128	18 13 26.9	-16 51 50
14.064	-0.526	18 15 02.5	-16 59 49
14.081	-0.151	18 13 42.0	-16 48 08
14.161	-0.223	18 14 07.4	-16 46 00
14.196	-0.125	18 13 50.1	-16 41 20
14.221	-0.287	18 14 28.7	-16 44 41
14.317	0.134	18 13 07.7	-16 27 30
14.330	-0.183	18 14 18.9	-16 35 57
14.427	-0.075	18 14 06.8	-16 27 44

l	b	α (1950)	δ(1950)
14°.445	-0°.651	18ʰ16ᵐ15ˢ.7	-16°43'19"
14.496	0.010	18 13 56.4	-16 21 39
14.600	0.014	18 14 08.0	-16 16 04
14.626	0.087	18 13 55.2	-16 12 36
14.677	-0.491	18 16 08.2	-16 26 30
14.931	-0.638	18 17 10.8	-16 17 19
15.032	-0.687	18 17 33.6	-16 13 23
15.143	-0.940	18 18 42.4	-16 14 44
15.181	-0.625	18 17 37.7	-16 03 45
15.198	-0.768	18 18 11.1	-16 06 56
16.313	-0.162	18 18 10.3	-14 50 47
16.368	-0.515	18 19 33.9	-14 57 56
16.431	-0.199	18 18 32.3	-14 45 37
16.614	-0.324	18 19 21.1	-14 39 31
16.808	-1.072	18 22 27.5	-14 50 28
16.936	0.758	18 16 03.4	-13 51 38
16.984	0.934	18 15 30.9	-13 44 03
16.995	0.868	18 15 46.5	-13 45 22
17.144	0.765	18 16 26.4	-13 40 28
18.143	-0.289	18 22 12.4	-13 17 41
18.185	-0.397	18 22 40.7	-13 18 31
18.197	-0.181	18 21 55.2	-13 11 46
18.252	1.892	18 14 32.9	-12 09 47
18.258	-0.297	18 22 27.5	-13 11 50
18.305	-0.391	18 22 53.4	-13 12 00
18.456	-0.007	18 21 47.5	-12 53 09
18.643	-0.288	18 23 10.2	-12 51 12
18.686	1.965	18 15 08.0	-11 44 49
18.881	-0.493	18 24 22.3	-12 44 23
18.954	-0.019	18 22 47.9	-12 27 08
19.044	-0.431	18 24 27.6	-12 34 00
19.050	-0.593	18 25 03.5	-12 38 15
19.066	-0.281	18 23 57.7	-12 28 36
19.485	0.138	18 23 15.3	-11 54 36
19.608	-0.235	18 24 50.2	-11 58 36
19.614	-0.132	18 24 28.6	-11 55 23
19.671	-0.137	18 24 36.3	-11 52 30
20.074	-0.141	18 25 23.5	-11 31 16
20.264	-0.894	18 28 28.3	-11 42 20
20.479	0.165	18 25 03.9	-11 01 12

l	b	α (1950)	δ (1950)
20°681	-0°136	18h26m32s0	-10°58' 57"
20.733	-0.087	18 26 27.4	-10 54 49
20.988	0.092	18 26 17.9	-10 36 16
21.871	0.008	18 28 16.8	-09 51 48
21.902	-0.368	18 29 41.4	-10 00 41
22.398	0.083	18 29 00.5	-09 21 45
22.760	-0.485	18 31 43.8	-09 18 24
22.947	-0.315	18 31 28.4	-09 03 43
22.982	-0.356	18 31 41.1	-09 03 00
23.067	-0.367	18 31 53.1	-08 58 48
23.072	-0.248	18 31 28.1	-08 55 13
23.115	0.556	18 28 40.2	-08 30 27
23.254	-0.268	18 31 52.9	-08 46 06
23.281	0.298	18 29 54.4	-08 28 52
23.421	-0.214	18 32 00.2	-08 35 44
23.538	-0.041	18 31 36.2	-08 24 41
23.613	-0.376	18 32 56.6	-08 30 03
23.706	-0.202	18 32 29.7	-08 20 15
23.706	0.171	18 31 09.7	-08 09 51
23.817	0.224	18 31 10.8	-08 02 28
23.869	-0.119	18 32 30.3	-08 09 17
23.909	0.066	18 31 55.1	-08 02 00
23.909	0.066	18 31 55.1	-08 02 00
23.956	0.152	18 31 41.9	-07 57 06
24.132	-0.067	18 32 48.7	-07 53 51
24.135	0.122	18 32 08.5	-07 48 26
24.194	0.203	18 31 57.8	-07 43 02
24.217	-0.053	18 32 55.3	-07 48 57
24.303	-0.151	18 33 26.0	-07 47 06
24.303	-0.151	18 33 26.0	-07 47 06
24.392	0.072	18 32 48.2	-07 36 10
24.460	-0.246	18 34 04.0	-07 41 24
24.467	0.489	18 31 27.2	-07 20 33
24.484	0.211	18 32 28.7	-07 27 24
24.502	-0.039	18 33 24.3	-07 33 25
24.517	-0.233	18 34 07.6	-07 38 01
24.677	-0.160	18 34 09.9	-07 27 29
24.720	-0.085	18 33 58.7	-07 23 06
24.742	-0.207	18 34 27.3	-07 25 20
24.742	-0.207	18 34 27.3	-07 25 20

l	b	α (1950)	δ (1950)
24°805	0°098	18h33m29s0	-07°13' 30"
25.161	0.069	18 34 15.1	-06 55 23
25.264	-0.317	18 35 49.4	-07 00 38
25.294	0.307	18 33 39.1	-06 41 41
25.382	-0.177	18 35 32.6	-06 50 28
25.386	-0.347	18 36 09.5	-06 54 59
25.396	0.034	18 34 49.0	-06 43 51
25.405	-0.254	18 35 51.7	-06 51 23
25.700	0.031	18 35 23.6	-06 27 47
25.700	0.031	18 35 23.6	-06 27 47
25.766	0.211	18 34 52.5	-06 19 16
26.103	-0.069	18 36 30.1	-06 09 07
26.103	-0.069	18 36 30.1	-06 09 07
26.433	0.614	18 34 40.9	-05 32 36
26.536	0.416	18 35 34.7	-05 32 37
26.555	-0.305	18 38 11.0	-05 51 37
26.600	-0.106	18 37 33.5	-05 43 43
26.981	-0.066	18 38 07.4	-05 22 20
27.132	0.000	18 38 10.1	-05 12 28
27.276	0.148	18 37 54.5	-05 00 42
27.307	-0.144	18 39 00.4	-05 07 09
27.491	0.189	18 38 09.7	-04 48 07
28.001	-0.031	18 39 53.4	-04 27 05
28.295	-0.377	18 41 39.9	-04 21 00
28.295	-0.377	18 41 39.9	-04 21 00
28.312	-0.023	18 40 26.2	-04 10 18
28.312	-0.023	18 40 26.2	-04 10 18
28.440	-0.002	18 40 36.0	-04 02 54
28.596	-0.363	18 42 10.3	-04 04 35
28.600	0.015	18 40 50.1	-03 53 55
28.638	0.194	18 40 16.1	-03 46 56
28.658	0.030	18 40 53.3	-03 50 25
28.787	0.252	18 40 20.3	-03 37 24
28.790	3.486	18 28 51.6	-02 07 29
28.801	0.174	18 40 38.4	-03 38 49
28.823	-0.226	18 42 06.2	-03 48 43
28.983	-0.603	18 43 44.4	-03 50 37
29.094	-0.713	18 44 20.2	-03 47 45
29.136	-0.042	18 42 01.7	-03 26 58
29.139	0.431	18 40 21.1	-03 13 43

ℓ	b	α (1950)	δ (1950)
29°.205	-0°.047	18^{h}42^{m}10^s.4	-03°23' 25"
29.944	-0.042	18 43 31.2	-02 43 56
30.069	-0.160	18 44 10.2	-02 40 32
30.227	-0.145	18 44 24.5	-02 31 43
30.277	-0.020	18 44 03.3	-02 25 36
30.404	-0.238	18 45 03.8	-02 24 51
30.467	0.429	18 42 48.7	-02 03 04
30.470	-0.039	18 44 28.7	-02 15 50
30.470	-0.039	18 44 28.7	-02 15 50
30.502	-0.290	18 45 25.8	-02 21 04
30.509	-0.447	18 46 00.0	-02 25 02
30.539	0.024	18 44 23.0	-02 10 25
30.539	0.024	18 44 23.0	-02 10 25
30.602	-0.106	18 44 57.6	-02 10 40
30.694	-0.261	18 45 40.9	-02 10 02
30.776	-0.029	18 45 00.4	-01 59 16
30.832	-0.186	18 45 40.1	-02 00 37
30.854	0.134	18 44 34.3	-01 50 36
30.854	0.134	18 44 34.3	-01 50 36
30.950	0.078	18 44 56.8	-01 47 02
30.999	-0.038	18 45 27.0	-01 47 38
31.050	0.480	18 43 42.2	-01 30 36
31.054	0.079	18 45 08.1	-01 41 28
31.054	0.079	18 45 08.1	-01 41 28
31.130	0.284	18 44 32.9	-01 31 46
31.165	-0.127	18 46 04.3	-01 41 15
31.239	-0.108	18 46 08.4	-01 36 47
31.239	-0.108	18 46 08.4	-01 36 47
31.275	0.056	18 45 37.5	-01 30 20
31.401	-0.259	18 46 58.6	-01 32 20
31.411	0.309	18 44 58.6	-01 16 06
31.580	0.101	18 46 01.7	-01 12 51
31.650	-0.649	18 48 49.4	-01 29 50
32.151	0.133	18 46 57.9	-00 41 33
32.797	0.192	18 47 56.8	-00 05 31
33.129	-0.094	18 49 34.6	+00 04 17
33.194	-0.010	18 49 23.3	+00 10 03
33.418	-0.004	18 49 47.0	+00 22 09
33.914	0.111	18 50 17.3	+00 51 45
34.254	0.144	18 50 47.8	+01 10 46

ℓ	b	α (1950)	δ (1950)
34°.550	-1°.110	18^{h}55^{m}47^s.7	+00°51' 54"
34.758	-0.681	18 54 39.3	+01 14 50
34.932	-0.018	18 52 37.3	+01 42 25
35.041	-0.498	18 54 31.6	+01 34 57
35.063	-1.506	18 58 08.8	+01 08 15
35.194	-1.750	18 59 15.3	+01 08 29
35.346	-1.827	18 59 48.5	+01 14 26
35.574	0.064	18 53 30.8	+02 18 52
35.588	-0.489	18 55 30.2	+02 04 20
35.603	-0.033	18 53 54.7	+02 17 44
35.673	-0.847	18 56 55.9	+01 58 57
36.289	-1.686	19 01 02.9	+02 08 31
36.289	0.734	18 52 27.0	+03 15 28
36.459	-0.179	18 56 00.6	+02 59 17
36.914	0.489	18 54 28.5	+03 41 59
36.914	0.489	18 54 28.5	+03 41 59
37.361	-0.228	18 57 51.1	+03 45 57
37.370	-0.067	18 57 17.7	+03 50 53
37.439	-0.040	18 57 19.6	+03 55 18
37.538	-0.113	18 57 46.2	+03 58 33
37.636	-0.113	18 57 57.0	+04 03 46
37.671	0.132	18 57 08.6	+04 12 25
37.749	-0.109	18 58 08.7	+04 09 54
37.763	-0.216	18 58 33.1	+04 07 41
37.871	-0.399	18 59 24.2	+04 08 21
38.051	-0.042	18 58 28.0	+04 27 49
39.252	-0.056	19 00 44.7	+05 31 21
39.904	-1.331	19 06 29.9	+05 30 32
40.504	2.537	18 53 47.9	+07 49 41
40.947	-0.567	19 05 43.6	+06 47 15
41.096	-0.213	19 04 44.5	+07 05 02
41.235	0.367	19 02 55.8	+07 28 33
41.517	0.033	19 04 39.1	+07 34 15
42.108	-0.623	19 08 06.3	+07 47 20
42.431	-0.264	19 07 25.8	+08 14 31
42.568	-0.143	19 07 15.3	+08 25 11
43.169	0.002	19 07 52.1	+09 01 08
43.182	-0.520	19 09 45.7	+08 47 13
43.890	-0.790	19 12 04.2	+09 17 11
44.264	0.100	19 09 35.3	+10 02 00

ℓ	b	α (1950)	δ (1950)
44.°786	-0.°490	19ʰ12ᵐ42.ˢ0	+10°13' 06"
45.125	0.136	19 11 05.8	+10 48 40
45.451	0.060	19 11 59.5	+11 03 49
45.475	0.130	19 11 47.1	+11 07 03
45.824	-0.290	19 13 57.9	+11 13 43
46.495	-0.247	19 15 06.0	+11 50 27
48.596	0.042	19 18 07.6	+13 49 45
48.642	0.227	19 17 32.7	+13 57 26
48.930	-0.286	19 19 58.2	+13 58 03
48.997	-0.295	19 20 08.0	+14 01 20
49.060	-0.260	19 20 07.8	+14 05 39
49.076	-0.377	19 20 35.2	+14 03 10
49.204	-0.345	19 20 43.3	+14 10 50
49.384	-0.298	19 20 54.3	+14 21 40
49.407	-0.193	19 20 34.1	+14 25 53
49.437	-0.465	19 21 36.9	+14 19 41
49.486	-0.381	19 21 24.4	+14 24 40
49.582	-0.381	19 21 35.8	+14 29 44
49.588	-0.456	19 21 52.8	+14 27 54
50.024	-0.076	19 21 21.5	+15 01 46
50.125	-0.670	19 23 43.1	+14 50 04
50.232	0.326	19 20 18.3	+15 24 14
51.060	0.162	19 22 32.7	+16 03 12
51.362	-0.001	19 23 44.6	+16 14 26
52.233	0.736	19 22 46.9	+17 21 29
52.240	-0.538	19 27 28.2	+16 45 06
52.753	0.335	19 25 18.2	+17 37 19
52.940	-0.588	19 29 04.3	+17 20 23
53.184	0.155	19 26 50.3	+17 54 47
53.639	0.235	19 27 28.1	+18 21 00
54.092	-0.066	19 29 30.3	+18 36 01
55.114	2.422	19 22 19.8	+20 41 36
57.541	-0.276	19 37 29.8	+21 30 06
59.529	-0.181	19 41 26.2	+23 16 17
59.796	0.237	19 40 26.6	+23 42 44
60.888	-0.127	19 44 13.9	+24 28 20
61.470	0.090	19 44 42.4	+25 05 02
62.941	0.084	19 48 03.7	+26 20 45
63.176	0.460	19 47 09.3	+26 44 25
64.140	-0.470	19 52 57.6	+27 05 09

ℓ	b	α (1950)	δ (1950)
68.°134	0.°917	19ʰ57ᵐ09.ˢ2	+31° 12' 49"
68.134	0.917	19 57 09.2	+31 12 49
69.942	1.517	19 59 16.7	+33 03 51
70.300	1.600	19 59 51.3	+33 24 41
71.603	2.824	19 58 10.8	+35 09 52
74.764	0.614	20 15 50.9	+36 36 04
75.363	-0.423	20 21 47.4	+36 29 59
75.767	0.344	20 19 49.0	+37 16 18
75.834	0.402	20 19 46.3	+37 21 35
76.152	-0.281	20 23 29.9	+37 13 30
76.383	-0.623	20 25 34.2	+37 12 46
77.977	-0.003	20 27 47.4	+38 51 58
78.032	0.607	20 25 25.0	+39 16 11
78.147	1.816	20 20 38.8	+40 03 54
78.163	-0.367	20 29 51.7	+38 48 00
78.300	1.372	20 23 00.0	+39 56 00
78.323	2.822	20 16 49.9	+40 47 00
78.350	1.496	20 22 37.5	+40 02 46
78.370	2.739	20 17 20.0	+40 46 30
78.455	-0.043	20 29 24.9	+39 13 39
78.502	1.223	20 24 14.8	+40 00 40
78.637	0.847	20 26 15.0	+39 54 01
78.683	0.939	20 26 00.1	+39 59 30
78.727	-0.606	20 32 35.0	+39 06 31
79.128	3.684	20 15 27.3	+41 56 00
79.157	-0.257	20 32 28.7	+39 39 43
79.224	-0.061	20 31 52.4	+39 50 00
79.235	0.342	20 30 13.3	+40 05 00
79.293	1.296	20 26 21.9	+40 41 42
79.306	0.282	20 30 41.7	+40 06 16
79.370	-0.806	20 35 25.0	+39 29 59
79.418	2.417	20 21 55.0	+41 26 58
79.822	0.074	20 33 11.5	+40 23 32
79.957	0.866	20 30 16.5	+40 58 31
79.982	-0.028	20 34 07.5	+40 27 29
80.039	2.108	20 25 11.5	+41 46 30
80.105	-0.093	20 34 47.4	+40 31 00
80.198	0.807	20 31 17.4	+41 08 00
80.346	0.721	20 32 07.6	+41 12 00
80.363	0.449	20 33 20.1	+41 03 00

ℓ	b	α (1950)	δ (1950)
80°.612	1°.465	20h 29m 47s.4	+41° 51' 29"
80.880	0.410	20 35 09.9	+41 26 16
80.936	-0.126	20 37 36.5	+41 09 18
80.942	-0.255	20 38 10.1	+41 04 50
81.253	1.123	20 33 19.9	+42 09 59
81.342	1.200	20 33 17.4	+42 17 01
81.480	0.561	20 36 28.9	+42 00 20
81.526	-0.037	20 39 10.1	+41 40 30
81.551	2.074	20 30 10.1	+42 58 29
81.681	0.540	20 37 14.0	+42 09 06
81.689	0.337	20 38 07.5	+42 02 01
82.036	2.330	20 30 37.5	+43 31 00
82.277	2.425	20 30 59.9	+43 45 59
82.454	2.369	20 31 50.0	+43 52 29
82.566	0.405	20 40 46.0	+42 45 56
83.783	3.308	20 32 04.6	+45 30 00
83.941	0.781	20 43 52.4	+44 04 29
84.813	3.771	20 33 29.9	+46 36 01
84.918	-1.155	20 55 35.1	+43 34 59
85.178	-0.074	20 51 57.4	+44 29 02
85.242	0.004	20 51 51.3	+44 34 59
93.060	2.810	21 10 45.5	+52 16 35
94.394	-5.489	21 51 29.9	+47 02 30
102.875	-0.721	22 17 43.5	+55 52 07
107.182	-0.953	22 45 51.7	+57 49 29
108.197	0.579	22 47 30.5	+59 39 00
108.760	-0.952	22 56 37.6	+58 30 52
110.106	0.044	23 03 04.3	+59 58 20
111.525	0.818	23 11 21.2	+61 13 45
111.612	0.374	23 13 21.3	+60 50 49
112.237	0.226	23 18 35.7	+60 55 39
113.589	-0.721	23 31 31.9	+60 27 34
115.784	-1.573	23 50 27.0	+60 12 22
118.148	4.962	23 58 59.6	+67 05 27
123.058	-6.297	00 49 24.9	+56 18 11
132.157	-0.725	02 04 29.1	+60 31 46
133.720	1.210	02 21 54.6	+61 51 57
133.790	1.410	02 23 04.0	+62 01 42
136.913	1.033	02 45 41.8	+60 27 00
138.486	1.635	02 59 14.3	+60 16 10

ℓ	b	α (1950)	δ (1950)
150°.590	-0°.950	03h 59m 29s.1	+51° 10' 48"
151.594	-0.228	04 07 19.3	+51 03 00
154.640	2.436	04 32 56.5	+50 46 49
155.357	2.609	04 36 46.8	+50 21 58
169.191	-0.903	05 10 01.8	+37 23 32
173.599	2.798	05 37 37.9	+35 49 34
173.607	-1.733	05 19 18.1	+33 19 00
173.898	0.284	05 28 06.9	+34 12 35
189.971	0.395	06 06 11.8	+20 30 59
192.616	-0.044	06 10 01.4	+17 59 31
192.632	-0.018	06 10 09.1	+17 59 26
196.448	-1.673	06 11 47.1	+13 51 00
206.540	-16.360	05 39 11.3	-01 56 09
206.791	-1.999	06 30 25.4	+04 35 00
209.010	-19.380	05 32 49.8	-05 25 07
213.709	-12.605	06 05 20.3	-06 22 54
218.714	1.844	07 06 06.3	-04 13 02
225.480	-2.550	07 03 02.7	-12 14 52
227.786	-0.116	07 16 17.0	-13 09 02
233.761	-0.191	07 27 52.8	-18 26 08
243.159	0.372	07 50 18.4	-26 17 53
253.588	-0.188	08 14 18.6	-35 23 23

M. Balister

NATIONAL RADIO ASTRONOMY OBSERVATORY

High-Resolution Imaging Spectroscopy
at Terahertz Frequencies
Part II: Management Plan and Cost Plan

*A Proposal to the National Aeronautics
and Space Administration
under A.O. No. OSSA 3–88*

National Radio Astronomy Observatory

November 1988

— Concept Study —

High-Resolution Imaging Spectroscopy at Terahertz Frequencies

Part II: Management Plan and Cost Plan

A Proposal to the National Aeronautics and Space Administration under A.O. No. OSSA 3–88

National Radio Astronomy Observatory

November 1988

Dr. Robert L. Brown
Associate Director, NRAO
Principal Investigator
(804–296–0222)

Dr. Paul A. Van den Bout
Director, NRAO

Mr. James L. Desmond
Associate Director for Administration
(804–296–0315)

The National Radio Astronomy Observatory (NRAO) is operated by Associated Universities, Inc., under Contract No. NSF AST 84–03744 with the National Science Foundation.

HIGH-RESOLUTION IMAGING SPECTROSCOPY AT TERAHERTZ FREQUENCIES

A Proposal to NASA Under A.O. No. OSSA 3-88

PART II: MANAGEMENT PLAN AND COST PLAN

November 9, 1988

SUMMARY

The goal of this mission is to determine the origin and propagation of ultraviolet radiation in the Galaxy by studying the excitation of atomic carbon and oxygen at submillimeter wavelengths. Obscured by the Galactic disk, ultraviolet (UV) radiation from most of the Galaxy is invisible at the earth. However, we can infer its presence from its effect on interstellar material. We intend to obtain spectroscopic images at high angular resolution of those submillimeter lines of C, O, and C^+ to which the Galactic disk is transparent and which are critical diagnostics of UV excitation.

The space station attached payload that will provide the high resolution images is a three (or more) element heterodyne submillimeter interferometer, HISAT (High-Resolution Imaging Spectroscopy at Terahertz Frequencies). Astronomical images of high fidelity will be obtained if (1) observations are made in an optimal way over the full internodal period of the space station; (2) low-noise receivers can be fabricated at frequencies approaching 1 THz; and (3) the IF and digital electronics can be designed to be robust and economical of electrical power. The management plan presents a mechanism for these questions to be answered in a timely manner.

The crux of the plan is the application to HISAT of expertise gained in millimeter/submillimeter instrumentation, in aperture synthesis, and in image processing at the National Radio Astronomy Observatory. The conduct and management of the HISAT concept investigation will enhance and share the resident infrastructure.

HIGH-RESOLUTION IMAGING SPECTROSCOPY AT TERAHERTZ FREQUENCIES

A Proposal to NASA Under A.O. No. OSSA 3-88

TABLE OF CONTENTS

1. Management Plan
   - 1.1. Organization 1
   - 1.2. Key Personnel Credentials 1
   - 1.3. Prior Management Experience 4
   - 1.4. Instrument Acquisition 5
   - 1.5. Schedule 5
   - 1.6. Subcontracts 5

2. Facilities and Equipment 7

3. Data Analysis Facilities 7

4. Cost Plan 7
   - 4.1. Cost Plan for HISAT Concept Investigation 8

Appendix A
- A.1. Key Personnel and Investigator Publications
  - A.1.1. Publications of Dr. Robert L. Brown 9
  - A.1.2. Publications of Dr. Anthony R. Kerr 16
  - A.1.3. Publications of Dr. A. Richard Thompson 22
  - A.1.4. Publications of Mr. Frederic R. Schwab 27

Appendix B. A Brief Profile of the National Radio Astronomy Observatory 28

Appendix C. UVA-SDL Estimate for SIS Device Subcontract 39

Appendix D. Technical Data Sheets 46

HIGH-RESOLUTION IMAGING SPECTROSCOPY AT TERAHERTZ FREQUENCIES

A Proposal to NASA Under A.O. No. OSSA 3-88

PART II: MANAGEMENT PLAN AND COST PLAN

November 9, 1988

1. Management

1.1. Organization

The concept investigation for High-Resolution Imaging Spectroscopy at Terahertz Frequencies (HISAT), a space station attached payload, is proposed by Dr. Robert L. Brown (Principal Investigator) with the full support of the National Radio Astronomy Observatory (NRAO).

The management structure for the HISAT concept investigation is shown in Figure 1. The Principal Investigator has overall responsibility for timely completion of the scheduled tasks. He is assisted by Co-Investigators Dr. Anthony R. Kerr, Mr. Frederic R. Schwab, and Dr. A. Richard Thompson whose responsibilities are as follows:

Dr. A. R. Kerr, head of millimeter-wave development in the NRAO Central Development Laboratory (CDL), is responsible for the low-noise receiver development.

Mr. Frederic R. Schwab, imaging analyst for The Very Large Array (VLA) and The Very Long Baseline Array (VLBA) synthetic aperture radio telescopes, is responsible for imaging simulations and evaluation of data-taking procedures.

Dr. A. Richard Thompson, head of VLBA Electronics, is responsible for HISAT system definition and instrument integration.

1.2. Key Personnel Credentials

Dr. Robert L. Brown (Principal Investigator): Born in Los Angeles in 1943, Dr. Brown received his B.A. in Physics from the University of California-Berkeley in 1965 and his M.S. and Ph.D. from the University of California-San Diego in 1969. His Ph.D. thesis explored the atomic physics processes which provide the opacity of the galactic disk to x-ray and ultraviolet radiation.

Following the Ph.D. degree, Dr. Brown joined the NRAO as a Research Associate and was appointed to the permanent NRAO Scientific Staff in 1971. His research work on the interstellar medium of our galaxy, and on extragalactic gas clouds using distant quasars as illuminating sources, led to an award of Tenure in 1978 from Associated Universities, Inc. (AUI), the governing board of the NRAO.

ORGANIZATION CHART
FOR NRAO PROPOSED CONCEPT INVESTIGATION:
HIGH RESOLUTION IMAGING SPECTROSCOPY
AT TERAHERTZ FREQUENCIES (HISAT)
1 November 1988

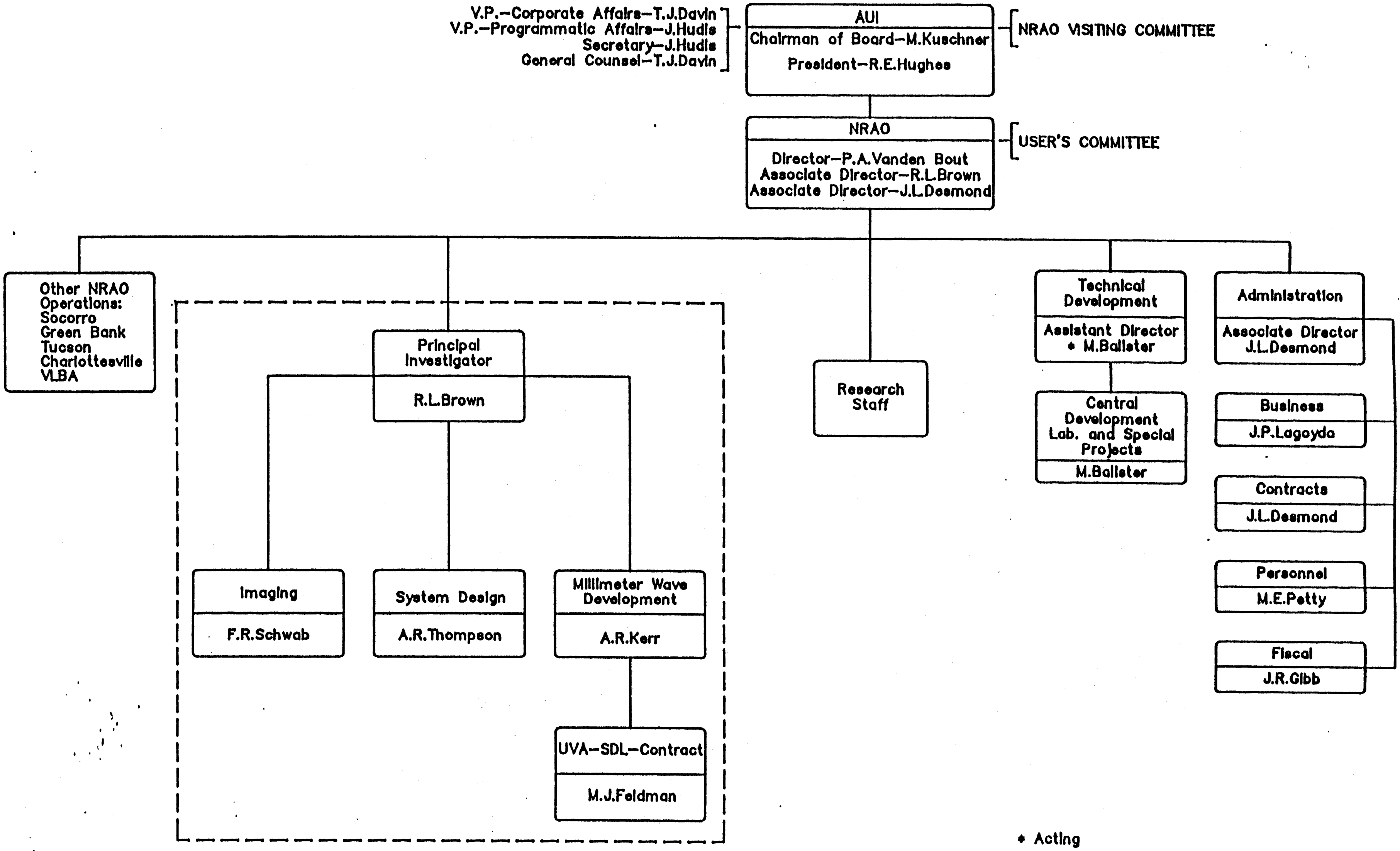

Figure 1

Dr. Brown has been involved with the management of the NRAO since 1979. He served as Assistant Director for Green Bank Operations from 1979-1982; Assistant Director for Tucson Operations, 1984-1985; and in 1985 was appointed to his present position as Associate Director for NRAO Operations.

Dr. Anthony R. Kerr (Millimeter-Wave Engineering): Anthony R. Kerr was born in England in 1941. He received the B.E., M.Eng.Sc., and Ph.D. degrees from the University of Melbourne, Australia, in 1964, 1967, and 1969, respectively.

In 1969, he joined the CSIRO to develop cryogenic parametric amplifiers for radio astronomy at X-band. From 1971 to 1974, he worked at the National Radio Astronomy Observatory, Charlottesville, VA, developing the first cryogenically-cooled Schottky-diode mixer receiver for millimeter-wavelength radio astronomy. Between 1974 and 1984, at the NASA/Goddard Institute for Space Studies, New York, he worked on the theory and design of Schottky, Josephson, and SIS mixers for millimeter-wave receivers. In 1984, he returned to the National Radio Astronomy Observatory, where he is responsible for development of new low-noise millimeter-wave receiver technology.

Dr. Kerr was co-recipient of the 1978 IEEE Microwave Prize, and received the 1983 NASA Exceptional Engineering Achievement Medal. In 1984 he was elected a Fellow of the Institute of Electrical and Electronics Engineers for "Contributions to Millimeter-Wave Receivers". He is a member of URSI Commission J and the Astronomical Society of Australia.

Dr. A. Richard Thompson: A. Richard Thompson was born in Hull, Yorkshire, England, on April 7, 1931. He received the B.Sc. degree with honors in physics from the University of Manchester, England. From 1952 to 1956 he was engaged in graduate studies in radio astronomy at Jodrell Bank Experimental Station of the University of Manchester and in 1956 received the Ph.D. degree.

From 1956 to 1957 he worked with E.M.I. Electronics Limited, Feltham, Middlesex, on missile guidance and telemetry problems. He joined the staff of Harvard University, Cambridge, MA, and held the position of Research Associate until 1961 and Research Fellow from 1961 to 1962. During this period he worked in the field of solar radio astronomy at the Fort Davis, TX, Radio Astronomy Station of Harvard College Observatory. In 1962 he joined Stanford University as a Radio Astronomer and held the position of Senior Research Associate from 1970 to 1972. During this period, from 1966 to 1972, he also held a visiting appointment at the Owens Valley Radio Observatory of the California Institute of Technology. In 1973 he joined the National Radio Astronomy Observatory, Socorro, NM, where he served as Deputy Manager of the VLA program during the initial construction period, and is currently Deputy Manager and Head of Electronics for the Very Long Baseline Array Program.

Dr. Thompson has served as Chairman of the Radio Astronomy Subcommittee of the Committee on Radio Frequencies (CORF) of the National Academy of Sciences, and Secretary of the Inter-Union Commission on Frequency

Allocations for Radio Astronomy and Space Science (IUCAF). He is currently subgroup Chairman for Radio Astronomy in U.S. Study Group II of the International Radio Consultative Committee (CCIR), and a member of CORF. He is also a member of U.S. Commission J of the International Union of Radio Science (URSI), Commission 40 of the International Astronomical Union, the American Astronomical Society, and a Senior member of the Institute of Electronics and Electrical Engineers.

Mr. Frederic R. Schwab: B.S. Mathematics, MIT, 1970. At the Arecibo Observatory (1971-1973) he was involved with both astronomy and ionospheric research groups and worked on ionospheric modification experiments. He joined the Computer Division at the NRAO in 1974 and was instrumental in developing image processing algorithms for radio interferometry; he participated in writing the data calibration and image processing software for the Astronomical Image Processing System (AIPS). In conjunction with astronomers at CalTech and Cambridge, he developed the "self-calibration" algorithm for use with connected element and VLBI radio interferometers. Mr. Schwab and W. D. Cotton devised the "global fringe search" algorithm used in Very Long Baseline Interferometry.

For nearly 15 years he has had responsibility for development and maintenance of the mathematical utility and applications software at the NRAO. Currently he is working on the site and configuration design for the National Millimeter-Wave Array telescope.

1.3. Prior Management Experience

NRAO has over 30 years experience in building radio astronomy instrumentation for its centimeter and millimeter-wave telescopes. The organization built and now operates the VLA telescope (76 M$) in New Mexico and is currently halfway through the construction of the VLBA telescope (83 M$). Both of these projects involved in-house electronic equipment development and construction, plus large subcontracts with industry.

In May 1985, the NSF and NASA entered into a Memorandum of Agreement (MOA) whereby the NRAO would develop, assemble, and install certain electronic equipment on the VLA antennas and then operate the VLA in conjunction with NASA's Voyager 2 Neptune mission. This work is now almost completed, and operational requirements to utilize the array will commence in April 1989 and terminate in October 1989. Funding for the Voyager 2 program is provided to NRAO through an interagency transfer between NASA and NSF for inclusion in AUI's contract with the Foundation.

NRAO constructed and for 20 years has operated a millimeter-wave radio telescope, the 12-m in Tucson, Arizona. Much experience has been gained in developing low-noise receivers and spectrometers for this telescope. The millimeter-wave development group in Charlottesville has performed much of the pioneering work in millimeter-wave mixer and frequency multiplier development and has an international reputation in this area.

1.4. Instrument Acquisition

This is a concept investigation for an instrument that will be built using existing technology except for the low-noise receivers which are not currently available. Thus the proposal emphasizes research, development, and fabrication of superconducting-insulating-superconducting (SIS) mixers for 500-800 GHz which meet the scientific requirements. During the early phase of the investigation, we will decide which type of SIS mixer is most suitable for these frequencies and later work will concentrate on the approach adopted.

1.5. Schedule

Figure 2 shows the schedule for the three-year concept investigation.

1.6. Subcontracts

A single subcontract with the Semiconductor Device Laboratory (SDL) of the University of Virginia is proposed. This group is led by Prof. Robert J. Mattauch and has been at the forefront of device development for millimeter- and submillimeter-wave mixers for the last 20 years. They have a worldwide reputation: Virtually all submillimeter astronomical observations world-wide done with heterodyne mixers have used Schottky diodes fabricated in Prof. Mattauch's laboratory. The collaboration between this group and Dr. Anthony R. Kerr's microwave group at the NRAO has extended over a similar length of time and has been very fruitful.

For these reasons and others such as proximity to the NRAO CDL and the ability to share resources, we feel that the SDL group at UVA is the only serious contender for the low-noise receiver development program needed for HISAT.

SCHEDULE FOR HISAT STUDY

FIGURE 2

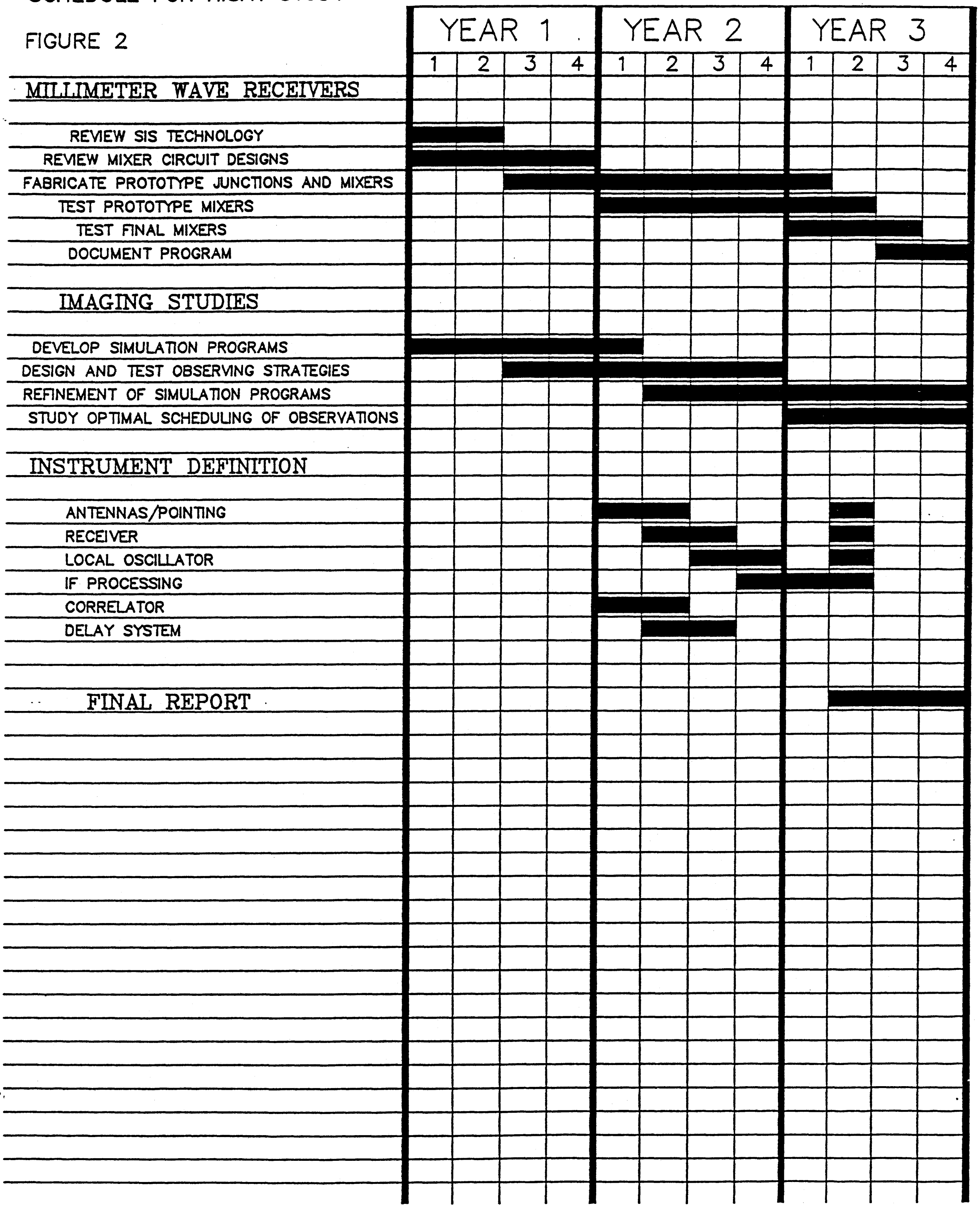

2. Facilities and Equipment

All major facilities and equipment for the concept investigation exist within NRAO or the SDL at UVA (the proposed subcontractor) and are available to the HISAT program at no direct cost. The cost plan includes spending a total of $50k on specialized test equipment that will be necessary to conduct the SIS mixer studies.

3. Data Analysis Facilities

The simulation of HISAT observations will be done using the NRAO Astronomical Image Processing System (AIPS) software. Modifications to this software for HISAT applications will be made in consultation with the AIPS programming staff and much of the work will be carried out on NRAO computing hardware. No direct charge is made for either staff support or computing time.

4. Cost Plan

The total cost of this program is $1,241,826 in 1988 $.

The following notes apply to the cost plan (Figure 4.1):

1) A 6% annual salary increase is applied to years 2 and 3. Fringe covers employee benefits and has been assumed to be 27.5% for all three years.

2) Materials and Supplies - covers expendable materials used in fabricating mixers, may also include electronic components.

3) Travel - covers cost of trips to administer the proposal and to meet with prospective vendors.

4) Subcontracts - see Appendix C for proposal.

5) Special Equipment - covers millimeter sources and test equipment.

7) Indirect Costs - 131.6% of direct labor. This is the current rate and is reviewed every year.

FIGURE 4.1 COST PLAN FOR HISAT CONCEPT INVESTIGATION

	% effort	Year 1	% effort	Year 2	% effort	Year 3
1. Salaries:						
Principal Investigator		*		*		*
Imaging Analyst	25	12,500	25	13,250	25	14,045
System Engineer	10	6,000	20	12,720	20	13,483
MM-wave Design Engineer	25	15,000	10	6,360	10	6,742
MM-wave Jr. Engineer	25	10,000	50	21,200	50	22,472
Assembly Technician			25	6,625	25	7,023
Machinist			10	3,180	10	3,371
Total Direct Labor		31,000		50,085		53,090
Fringe at 27.5% (all years)		8,525		13,773		14,600
Total Salaries and Fringe		39,525		63,858		67,690
2. Material and Supplies		20,000		20,000		20,000
3. Travel		5,000		5,000		5,000
4. Major Subcontracts						
UVA Semiconducter Device Lab.		261,816		272,858		284,504
5. Special Equipment		25,000		25,000		
Total Direct Costs		326,341		361,716		377,194
7. Indirect Costs						
131.6% of direct labor(all years)		40,796		65,912		69,867
TOTAL ESTIMATED COST		367,137		427,628		447,060
TOTAL ALL YEARS						1,241,82[illegible]

* No direct charge to project

APPENDIX A

A.1. Key Personnel and Investigator Publications

A.1.1. Publications of Dr. Robert L. Brown

1. "Simultaneous Photoionization and Photoexcitation in Helium," Phys. Rev., 1, 341, 1970.

2. "Double Photoionization of Helium," Phys. Rev., 1, 586, 1970.

3. "Interstellar Absorption of Cosmic X-rays," Phys. Rev. D., 2252, 1970 (with R. J. Gould).

4. "Theoretical Continuous Spectra of Gaseous Nebulae," Ap. J., 160, 939, 1970 (with W. G. Mathews).

5. "Production of the Diffuse Background X-ray Flux at 44 Å by Superthemal Proton Bremsstrahlung," Ap. J. (Lett.), 159, L187, 1970.

6. "Photoionization of Molecular Hydrogen at X-ray Energies," J. Chem. Phys., 52, 4177, 1970.

7. "On the Photoionization of Hydrogen and Helium," Ap. J., 164, 387, 1971.

8. "On the Origin of the Diffuse Gamma Ray Background," Lettere al Nuova Cimento, Serie I, 4, 941, 1970.

9. "The 1/4 KEV X-ray Background: A Reply," Nature Phys. Sci., 229, 85, 1971.

10. "Near the Resonant Charge Transfer at Thermal Energies," Astrophys. & Space Science, 16, 274, 1972.

11. "On the Ultraviolet Absorption Line Spectra Produced by HI Regions," Ap. J., 163, 495, 1971 (with Joseph Silk).

12. "First Epoch Radio Observations of Supernova 1970g," Ap.J., 174, 383, 1972, (with S. Gottesman, J. Broderick, B. Balick and P. Palmer).

13. "Ionization Equilibria of Calcium and Sodium in Interstellar Clouds," Ap. J., 173, 593, 1972.

14. "The Charge Transfer Reaction $C^{+2} + He \rightarrow He^{+}C^{+}$ and its Application to the Interstellar Medium," Ap. J., 174, 511, 1972.

15. "The Latitude Extent of Diffuse Ionization in the Galaxy," Ap. J., 178, 119, 1972 (with M. A. Gordon and S. T. Gottesman).

16. "Chemical Composition of the Interstellar Gas: X-ray Determinations," Astrophys. & Space Science, 18, 329, 1972.

17. "Evidence for a Third Thermally Stable Phase of the Interstellar Gas," Ap. J., 182, 755, 1973 (with Riccardo Giovanelli).

18. "The Dependence of Compton X-ray Emission from Clusters of Galaxies on the Velocity Dispersion of the Cluster," Ap. J., 180, L49, 1973.

19. "The Ionization of Dark Clouds: Implications from Searches for Radio Recombination Lines," Ap. J., 184, 693, 1973.

20. "Observations of Intense 100-Micron Objects at 3.5 Millimeter Wavelength," Ap. J., 181, 125, 1973 (with John J. Broderick).

21. "21-Centimeter Absorption at $z = 0.692$ in the Quasar 3C 286," Ap. J., 184, L7, 1973 (with M. S. Roberts).

22. "Observations of the Recombination Line Region Toward Sagittarius A," Ap. J., 185, 843, 1973 (with Bruce Balick).

23. "The He^+/H^+ Ratio in Dark Clouds," Ap. J., 188, 475, 1974 (with Gomez Gonzalez).

24. "A Green's Function Approach to Inverse Compton Scattering," Phys. Rev. D., 8, 4286, 1974 (with Patrick S. Yeung).

25. "Detection of Radio Recombination Line Emission from the RHO Ophicuchi Dark Cloud," Ap. J., 189, 253, 1974 (with G. R. Knapp).

26. "Compact Radio Structure in the HII Region G351.6-1.3," Ap. J., 192, 343, 1974 (with J. J. Broderick).

27. "The Nature and Distribution of Carbon Recombination Line Emission in the ρ Oph Dark Cloud," Ap. J., 192, 607, 1974 (with R. H. Gammon, G. R. Knapp and Bruce Balick).

28. "Intense Sub-Arcsecond Structure in the Galactic Center," Ap. J., 194, 265, 1974 (with Bruce Balick).

29. "Galactic Nonthermal Continuum Emission," 1974, in Galactic and Extragalactic Radio Astronomy, ed. Verschuur and Kellermann (Springer-Verlag), p. 1.

30. "Some Problems with the Radio Source Cyg X-3," Ap. J., 194, L13, 1974 (with R. M. Hjellming and L. C. Blankenship).

31. "Radio Observations of the Infrared Source AFCRL 809-2992," Ap. J., 194, L9, 1974.

32. "Two New Recombination Line Results," 1974, IAU Symp. No. 60, (D. Reidel), p. 76 (with F. J. Kerr, P. D. Jackson and G. R. Knapp).

33. "Radio Recombination Line Observations of the CII Region NGC 2023," Ap. J., 196, 167, 1975 (with G. R. Knapp and T.B.H. Kuiper).

34. "The Transfer of Radio Recombination Line Radiation Through a Cold Gas I: Hydrogen and Helium Lines in HII Regions," Ap. J., 200, 598, 1975.

35. "Observations of Carbon Recombination Line Emission in the Reflection Nebula M87," Ap. J., 195, L23, 1975 (with G. R. Knapp, T.B.H. Kuiper and E.N.R. Kuiper).

36. "The Radio Recombination Line Spectrum of Orion A: Observation and Analysis," Ap. J., 201, 134 (with Felix J. Lockman).

37. "An Interpretation of the Radio Outbursts of Cygnus X-3," Ap. J., 200, 719, 1975 (with Alan P. Marscher).

38. "Recombination Line Observations of a Normal Helium Abundance in the Galactic Center HII Region Sgr B2," Ap. J., 200, L155, 1975 (with Felix J. Lockman).

39. "Fine Structure in HII Regions: III. A Search for Sub-Arcsecond Structure," P.A.S.P., 88, 156, 1976.

40. "Intense Sub-arcsecond Structure in the Galactic Center," in HII Regions and the Galactic Center, Proc. of Eighth ESLBA Symp., 1975, ed. A.F.M. Moorwood, p. 261 (with B. Balick).

41. "Compact HII Regions in the Ophiuchus and R Coronae Austrinae Dark Clouds," Ap. J., 202, L125, 1975.

42. "OH and H_2O Masers in the Monoceros-R2 Molecular Cloud," Ap. J., 204, 21, 1976 (with G. R. Knapp).

43. "CO Observations of the Expanding Envelope of IRC+10216," Ap. J., 204, 781, 1976 (with T.B.H. Kuiper, G. R. Knapp and S. L. Knapp).

44. "On the Derivation of Nebular Electron Temperatures from Radio Recombination Line Observations," Ap. J., 207, 436, 1976 (with Felix J. Lockman).

45. "Carbon Recombination Line Observations of the Sharpless 140 Region," Ap. J., 204, 781, 1976 (with G. R. Knapp, T.B.H. Kuiper and R. K. Kakar).

46. "CO Observations of NGC 1579 (S222) and S239," Ap. J., 206, 443, 1976 (with G. R. Knapp and T. Kuiper).

47. "Observations of Heavy Element Recombination Lines in the Rho Ophiuchi Dark Cloud at 13 cm," Ap. J., 206, 109, 1976 (with G. R. Knapp and T.B.H. Kuiper).

48. "Further Joint X-Ray, Infrared and Radio Observations of Cygnus X-3," Ap. J., 207, 78, 1976 (with K. O. Mason, E. E. Becklin, L. Blankenship, J. Elias, R. M. Hjellming, K. Mathews, P. A. Murdin, G. Neugebauer, P. W. Sanford and S. Willner).

49. "Radio Telescopes," in McGraw-Hill Encyclopedia of Science and Technology, 1976 edition.

50. "Radio Astronomy," in McGraw-Hill Encyclopedia of Science and Technology, 1976 edition.

51. Detection of Z 0.5 of a 21-cm Absorption Line in AO 0235+164: The First Coincidence of Large Radio and Optical Redshift," A. J., 81, 293, 1976 (with M. S. Roberts, W. D. Brundage, A. H. Rots, M. P. Haynes and A. M. Wolfe.

52. "Limits on the Variation of Fundamental Atomic Quantities over cosmic Time Scales," Phys. Rev. Letters, 37, 179, 1976 (with A. M. Wolfe and M. S. Roberts).

53. "The Structure of the Radio Emission from the NGC 1579/LkH⟩101 Region," M.N.R.A.S., 175, 87p, 1976 (with J. J. Broderick and G. R. Knapp).

54. "Energetic Secondary Electrons in Dense Interstellar Clouds," Ap. J., 212, 659, 1977.

55. "CO Observations of Galactic Reflection Nebulae," Ap. J., 214, 78, 1977 (with G. R. Knapp, T.B.H. Kuiper and S. L. Knapp).

56. "On the Nature of Radio Sources near Flare Stars," Ap. J., 217, 716, 1977 (with W. S. Gilmore and B. Zuckerman).

57. "On the Interpretation of Carbon Monoxide Self-Absorption Profiles Seen Toward Embedded Stars in Dense Interstellar Clouds," Ap. J., 214, L73, 1977 (with Chun Ming Leung).

58. "The Analysis of Radio Emission from HII Regions: Consequences of Improper Analytical Methods," Ap. J., 222, 153, 1978 (with F. J. Lockman).

59. "Energetic Secondary Electrons and the Non-Thermal Galactic Radio Background: A Probe of the Magnetic Field in Interstellar Clouds," 1978 (with Alan H. Marscher).

60. "Origin and Evolution of the Radio Emission from Immediate Post-Outburst Supernovae," Ap. J., 220, 474, 1978 (with A. P. Marscher).

61. "Are Supernovae Radio Sources? A Search for Radio Emission from Young Supernova Remnants," Ap. J., 220, 467, 1978 (with A. P. Marscher).

62. "A Search for Atomic Hydrogen in Clusters of Galaxies," Ap. J., 221, 414, 1978 (with M. P. Haynes and M. S. Roberts).

63. "Energetic Secondary Electrons and the Non-thermal Galactic Radio Background: A Probe of the Magnetic Field in Interstellar Clouds," Ap. J., 221, 588, 1978 (with Alan P. Marscher).

64. "The Radio Spectrum of the Compact Source at the Galactic Center," Astron. J., 83, 1594, 1978 (with K. Y. Lo and K. J. Johnston).

65. "Radio Recombination Lines," 1978, Annual Review of Astronomy and Astrophysics, vol. 16, p. 445 (with Felix J. Lockman and G. R. Knapp).

66. "On the Rapidly Variable Circular Polarization of HR 1099 at Radio Frequencies," Astron. J., 83, 2504, 1978 (with P. C. Crane).

67. "Type I OH Masers: A Study of Positions, Polarization, Nearby Water Masers, Radio Continuum and Infrared Properties," Ap. J., 227, 450, 1979 (with N. J. Evans II, S. Beckwith, and W. Gilmore).

68. "21-Centimeter Absorption at z = 0.395 in the Quasar 1229-021," Ap. J., 230, L1, 1979 (with R. E. Spencer).

69. "Carbon Radio Recombination Line Emission from Dark Clouds," Radio Recombination Lines, 127, 1980.

70. "The Importance of Non-LTE Effects to the Interpretation of Radio Recombination Lines," Radio Recombination Lines, 51, 1980.

71. "Search for Radio Emission from the Young Supernova Remnants in NGC 6946," Nature, 285, 151, 1980.

72. "On the Ionized Regions Associated with Tauri Stars," Astron. J., 84, 1709, 1980 (with S. P. Maran, R. W. Hobbs, M. Jura and G. R. Knapp).

73. "A Confusion-Limited Extragalactic Source Survey at 4.755 GHz. I. Source List and Areal Distributions," Astron. J., 85, 780, 1980 (with J. E. Ledden, J. J. Broderick and J. J. Condon).

74. "Analysis and Interpretation of HI Self-Absorption Lines. I." Ap. J., 242, 416, 1980 (with Frank H. Levinson).

75. "Structure of the Compact Nuclear Radio Source in M82," Ap. J., 241, 561, 1980 (with Susan Neff).

76. "Quasi-Simultaneous Observations of the BL Lac Object MK 501 in X-ray, UV, Visible, IR and Radio Frequencies," Ap. J., 243, 690, 1981 (with Y. Kondo, D. M. Worrall, R. F. Mushotzky, R. L. Hackney, K.R.H. Hackney, J. B. Oke, H.K.C. Yee, G. Neugebauer, K. Matthews, P. A. Feldman).

77. "Isocyanic Acid in the Taurus Molecular Cloud 1," Ap. J., 248, L119, 1981.

78. "High Resolution VLA Observations of the Galactic Center," Ap. J., 250, 155, 1981 (with K. J. Johnston and K. Y. Lo).

79. "A Survey of Ionized Helium in Galactic HII Regions," Ap. J., 259, 595, 1982 (with F. J. Lockman).

80. "The Variable Radio Structure of 3C 446," Ap. Letters, 21, 105, 1981 (with K. Johnston, F. Briggs, R. C. Walker, S. Neff and A. Wolfe).

81. "Galactic Non-Thermal Radiation," in The Phases of the Interstellar Medium, ed. J. M. Dickey (Proc. of an NRAO Green Bank Workshop), p. 163.

82. "Variability of the Compact Radio Source at the Galactic Center," Ap. J., 253, 108, 1982 (with K. Y. Lo).

83. "Precessing Jets in Sgr A: Gas Dynamics in the Central Parsec of the Galaxy," Ap. J., 262, 110, 1982.

84. "Radio Observations of the Galactic Center: Future Directions 1982, in The Galactic Center, ed. G. R. Riegler and R. D. Blandford (New York: AIP), p. 204.

85. "The Gas Density and Distribution within 2 pc of the Galactic Center," Ap. J., 268, L85, 1983 (with K. J. Johnston).

86. "Radio Recombination Lines from Quasars I. Level Populations of Hydrogenic Ions in a Strong, Nonthermal Radiation Field," Ap. J. Suppl., 53, 351, 1983 (with E. James Wadiak and Craig L. Sarazin).

87. "Discovery of an X-ray Bright BL Lacertae Object: 0414+009," Ap. J., 270, L1, 1983 (with M. P. Ulmer, D. A. Schwartz, J. Patteson and R. G. Cruddace).

88. "Neutral Hydrogen Absorption in the Double Galaxy UGC 6081," Astron. J., 88, 1749, 1983 (with B. A. Williams).

89. "21 cm HI Absorption at $z = 0.437$ Against the Extended Radio Structure of 3C 196," Ap. J., 264, 87, 1983 (with Kenneth J. Mitchell).

90. "The Relation Between Magnetic Field and Gas Density in Interstellar Clouds," Ap. J., 264, 134, 1983 (with Chong-An Chang).

91. "Cosmic Rays and Magnetic Fields in the Galaxy," in Kinematics, Dynamics, and Structure of the Milky Way, ed. W. L. Shuter (Dordrecht: Reidel), p. 197, 1983.

92. "A VLBI Survey of Interstellar Broadening of Extragalactic Radio Sources Seen at Low Galactic Latitudes," Astron. Astrophys., 135, 199, 1984 (with Brian Dennison, M. Thomas, R. S. Booth, J. J. Broderick and J. J. Condon).

93. "Large Scale Emission in Radio Quasars: Confined Radio Lobes Excited by Fast Jets," Astron. J., 89, 195, 1984 (with S. G. Neff).

94. "Sagittarius A and Its Environment," Ann. Rev. Astron. and Astrophys., 22, 223, 1984 (with H. S. Liszt).

95. "Star Formation in the Inner Galaxy: A Far Infrared and Radio Study of Two HII Regions," <u>Ap. J.</u>, 1985 (with D. F. Lester, H. L. Dinerstein, M. W. Werner, P. M. Harvey and N. J. Evans II).

96. "An Attempt to Detect Mass Loss from ⟩Lyrae with the VLA," <u>Ap. J.</u>, 294, 646, 1985 (with J. M. Hollis and G. Chin).

97. "Confirming Hot Spots in 3C 196: Implications for QSO-Companion Galaxies," <u>Ap. J.</u>, 306, 107, 1986 (with J. Broderick and K. Mitchell).

98. "Radio Observations of HII Regions in <u>Spectroscopy of Astrophysical Plasmas</u>, ed. A. Dalgarno and D. Layzer (Cambridge University Press, 1987), 35-58.

99. "Galactic Non-thermal Continuum Emission," in <u>Galactic and Extragalactic Radio Astronomy</u>, 2nd edition, ed. K. Kellermann and G. Verschuur (Springer-Verlag), 1987.

100. "The Size of the $z = 0.437$ HI Absorption Cloud Toward the QSO 3C 196," 1987 (with J. J. Broderick, K. J. Johnston, J. M. Benson, K. J. Mitchell, and W. B. Waltman), accepted for <u>Ap. J.</u>, June 1988.

<u>Technical Reports</u>

101. "High Frquency Performance of the 140-foot Telescope I: Observations at 10650 MHz" (Engineering Memo. 132).

102. "High Frequency Performance of the 140-foot Telescope II. Observations at 22235 MHz (Engineering Memo. 133).

103. "K-Band Performance of the 140-foot Telescope" (Engineering Memo 138).

104. "A First Look at the Model IV Autocorrelator and the X-Band Maser/Upconverter Receiver."

A.1.2. <u>Publications of Dr. Anthony R. Kerr</u>

1. "On Two-Idler Parametric Amplifiers," <u>IEEE Trans. Microwave Theory Tech</u>., vol. MTT-17, no. 1, p. 39, January 1969.

2. "A Comparison of One- and Two-Idler Parametric Amplifiers," <u>IEEE Trans. Microwave Theory Tech.</u>, vol. MTT-18, no. 5, May 1970.

3. "Stability of Parametric Networks," with P. H. Gerrand, Electronics Letters, vol. 7, no. 2, p. 40, 28 January 1971.

4. "A Cryogenic Receiver for 8.6-9.2 GHz," Radiophysics Laboratory Report No. RPL 185, Commonwealth Scientific and Industrial Research Organization, Sydney, Australia, September 1972.

5. "The Cyanoacetylene Cloud in Sagittarius B2," with R. X. McGee, L. M. Newton, R. A. Batchelor, Astrophysical Letters, vol. 13, pp. 25-32, 1973.

6. "8.8 GHz Radio Observations of 12 Suggested Supernova Remnants," with J. R. Dickel, D. K. Milne, J. G. Ables, Australian Journal of Physics, vol. 26, pp. 379-388, 1973.

7. "Cryogenic Cooling of Mixers for Millimeter and Centimeter Wavelengths," with S. Weinreb, IEEE Journal of Solid State Circuits, vol. SC-8, no. 1, pp. 58-63, February 1973.

8. "Room Temperature and Cryogenic Mixers for 80-120 GHz," Electronics Division Internal Report No. 145, National Radio Astronomy Observatory, Charlottesville, VA, July 1974.

9. "Schottky Diode Mixers for Millimeter-Wave Radio Astronomy Receivers," URSI/USNC Annual Meeting, Boulder, CO, October 1975, Invited Paper.

10. "Anomalous Noise in Schottky Diode Mixers at Millimeter Wavelengths," IEEE International Microwave Symposium Digest of Technical Papers, pp. 318-320, June 1975.

11. "A Technique for Determining the Local Oscillator Waveforms in a Microwave Mixer," IEEE Trans. Microwave Theory Tech., vol. MTT-23, no. 10, pp. 828-831, Oct. 1975.

12. "Low-Noise Room Temperature and Cryogenic Mixers for 80-120 GHz," IEEE Trans. Microwave Theory Tech., vol. MTT-23, no. 10, pp. 781-787, October 1975.

13. "The Microwave Limb Sounder Experiment: Observations of Stratospheric and Mesospheric H_2O," in "Inter-Hemispheric Survey of Minor Upper Atmospheric Constituents During October-November 1976," NASA Technical Memorandum TMX-73630, 1977.

14. "Microwave Aircraft Measurements of Stratospheric Molecules," with J. W. Waters, J. J. Gustincic, R. K. Kakar, R. J. Mattauch, H. K. Roscoe, and P. N. Swanson, International Conference of Stratospheric and Related Problems, Utah State Univ., September 1976; JPL Publication No. 77-12, p. 108-110, 1977.

15. "A New Mixer Design for 140-220 GHz," with R. J. Mattauch and J. Grange, IEEE Trans. on Microwave Theory and Tech., vol. MTT-25, no. 5, pp. 399-401, May 1977.

16. "Analysis of Noise in Room-Temperature Millimeter-Wave Mixers," with D. Held, 1977 IEEE International Microwave Symposium Digest of Technical Papers, pp. 483-486.

17. "A Quasi-Optical Mixer for 100 GHz," with P. Siegel and R. J. Mattauch, 1977 IEEE International Microwave Symposium Digest of Technical Papers, pp. 96-98.

18. "A Recyclable Josephson Junction Mixer at 115 GHz," with Y. Taur, presented at the URSI/USNC meeting, Boulder, CO, October 1977.

19. "Conversion-Loss and Noise of Microwave and Millimeter-Wave Mixers: II - Experiment," with D. Held, IEEE Trans. on Microwave Theory and Tech., vol. MTT-26, no. 2, pp. 55-61, February 1978.

20. "Conversion-Loss and Noise of Microwave and Millimeter-Wave Mixers: I - Theory," with D. Held, IEEE Trans. on Microwave Theory and Tech., vol. MTT-26, no. 2, pp. 49-55, February 1978.

21. "Microwave Measurements of Upper Atmospheric Gasses: H_2O, O_3, CO, CLO, N_2O," with Waters *et al.*, presented at the World Meteorological Organization Symposium on the Geophysical Aspects and Consequences of Changes in the Composition of the Stratosphere, Toronto, 26-30 June 1978.

22. "Contact Whiskers for Millimeter Wave Diodes," with J. A. Grange and J. A. Lichtenberger, NASA Technical Memorandum #79616, August 1978.

23. "Low-Noise Josephson Mixers at 115 GHz using Recyclable Point Contacts," with Y. Taur, Applied Phys. Lett., vol. 32, p. 775, June 1978.

24. "Progress on Millimeter-Wave Josephson Junctions," with Y. Taur, American Institute of Physics Conference Proceedings No. 44, on Future Trends in Superconductive Electronics, p. 254, 1978.

25. "Aircraft Search for Millimeter-Wavelength Emission by Stratospheric CO," with Waters *et al.*, J. Geophys. Research, vol. 84, no. 20, pp. 7034-7040, Nov. 1979.

26. "Shot Noise in Resistive-Diode Mixers, and the Attenuator Noise Model," IEEE Trans. on Microwave Theory and Tech., vol. MTT-27, no. 2, Feb. 1979.

27. "Transport of Majority and Minority Carriers in 2-m Diameter Pt-GaAs Schottky Barriers," with E. Y. Chen, *et al.*, IEEE Trans. Electron Devices, vol. ED-26, no. 3, pp. 214-219, March 1979.

28. "Noise and Conversion Loss Analysis of Two-Diode Subharmonically Pumped and Balanced Mixers," IEEE International Microwave Symposium Digest, pp. 17-19, May-June 1979.

29. "The Low-Noise 115-GHz Receiver on the Columbia-GISS Four-Foot Telescope," with H. Cong and R. J. Mattauch, IEEE Trans. Microwave Theory Tech., vol. MTT-27, no. 3, pp. 245-248, March 1979.

30. "Noise and Loss in Balanced and Subharmonically Pumped Mixers, Part 1: Theory," and "Noise and Loss in Balanced and Subharmonically Pumped Mixers, Part 2: Application," IEEE Trans. Microwave Theory Tech., vol. MTT-27, no. 12, pp. 938-950, December 1979.

31. "Observations of Interstellar H_2O Emission at 183 Ghz," with J. Waters *et al.*, Astrophys. J., vol. 235, pp. 57-62, Jan. 1980.

32. "Measurements of Upper Atmospheric H_2O Emission at 183 GHz," with J. W. Waters, J. J. Gustinic, P. N. Swanson, in Proceedings of International Workshop on Atmospheric Water Vapor, Vail CO, Sept. 1979, A. Deepak *et al.* editors, pp. 229-240, NY:Academic Press, 1980.

33. "A User-Oriented Computer Program for the Analysis of Microwave Mixers, and a Study of the Effects of the Series Inductance and Diode Capacitance on the Performance of Some Simple Mixers," with P. H. Siegel, NASA Goddard Space Flight Center, Greenbelt, Md., NASA Tech. Memo. No. 80324, July 1979.

34. "Computer Analysis of Microwave and Millimeter-Wave Mixers," with P. H. Siegel, IEEE Trans. Microwave Theory Tech., vol. MTT-28, no. 3, pp. 275-276, March 1980.

35. "Low Cost, High Burnout Millimeter GaAs Schottky Barrier Flip-Chip Diodes," with Y. Anand *et al.* 1980, IEEE International Electron Devices Meeting, Digest of Technical Papers, p. 841, Dec. 1980.

36. "Infinite Available Gain in a 115 SIS Mixer," with S-K. Pan, M. J. Feldman, and A. Davidson, Physica, vol. 108 B, p. 1369, 1981.

37. "Millimeter-Wave Detectors with Improved Sensitivity and Dynamic Range Using Zero-Bias Low-Barrier Schottky Diodes," with Y. Anand, Microwave Journal, v. 24, no. 12, pp. 67-71, Dec. 1981, and v. 25, no. 1, p. 118, Jan. 1982.

38. "SIS Mixer Analysis Using a Scale Model", with M. J. Feldman, S-K. Pan, and A. Davidson, IEEE Trans. on Magnetics, vol. MAG-19, no. 3, pp. 494-497, May 1983.

39. "Design & Analysis of the Channel Waveguide Transformer," with P. H. Siegel and D. W. Peterson, IEEE Trans. Microwave Theory Tech., vol. MTT-31, no. 6, pp. 473-484, June 1983.

40. "The Channel Waveguide Transformer: an Easily Fabricated H-Plane Transition for the Rectangular TE-10 Mode," with P. H. Siegel and D. W. Peterson, IEEE International Microwave Symposium, Digest of Technical Papers, June 1983.

41. "Low-Noise 115-GHz Receiver Using Superconducting Tunnel Junctions," with S-K. Pan, M. J. Feldman, and P. Timbie, Appl. Phys. Lett., 15 Oct. 1983.

42. "Superconducting Tunnel Junction Receivers for 2.6 mm", with S.-K. Pan, M. J. Feldman, E. S. Palmer, J. A. Grange and P. Timbie, 8th International Conf. on Infrared and Millimeter Waves, Digest of Technical Papers, Dec. 1983.

43. "A Comparison of the Measured and Theoretical Performance of a 140-220 GHz Schottky Diode Mixer", with P. H. Siegel and R. J. Mattauch, IEEE International Microwave Symposium, Digest of Technical Papers, pp. 549-551, June 1984.

44. "The Measured and Computed Performance of a 140-220 GHz Schottky Diode Mixer," with P. H. Siegel, IEEE Trans. Microwave Theory Tech., vol. MTT-32, no. 12, pp. 1579-1590, December 1984.

45. "A General Analysis Program for the Superconducting Quasi-Particle Mixer," with R. G. Hicks and M. J. Feldman, NASA Goddard Space Flight Center, Greenbelt, MD, NASA Technical Memo TM 86145, July 1986.

46. "A Superconducting Tunnel Junction Receiver for Millimeter-Wave Radio Astronomy," with S.-K. Pan, NASA Goddard Space Flight Center, Greenbelt, MD, NASA Technical Memo TM 87792, July 1986.

47. "SIS Mixers at 115 GHz Using Nb/Al-Al_2O_3/Nb Junctions," with S.-K. Pan, M. J. Feldman, and J. W. Lamb, National Radio Astronomy Observatory, Charlottesville, VA, NRAO Electronics Division Internal Report No. 268, April 1987.

48. "SIS Mixer Design by Frequency Scaling, Including Saturation Effect," with M. J. Feldman and S.-K. Pan, National Radio Astronomy Observatory, Charlottesville, VA, NRAO Electronics Division Internal Report No. 267, April 1987.

49. "Saturation of the SIS Mixer," with M. J. Feldman and S.-K.Pan, International Superconductivity Electronics Conference, Tokyo, Digest of Technical Papers, pp. 290-292, Aug. 1987.

50. "Integrated Tuning Elements for SIS Mixers," with S.-K. Pan and M. J. Feldman, International Superconductivity Electronics Conference, Tokyo, Digest of Technical Papers, pp. 372-375, Aug. 1987.

51. "Integrated Tuning Elements for SIS Mixers," with S.-K. Pan and M. J. Feldman, Int. J. Infrared Millimeter Waves, vol. 9, no. 2, pp. 203-212, Feb. 1988.

52. "A 85-116 GHz SIS Mixer Using Inductively Shunted Edge-Junctions," with S.-K. Pan, M.J. Feldman, A. Kleinsasser, J. Stasiak, R.L. Sandstrom, and W.J. Gallagher, IEEE International Microwave Symposium, Digest of Technical Papers, pp. 465-468, June 1988.

53. "A 85-116 GHz SIS Receiver Using Inductively Shunted Edge-Junctions," with S.-K. Pan, M. J. Feldman, A. Kleinsasser, J. Stasiak, R. L. Sandstrom, and W.J. Gallagher, to appear in IEEE Trans. Microwave Theory Tech.

54. "Fabrication of Nb/Al-Al_2O_3/Nb Junctions With Extremely Low Leakage Currents," with A. W. Lichtenberger, C. P. McClay, R. J. Mattauch, M. J. Feldman, and S.-K. Pan, to appear in IEEE Trans. on Magnetics.

A.1.3. Publications of Dr. A. Richard Thompson

1. Hanbury Brown, R., Palmer, H. P., and Thompson, A. R. (1954), "Galactic Radio Sources of Large Angular Diameter," Nature (London), 173, 945-946.

2. Hanbury Brown, R., Palmer, H. P., and Thompson, A. R. (1955), "A Rotating-Lobe Interferometer and Its Application to Radio Astronomy," Phil. Mag., 46, 857-866.

3. Hanbury Brown, R., Palmer, H. P., and Thompson, A. R. (1955), "Polarization Measurements on Three Intense Radio Sources," Monthly Not. Roy. Astron. Soc. 115, 487-492.

4. Morris, D., Palmer, H. P., and Thompson, A. R. (1957), "Five Radio Sources of Small Angular Diameter," The Observatory, 77, 103-106.

5. Maxwell, A., Swarup, G., and Thompson, A. R. (1958), "The Radio Spectrum of Solar Activity," Proc. I.R.E., 46, 142-148; reprinted in The Radio Noise Spectrum, D. H. Menzel, Ed., Harvard Univ. Press, 1960, pp. 101-110.

6. Thompson, A. R. (1959), "The Correlation of Solar Radio Bursts With Magnetic Activity and Cosmic Rays," Paris Symposium on Radio Astronomy, R. N. Bracewell, Ed., Stanford University Press, pp. 210-213.

7. Thompson, A. R. (1959), "Solar Radio Astronomy at Fort Davis, Texas," I.G.Y. Bulletin, Nat. Acad. Sci., Wash., no. 29, pp. 16-18; also printed in Trans. Am. Geophys. Union, Suppl., 40, no. 4.

8. Maxwell, A. Thompson, A. R., and Garmire, G. (1959), "The Association of Solar Radio Bursts with Auroral Streams," Planet. Space Sci., 1, 325-332.

9. Thompson, A. R., and Maxwell, A. (1960), "Solar Radio Bursts and Low-Energy Cosmic Rays," Nature (London), 185, 89-90.

10. Thompson, A. R., and Maxwell, A. (1960), "Solar Radio Bursts and Cosmic Rays," Planet. Space Sci., 2, 104-109.

11. Thompson, A. R. (1961), "Spectral Observations of Solar Radio Bursts: I. Receiving Equipment," Astrophys. J., 133, 643-648.

12. Thompson, A. R. (1961), "Sweep Frequency Observations of Meteor Scatter Bursts," J. Atmos. Terrest. Phys., 22, 161-165.

13. Maxwell, A., and Thompson, A. R. (1962), "Spectral Observations of Solar Radio Bursts: II. Slow-Drift Bursts and Coronal Streamers," Astrophys. J., 135, 138-150.

14. Thompson, A. R. (1962), "Type IV (Continuum) Radio Bursts from the Sun," J. Phys. Soc. Japan, 17 Suppl. A-II (Proc. of International Conference on Cosmic Rays and the Earth Storm), 198-203.

15. Thompson, A. R., and Maxwell, A. (1962), "Spectral Observations of Solar Radio Bursts: III. Continuum Bursts," Astrophys. J., 136, 546-558.

16. Maxwell, A., Hughes, M. P., and Thompson, A. R. (1963), "Catalog of Type II (Slow-Drift) and Type IV (Continuum) Solar Radio Bursts," J. Geophys. Res., 68, 1347-1354.

17. Swarup, G., Thompson, A. R., and Bracewell, R. N. (1963), "The Structure of Cygnus A," Astrophys. J., 138, 305-309.

18. Thompson, A. R., and Krishnan, T. (1965), "Observations of the Six Most Intense Radio Sources with a 1.0′ Fan Beam," Astrophys. J., 141, 19-33.

19. Moffet, A. T., Schmidt, M., Slater, C. H., and Thompson, A. R. (1967), "The Radio Source 3C17," Astrophys. J., 148, 283-286.

20. Thompson, A. R., Colvin, R. S., and Stanley, G. J. (1967), "Measurements of the Flux Densities, Positions and Angular Widths of Planetary Nebulae at 10- and 21-cm Wavelengths," Astrophys. J., 148, 429-442.

21. Thompson, A. R., and Colvin, R. S. (1967), "Further Observations of Planetary Nebulae at 10 cm Wavelength, Including the Peculiar Nebula NGC 6302," Astrophys. J., 150, 345-348.

22. Thompson, A. R. (1967), "Optical Depths and Electron Temperatures of Two Planetary Nebulae Derived From Their Radio-Frequency Spectra," Astrophys. Letters, 1, 25-29.

23. Downs, G. S., and Thompson, A. R. (1968), "The Distribution of Polarization in the Crab Nebula at a Wavelength of 9.8 cm," Astrophys. J., 152, L65-L69.

24. Thompson, A. R. (1968), "Radio Measurements of Planetary Nebulae," I.A.U. Symposium No. 34, Planetary Nebulae, D. E. Osterbrock and C. R. O'Dell, Eds., D. Reidel, pp. 112-121.

25. Thompson, A. R. (1968), "Electron Temperatures in the Outer Regions of Planetary Nebulae," Astrophys. Letters, 2, 201-204.

26. Thompson, A. R., Riddle, A. C., and Lang, K. R. (1969), "Observations of the Occultation of Sagittarius A by the Moon," Astrophys. Letters, 3, 49-50.

27. Thompson, A. R., Colvin, R. S., and Hughes, M. P. (1969), "The 21-cm Absorption Profiles of DR 21 and the Source Near NGC 6857," Astrophys. J., 158, 939-951.

28. Thompson, A. R., and Colvin, R. S. (1970), "An Attempt to Detect Neutral Hydrogen in Planetary Nebulae," Astrophys. J., 160, 363-368.

29. Colvin, R. S., Hughes, M. P., Thompson, A. R., and Verschuur, G. L.(1970), "Galactic Hydrogen Absorbtion at 21-cm Wavelength in the Direction of Virgo A," Astrophys. Letters, 6, 211-214.

30. Bracewell, R. N., Colvin, R. S., Price, K. M., and Thompson, A. R. (1971), "Stanford's High-Resolution Radio Interferometer," Sky & Telescope, 42, 2-7.

31. Hughes, M. P., Thompson, A. R., and Colvin, R. S. (1971), "An Absorbtion-Line Study of the Galactic Neutral Hydrogen at 21 Centimeters Wavelength," Astrophys. J. Suppl., 23, 323-370.

32. Downs, G. S., and Thompson, A. R. (1972), "The Distribution of Linear Polarization in Cassiopeia-A at Wavelengths of 9.8 and 11.1 Cm," Astron. J., 77, 120-133.

33. Bracewell, R. N., and Thompson, A. R. (1973), "The Main Beam and Ring-Lobes of an East-West Rotation-Synthesis Array," Astrophys. J., 182, 77-94.

34. Thompson, A. R., and Bracewell, R. N. (1974), "Interpolation and Fourier Transformation of Fringe Visibilities," Astron. J., 79, 11-24.

35. Bracewell, R. N., Colvin, R. S., D'Addario, L. R., Grebenkemper, C. J., Price, K. M., and Thompson, A. R. (1973), "The Stanford Five-Element Radio Telescope," Proc. IEEE, 61, 1249-1257.

36. Thompson, A. R. (1974), "The Planetary Nebulae as Radio Sources," Vistas in Astronomy, vol. 16, A. Beer, Ed., Pergammon Press, pp. 309-328.

37. Granlund, J., Thompson, A. R., and Clark, B. G. (1978), "An Application of Walsh Functions in Radio Astronomy Instrumentation," IEEE Trans.Electromagn. Compat., EMC-20, 451-453.

38. Johnson, H. M., Balick, B., and Thompson, A. R. (1979), "VLA Observations of Stellar Planetary Nebulae," Astrophys. J., 233, 919-924.

39. Thompson, A. R. (1980), "The Effects of the Proposed Satellite Power System on the VLA," Workshop on Satellite Power Systems (SPS) Effects on Optical and Radio Astronomy, CONF-7905143, P. A. Ekstrom and G. M. Stokes, Eds., U.S. Dept. of Energy, Office of Energy Res., PS Proj. Div., Washington, D.C., pp. 135-142.

40. Thompson, A. R., and Sinha, R. P. (1980), "An Upper Limit to the Mass Loss Rate from the Nuclei of Planetary Nebulae," Astron. J., 85, 1240-1241.

41. Thompson, A. R. (1980), "The Effects of a Satellite Power System on Ground-Based Astronomy," Final Proceedings of the Solar Power Satellite Program Review, Conf-800491, U.S. Dept. of Energy, SPS Project Div., Washington, D.C., pp. 419-422.

42. Thompson, A. R., Clark, B. G., Wade, C. M., and Napier, P. J. (1980), "The Very Large Array," Astrophys. J. Suppl., 44, 151-167.

43. Thompson, A. R. (1981), "Effects of a Satellite Power System on Ground-Based Radio and Radar Astronomy," Radio Science, 16, 35-45.

44. Thompson, A. R. (1982), "The Response of a Radio-Astronomy Synthesis Array to Interfering Signals," IEEE Trans. Antennas Propagat., AP-30, 450-456.

45. Thompson, A. R., and D'Addario, L. R. (1982), "Frequency Response of a Synthesis Array: Performance Limitations and Design Tolerances," Radio Science, 17, 357-369.

46. Thompson, A. R. (1983), "Early Interferometry at Jodrell Bank," in Serendipitous Discoveries in Radio Astronomy, Proceedings of NRAO Workshop No. 7, Green Bank, May 4-6, 1983, K. I. Kellermann and B. Sheets, Eds., National Radio Astronomy Observatory, Green Bank, West Virginia, pp. 146-153.

47. Napier, P. J., Thompson, A. R., and Ekers, R. D. (1983), "The Very Large Array: Design and Performance of a Modern Synthesis Radio Telescope," Proc. IEEE, 71, 1295-1320.

48. D'Addario, L. R., Thompson, A. R., Schwab, F. R., and Granlund, J. (1984), "Complex Cross Correlators with Three-Level Quantization: Design Tolerances," Radio Science, 19, 931-945.

49. Layland, J. W., Napier, P. J., and Thompson, A. R. (1985), "A VLA Experiment - Planning for Voyager at Neptune," Telecommunications and Data Acquisition Progress Report 42-82, April-June 1985, Jet Propulsion Laboratory, Pasadena, California, pp. 136-142.

50. Kellermann, K. I., and Thompson, A. R. (1985), "The Very Long Baseline Array," Science, 229, 123-130.

51. Thompson, A. R. (1986), "The Interferometer in Practice," in Synthesis Imaging, Proceedings of NRAO Workshop No. 13, Socorro, New Mexico, Aug. 5-9, 1985, R. A. Perley, F. R. Schwab, and A. H. Bridle, Eds., National Radio Astronomy Observatory, Green Bank, West Virginia, pp. 9-30.

52. Kellermann, K. I., and Thompson, A. R. (1988), "The Very Long Baseline Array," Scientific American, 258, no. 1 (Jan.), 54-63.

53. "Synthesis Mapping", Proceedings of NRAO Workshop No. 5, Socorro, New Mexico, June 21-25, 1982, A. R. Thompson and L. R. D'Addario, Eds., National Radio Astronomy Observatory, Green Bank, West Virginia, 1982. (A. R. Thompson is also author of Lectures 1 and 5 in this volume.)

54. Thompson, A. R., Moran, J. M., and Swenson, G. W., Jr., Interferometry and Synthesis in Radio Astronomy, John Wiley and Sons, New York, 1986, (534 pages).

A.1.4. Publications of Mr. Frederic R. Schwab

1. A. Wootten and Fred Schwab, Eds., Science with a Millimeter Array: Proceedings of an NRAO Workshop Held at the National Radio Astronomy Observatory, Green Bank, West Virginia, September 30-October 1, 1985, NRAO, Green Bank, 1988.

2. R. A. Perley, F. R. Schwab, and A. H. Bridle, Eds., Synthesis Imaging: Course Notes from an NRAO Summer School Held in Socorro, New Mexico, August 5-9, 1985, NRAO, Green Bank, 1986; R. A. Sramek and Fred Schwab, "Imaging," Chapter V of this volume.

3. Fred Schwab, "Self-Calibration at Meter Wavelengths," in Low Frequency Radio Astronomy: Proceedings of a Workshop Held at the NRAO, Green Bank, West Virginia, on November 16-17, 1984, NRAO, Green Bank, 1986.

4. P. P. Kronberg, P. Biermann, and Fred Schwab, "The Nucleus of M82 at Radio and X-Ray Bands: Discovery of a New Radio Population of Supernova Candidates," Astrophys. J., 291 (1985) 693-707.

5. Fred Schwab, "Relaxing the Isoplanatism Assumption in Self-Calibration: Applications to Low-Frequency Radio Interferometry," Astron. J., 89 (1984) 1076-1081.

6. L. R. D'Addario, A. R. Thompson, Fred Schwab, and J. Granlund, "Complex Cross-Correlators with Three-Level Quantization: Design Tolerances," Radio Sci., 19 (1984) 931-945.

7. Fred Schwab, "Optimal Gridding of Visibility Data in Radio Interferometry," in Indirect Imaging, J. A. Roberts, Ed., Cambridge Univ. Pr., 1984, 333-346.

8. Fred Schwab and W. D. Cotton, "Global Fringe Search Techniques for VLBI," Astron. J., 88 (1983) 688-694.

9. P. P. Kronberg, P. Biermann, and Fred Schwab, "The Continuum Radio Structure of the Nucleus of M82," Astrophys. J., 246 (1981) 751-760.

10. Fred Schwab, "Adaptive Calibration of Radio Interferometer Data," in 1980 International Optical Computing Conference, W. T. Rhodes, Ed., Proc. Soc. Photo-Opt. Instrum. Eng., 231 (1980) 18-25.

APPENDIX B

A Brief Profile of the National Radio Astronomy Observatory

Since its founding in 1957, the National Radio Astronomy Observatory (NRAO) has been a major force in the development of radio astronomy. This field, pioneered in the United States, has blossomed to become a central element of modern astronomy throughout the world.

At the present time, the NRAO manages the operation of three major observing sites from its headquarters in Charlottesville, Virginia. The 300-foot diameter meridian transit telescope and the 140-foot diameter fully steerable telescope are both located at the original Green Bank, West Virginia site; the Very Large Array (VLA) telescope, a mobile array of twenty-seven 25-meter antennas, is located on the Plains of San Agustin near Socorro, New Mexico; and the 12-meter diameter millimeter-wave telescope is located on Kitt Peak near Tucson, Arizona. (Operation of the three-element Interferometer, also located in Green Bank, West Virginia, was discontinued for astronomical observing in 1978 when the VLA became operational; it is now operated by the NRAO exclusively for the U.S. Naval Observatory for purposes of time-keeping.) NRAO is constructing a new telescope, the Very Long Baseline Array (VLBA). The VLBA, like the VLA, is a synthesis telescope simulating an extremely large single antenna by a distribution of smaller antennas operating in concert. In the case of the VLBA, the ten individual antennas will be spaced from Hawaii to the Virgin Islands and controlled from an operations center in Socorro, New Mexico.

The NRAO is operated by Associated Universities, Inc. (AUI), an independent, not-for-profit research management corporation, under the terms of a contract between the National Science Foundation (NSF) and AUI. The following responsibilities for AUI are included in the Scope of Work of this contract:

- Staff, manage, operate, and maintain the facilities ... of [the] Observatory ...;

- Provide scientific, managerial, and logistic support in the conduct of research programs in radio astronomy and related fields. The research shall be carried out by the staff of the Observatory, and visiting scientific investigators. The scientific merit of research proposed by visiting scientific investigators and by the Observatory staff shall be given the same consideration. The major criteria for the utilization of Observatory facilities shall be the scientific merit of the proposal, the competence of the individual or individuals, and the suitability of the Observatory facilities.

- Maintain a broad base research program at the Observatory in order to promote advances in and the utilization of knowledge in astronomy.

- Provide facility and logistic support to university and NRAO research programs in radio astronomy and related fields.

- Engage in education programs in radio astronomy and related fields as may be appropriate to the operation of the Observatory and as is consistent with the Program Plan.

These contractual requirements have characterized the role of the NRAO since it was founded.

The concept of a national observatory was unique when it was proposed in 1954 -- NRAO was the first national astronomical observatory. There were some who doubted that an open, visitor-oriented, national facility could efficiently serve its user community and at the same time provide a research environment that would be conducive to competitive research. The fact that NRAO has established and maintained the world standard in radio instrumentation and user service, together with the remarkable flood of scientific results from its users, is ample justification for the wisdom of providing such facilities.

Users

The principal responsibility of the Observatory is to provide the astronomy community access to forefront research capabilities through the development of major national facilities.

Figure B-1 shows the annual growth in the user group over the history of the Observatory, from the modest beginnings, before the first major telescopes were built, to over 650 long and short-term visitors today. The largest increase in the number of visitor-users occurred as the VLA entered full operation in 1981. The use by Observatory staff, both permanent scientists and postdoctorals (Research Associates) can be seen to represent about 7% of all Observatory users.

The number of institutions using NRAO telescopes has also grown dramatically over the years, with a 50% increase attributable to the VLA. Universities represent 64% of the institutions, other observatories and government laboratories 33%, and private industries the remaining 3%. The overwhelming majority of these institutions lack the resources to design, build, maintain, and operate telescopes comparable to those at NRAO. Nevertheless, many of these institutions actually participate with NRAO in the design and fabrication of sub-elements of advanced systems. This includes not only individual university groups who bring their own observing equipment to NRAO telescopes but also working teams operating out of universities and government laboratories who assist in the design and, in some cases, actual construction of new instrumentation. Maintenance of such capabilities in these institutions is important to the future of NRAO as a national observatory.

Number of People Observing With NRAO Telescopes

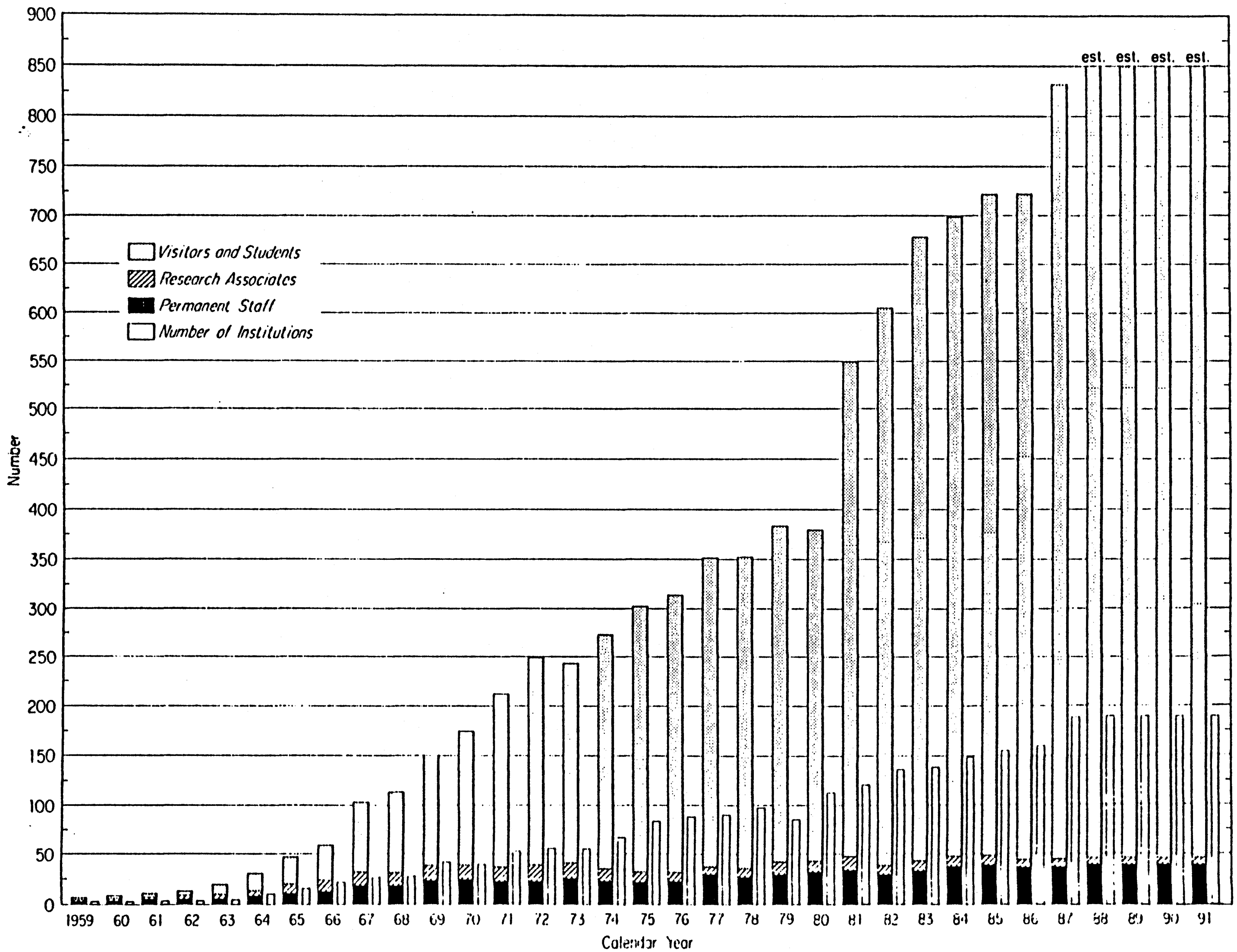

Figure B-1. This bar chart shows for each calendar year the number of NRAO permanent research staff and the number of NRAO research associates (postdoctorals) who use the telescopes. In addition, it shows the total number of visitor-users of NRAO telescopes and the number of institutions from which the NRAO visitors come. The significant jump in these last categories for 1981 reflects the increased use of the VLA.

It is also important to note that in keeping with a growing interdependence of all areas of astronomy, the NRAO user community is rapidly growing to accommodate new observers from the optical, infrared, X-ray, and related areas.

The NRAO Student Program is illustrated in Figure B-2. The vast majority of the student users are graduate students from universities having Ph.D. programs in astronomy. A large increase in graduate student users occurred when the VLA began operations. As with the other categories of users, this increase is due not only to the research opportunities the VLA presents but also to the operational convenience of this instrument which has been facilitated by the efforts of the Observatory staff.

The Summer Student and Co-op Programs are a much smaller component of student usage of NRAO facilities, but these are important in the national programs. Both serve to introduce senior undergraduate and beginning graduate students to radio astronomy. The Summer Student Program focuses on astronomical research; the Co-op Program is conducted with university groups of engineers, applied physicists, and computer scientists. Both are important mechanisms for acquainting skilled scientists with issues of importance to the field of radio astronomy.

The extent to which NRAO is dedicated to its user community can be seen by examining Figures B-3 and B-4. Approximately 35,000 observing hours exist in principle in one year for all four of NRAO's telescopes taken together (4x24x365). The actual hours scheduled for observing with these telescopes are shown in Figure B-3, where the recent totals are approximately 30,000, or 86%. The remaining 14% is scheduled for tests, calibration, preventative maintenance, installation of new equipment, and repairs.

The only periods when less than about 85% of the available time was scheduled for observing was in 1979-80 after the three-element Interferometer was closed and before the VLA began full operation, and in 1982-83 when the 36-foot millimeter-wave telescope was re-surfaced and re-christened as the 12-meter telescope. The telescopes, which operate 24 hours a day, are efficiently scheduled to produce as much observing as possible.

How is the observing time allocated to staff and visitor users? Different projects require differing amounts of time, but all grants of observing time are made on the basis of scientific merit. All proposals, from staff and visitors alike, are refereed and graded for merit by anonymous referees selected from the community. The detailed scheduling is done by the site directors, with the assistance of a special committee in the case of the VLA. The rule that Observatory staff compete for time on the same footing as visitors is fundamental and has contributed a great deal to the excellent relationship between the Observatory and its user community.

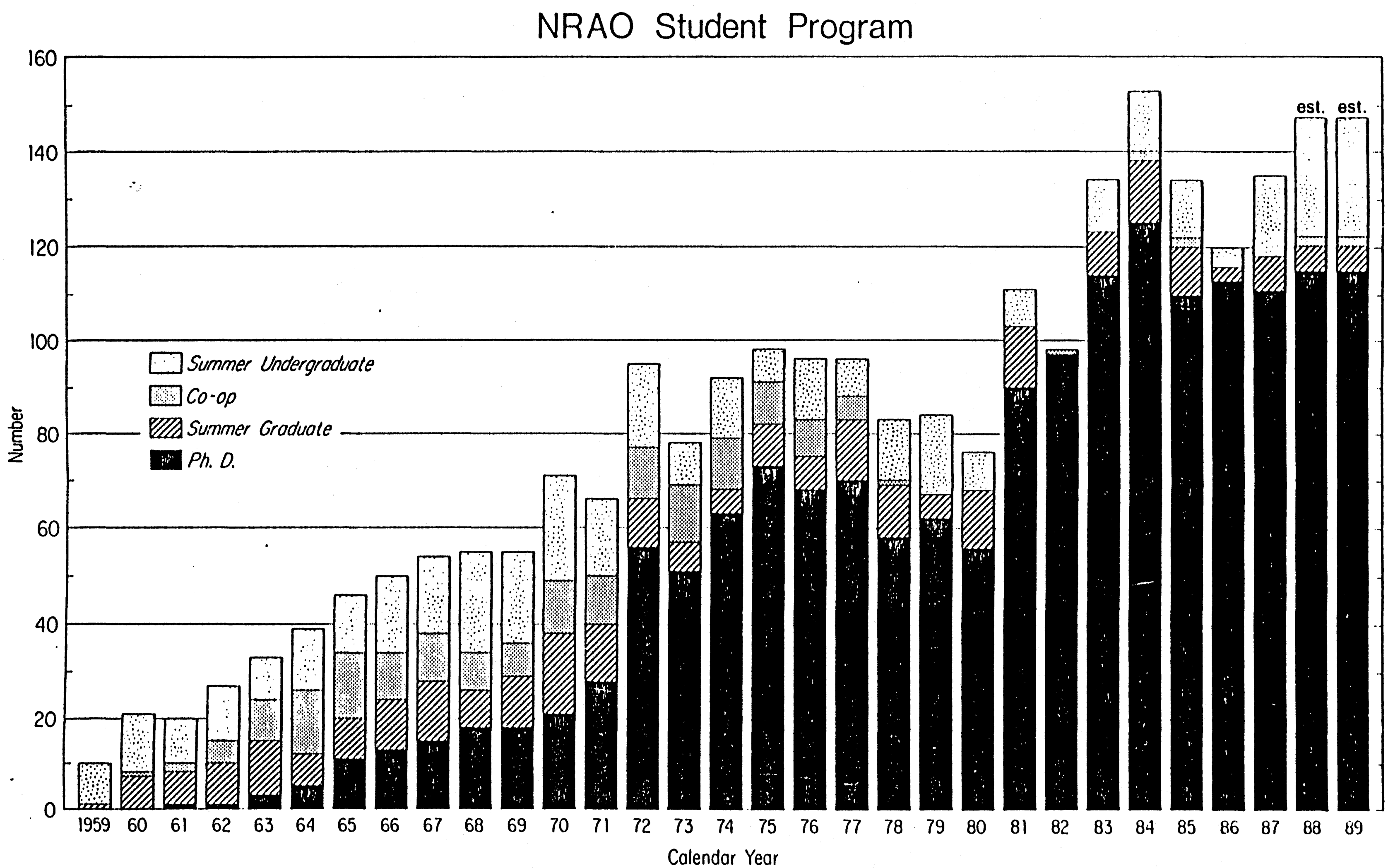

Figure B-2. This figure shows for each calendar year the number of Ph.D. students (including those few salaried at NRAO), NRAO co-op students, and NRAO summer students (undergraduate and graduate) who observed or worked at the NRAO during that year.

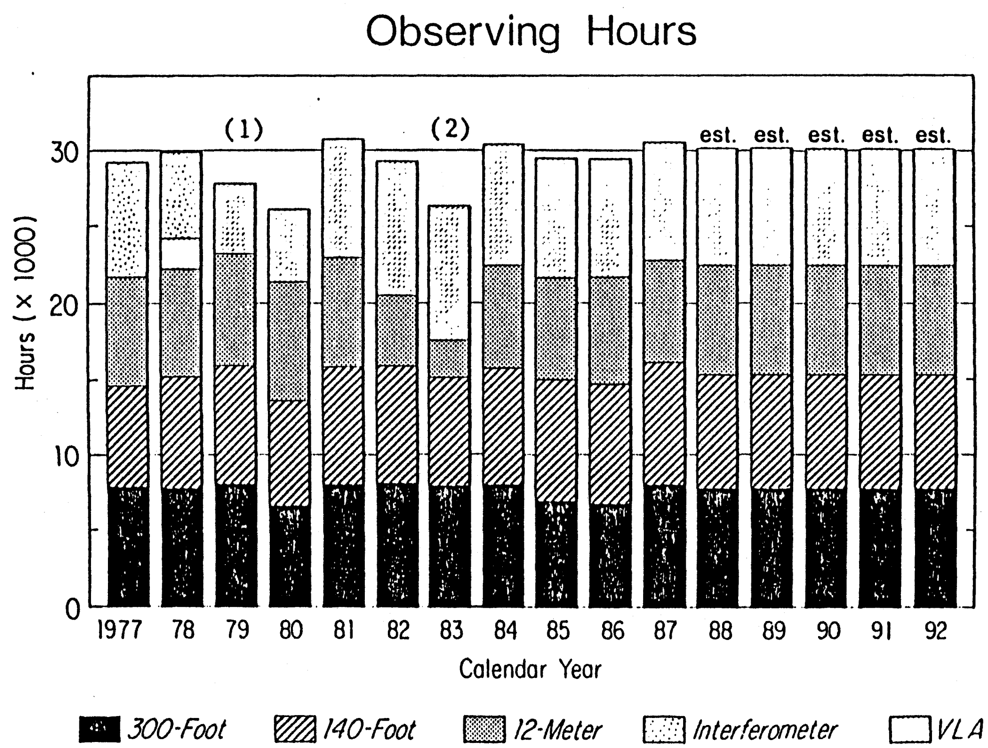

Figure B-3. Hours scheduled for observing on each telescope during the last decade.
(1) Shutdown of observing on 3-element Interferometer and commissioning of the VLA.
(2) Resurfacing of the 12-meter millimeter wave telescope.

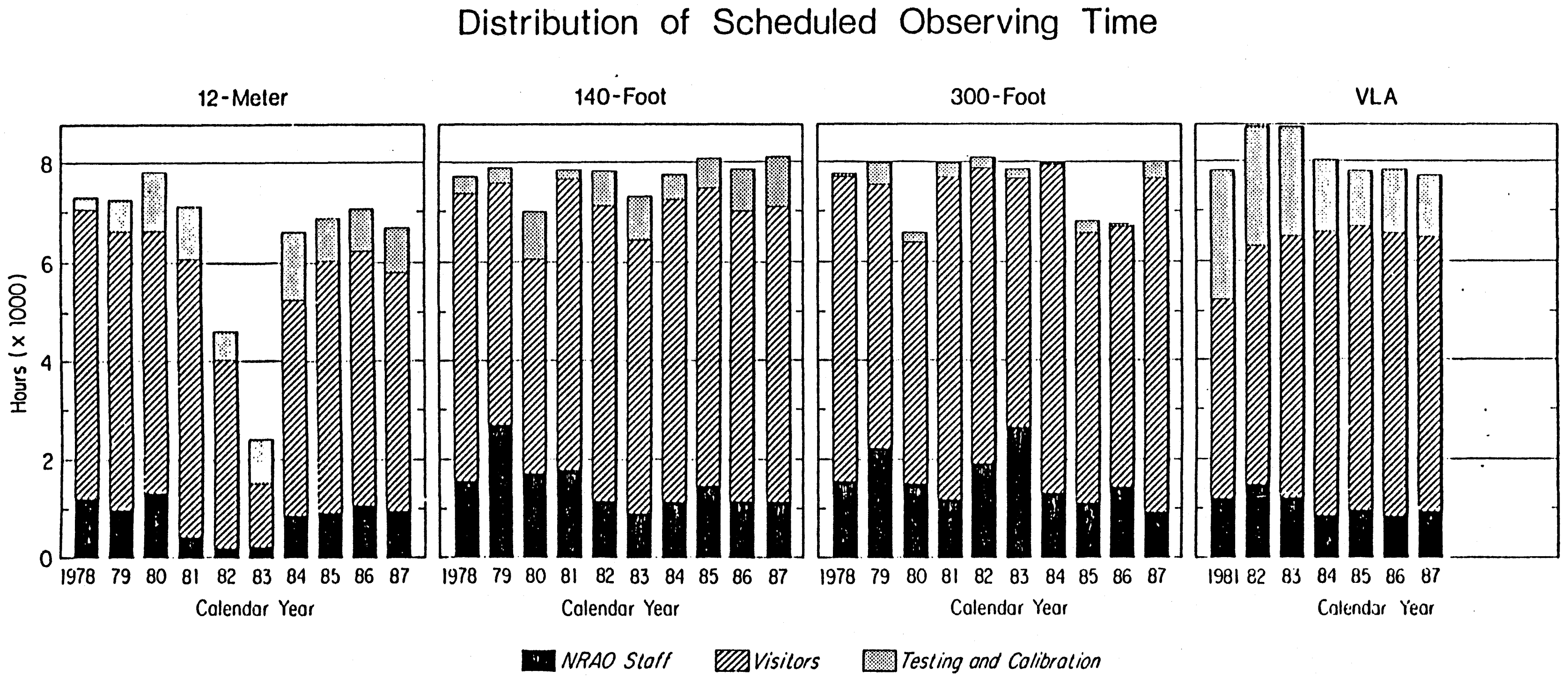

Figure B-4. These graphs show the number of hours scheduled for calibration and for observing by the NRAO staff and by visitors on each telescope system during the last decade.

Figure B-4 shows the actual observing time distribution among NRAO scientific staff, visitors, and calibration and test time. Over time, the NRAO staff has qualified to utilize about 15% of the observing time, with some variation from telescope to telescope. This level of use is judged to be adequate to enable the Observatory staff to maintain a competitive research program of its own, which is necessary if the Observatory is to continue to provide effective leadership within the U.S. radio astronomy community.

Staff and Operations

The growth of NRAO's permanent full-time staff over the history of the Observatory is shown in Figure B-5. The steady, smooth growth up to 1970 accompanied the construction of the 300-foot, 140-foot, millimeter-wave, and three-element Interferometer. The size of the operations staff was constant throughout most of the VLA construction period and increased in response to major new user requirements as operation of that instrument began in 1979.

The composition of the scientific staff at NRAO is given in Table 1, where the scientific staff is defined as all professional employees holding a Ph.D degree. The total Ph.D. staff is 65 employees, 18% of all full-time permanent employees. Of these 65, 28 form the basic research staff, or 8% of all full-time permanent employees. Twenty-two of the 65 members of the Ph.D. staff hold tenured positions, or 6% of the staff. These numbers are consistent with the original intention that the Observatory have a small, dedicated research and development staff.

Organization Chart

The NRAO Organization Chart is shown as Figure B-6.

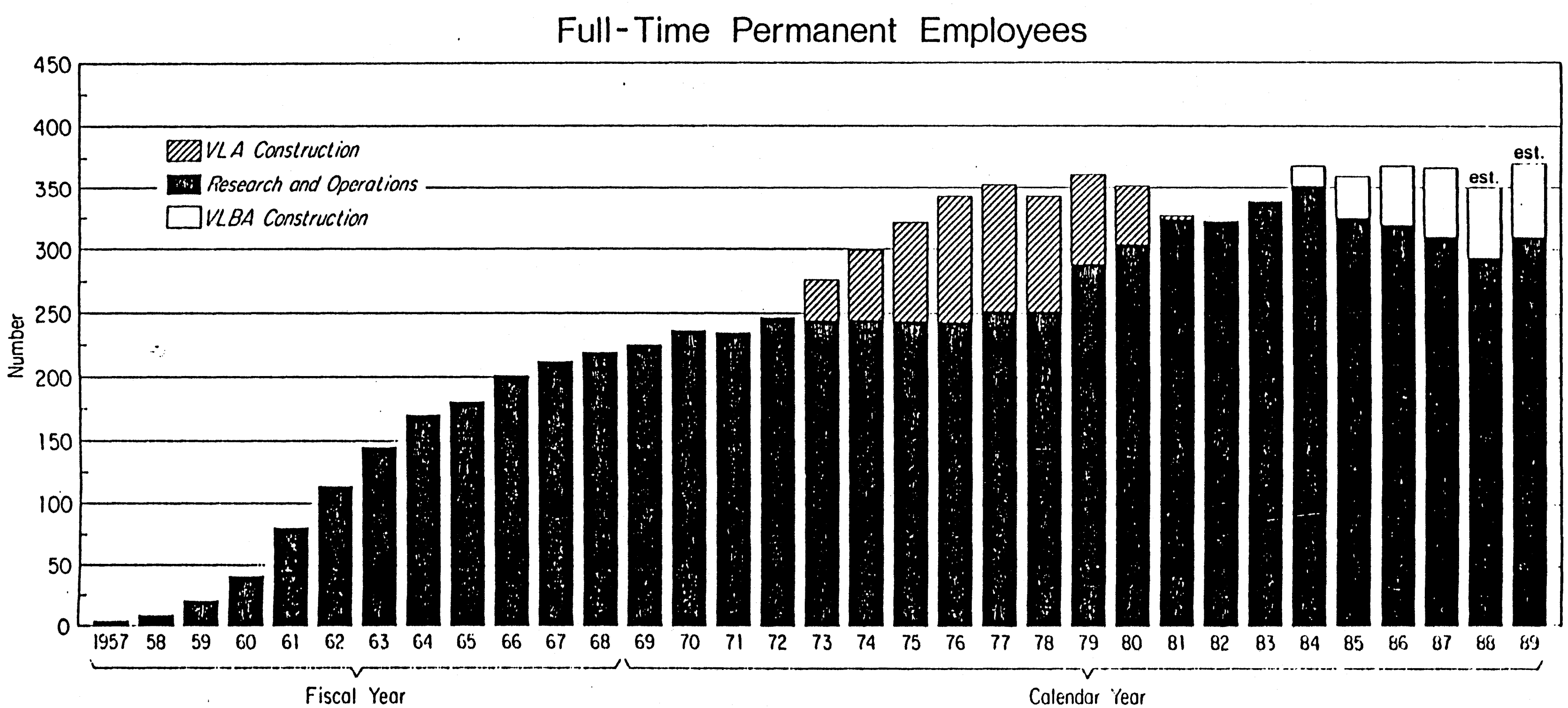

Figure B-5. This figure shows the total number of NRAO full-time, permanent employees at the end of each year, projected into the future.

TABLE 1. Ph.D. Staff Classification/Distribution

Basic Research Staff	Total
Postdoctorals	6
Associate Scientists	3
Scientists	15
Senior Scientists	4
Total	28
Other Ph.D. Staff	
Operations/Management	14
Electronics	8
Computing	4
VLBA Construction	11
Total (6 tenured)	37
Total Ph.D. Staff (22 tenured)	65
NRAO Staff	
Operations	295
Construction: VLBA	64
Voyager	8
Total Staff	367
Fraction of staff with Ph.D. degree	- 18%
Fraction of Ph.D. staff with tenure	- 34%
Fraction of total staff with tenure	- 6%

NATIONAL RADIO ASTRONOMY OBSERVATORY
ORGANIZATION CHART
1 OCTOBER 1988

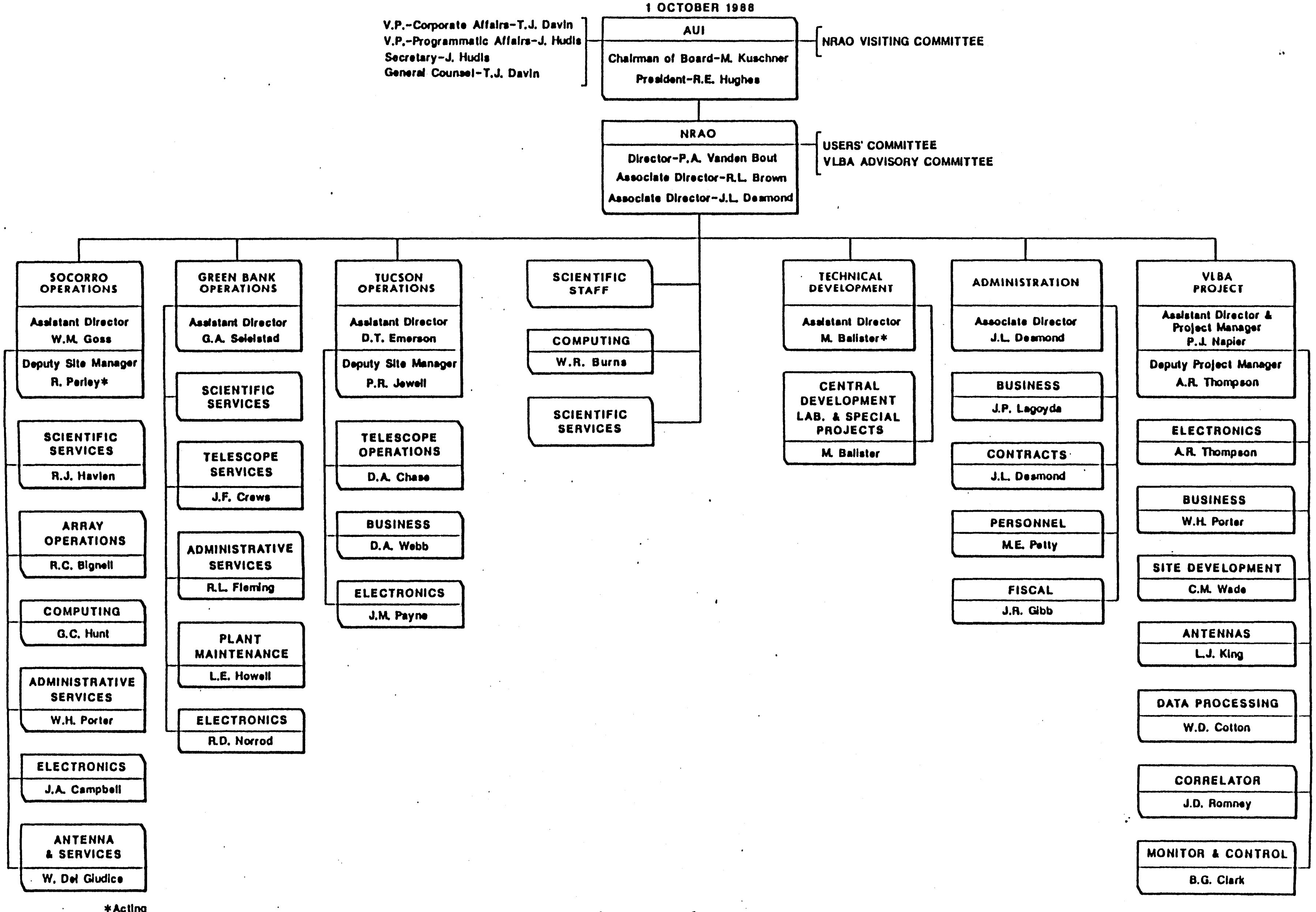

Figure B-6.

APPENDIX C. UVA-SDL Estimate for SIS Device Subcontract

(see attached)

University
of Virginia

SCHOOL OF ENGINEERING AND APPLIED SCIENCE
DEPARTMENT OF ELECTRICAL ENGINEERING

(804) 924-6112

November 2, 1988

Dr. Robert Brown
National Radio Astronomy Observatory
Edgemont Road
Charlottesville, VA 22901

Dear Dr. Brown:

I hereby agree that the SIS receiver element research team of the University of Virginia Semiconductor Device Laboratory, SDL, will work in close conjunction with the research team of the National Radio Astronomy Observatory on the project entitled "Submillimeter Interferometer as a Space Station Attached Payload". Researchers at the SDL have extensive knowledge of the fabrication of very high quality trilayer and edge junction SIS devices. Furthermore, all major pieces of device fabrication equipment are available in the SDL. An approximate budget for this portion of the proposed joint research interaction is attached.

Sincerely yours,

Robert J. Mattauch
Director, SDL
Chairman, Department of Electrical
Engineering

RJM:pm

attach: budget

THORNTON HALL • CHARLOTTESVILLE, VIRGINIA 22901

NRAO Subcontract

		Year 1	Year 2	Year 3
I.	Personnel			
	A. Dr. M. J. Feldman			
	10% c/y	$ 5,800	6,148	6,517
	B. Ph.D. Research Engineer			
	100% c/y	48,000	50,880	53,933
	C. Technician			
	100% c/y	35,000	37,100	39,326
	D. Graduate Research Assistant			
	50% a/y 100% summer	8,316	8,712	9,108
	@$10.50/hr,$11.00/hr,$11.50/hr	5,544	5,808	6,072
	E. Secretary			
	10% c/y	2,000	2,120	2,247
	Salaries	$104,660	110,768	117,203
	Fringe Benefits	20,884	22,137	23,466
II.	Supplies	36,000	36,000	36,000
III.	Photomasks	5,000	5,000	5,000
IV.	Travel	3,000	3,000	3,000
V.	Publications	2,000	2,000	2,000
VI.	OCS	3,000	3,000	3,000
		$174,544	181,905	189,669
	Overhead 50%	87,272	90,953	94,835
	TOTAL	$261,816	272,858	284,504

Robert J. Mattauch **January 1988**

Born: Rochester, Pennsylvania, 1940

Education:

Ph.D. (Electrical Engineering), North Carolina State University, 1967

Dissertation: *"A Study on the Effects of* Co^{60} *- radiation on the steam-grown* SiO_2 *MOS structures"*

M.E.E.E. (Electrical Engineering), North Carolina State University, 1963

B.S. (Electrical Engineering), Carnegie Institute of Technology, 1962

Experience:

Department of Electrical Engineering, University of Virginia, Charlottesville, Virginia

Chairman, 1987 - present
Standard Oil Co. (OHIO) Professor, 1987 - present
Wilson Professor, 1983 - 1986
Professor, 1976 - 1983
Associate Professor, 1970 - 1976
Assistant Professor, 1966 - 1970

Professional Societies:

Fellow, IEEE, 1986
Senior Member, IEEE, 1981
Member, IEEE University Microelectronics Committee, 1974--
Institute of Electrical and Electronics Engineers
Eta Kappa Nu, National Electrical Engineering Honorary Society
Sigma Xi, National Research Honorary Society
Tau Beta Pi, National Engineering Honorary Society
Phi Kappa Phi, National Scientific Scholastic Honorary Society
Pi Mu Epsilon, National Mathematics Honorary Society

Honors and Academic Awards:

Elected Standard Oil Company of Ohio Professor, 1986
Elected Fellow of The Institute of Electrical and Electronics Engineers "For contributions to the development of low-noise millimeter-wave diode technology," January 1986
Recipient of IEEE Centennial Medal for Fundamental Contributions in the Field of Low-Noise Metal-Semiconductor Junctions and Microfabrication, 1984
Elected Alice M. and Guy A. Wilson Professor of Electrical Engineering, 1983
Elected to University of Virginia Faculty Senate, 1983
Recipient of American Society of Engineering Education Western Electric Fund Award for Excellence in the Instruction of Engineering Students, 1980
Recipient of T. Holmes MacDonald, Eta Kappa Nu Award "An Outstanding Electrical Engineering Professor in USA for 1975"

Robert J. Mattauch January 1988

Recipient of 1975 Eta Kappa Nu Award, Gamma Pi Chapter for Advances in the Area of Semiconductor
Devices
Ford Fellow, North Carolina State University, 1962
O.G. Richter Scholarship, Carnegie Institute of Technology, 1961
Elk's Scholarship, Carnegie Institute of Technology, 1958

Research Record:

Robert J. Mattauch joined the University of Virginia Department of Electrical Engineering in September 1966 and within months began the Semiconductor Device Laboratory. The lab initiated work in the area of infrared detectors and in 1969 initiated work on millimeter wave receiver elements for use in radio astronomy. In less than two years, Dr. Mattauch and his graduate students had set world records in millimeter wave mixer element noise temperature, conversion loss, and cutoff frequency. This lab staff now consists of four faculty members, a research scientist, technician, research administrator, and 11 graduate students. This lab and its associated research team under Mattauch's direction is known internationally for its expertise in the area of millimeter/sub-millimeter wave receiver elements. Lab visitors include eminent scientists from all major countries with an occasional visitor spending his sabbatical period at the lab.

Recent Publications:

R.J. Mattauch and T.W. Crowe, "GaAs Schottky Devices for Submillimeter Wavelengths," International Journal of Infrared and Millimeter Waves, 8, No. 10, October 1987.

T.W. Crowe and R.J. Mattauch, "Analysis and Optimization of Millimeter- and Submillimeter-Wavelength Mixer Diodes," IEEE Trans. Microwave Theory and Techniques, Vol. MTT-35, No. 2, pp. 159-168, February 1987.

K.M. Kattmann, T.W. Crowe, and R.J. Mattauch, "Noise Reduction in GaAs Schottky Barrier Mixer Diodes," IEEE Trans. Microwave Theory and Techniques, Vol. MTT-35, No. 2, pp. 212-214, February 1987.

T.W. Crowe and R.J. Mattauch, "Conversion Loss in GaAs Schottky Barrier Mixer Diodes," IEEE Trans. Microwave Theory and Techniques, Vol. MTT-34, No. 7, pp. 753-760, July 1986.

W.L. Bishop and R.J. Mattauch, "Photolithography and Etching for Submicron Schottky Diode Anode Features," Proc. for Southeastcon '86, pp. 147-152, April 1986.

R.J. Mattauch, M. Faber and J. Archer, "A Frequency Doubler with 35% Efficiency at W-Band," Microwave Journal, July 1985.

K. McKinney, R. Mattauch, and W. Bishop, "Design, Fabrication, and Performance of a Whiskerless Schottky Diode for Millimeter and Submillimeter Wave Applications,"Proc. of Southeastcon '85, pp. 111-115, April 1985.

A. Lichtenberger, A. Lewis, andd R. Mattauch, "Design and Optimization of NbCN/PbBi Mixer Elements for Heterodyne Receivers," Proc. for Southeastcon '85, pp. 102-105, April 1985.

T.W. Crowe, R.J. Mattauch, and W.L. Bishop, "Frequency & Noise Limits of Schottky Barrier Mixer Diodes," Microwave Journal, pp. 101-116, March 1985.

M.T. Faber, J.W. Archer, and R.J. Mattauch, "A High Efficiency -[';/.Frequency Doubler for 100 GHz," Proc. of 1985 IEEE, MTT-S International Microwave Symposium Digest, June 1985.

Marc J. Feldman **January 1988**

Born: Philadelphia, Pennsylvania, June 21, 1945

Education:

B.A. (physics) University of Pennsylvania, 1967

M.S. (physics) University of Pennsylvania, 1967
Thesis: "Energy Dynamics of the Interstellar Clouds"

Ph.D. (physics) University of California at Berkeley, 1975
Thesis: "Theory of the Unbiased Josephson Junction Parametric Amplifier"
Advisor: R.Y. Chiao, C.H. Townes

Professional Experience:

Department of Physics, University of California, Berkeley, California

National Science Foundation Graduate Traineeship, 1967-1971
Teaching Assistant, 1968-1970 (unpaid)
Research Assistant, 1971-1975
Post-Graduate Research Physicist, 1975-1978

Swedish National Science Research Council Visiting Scientist, at Chalmers University, Gothenburg, Sweden; NORDITA Fellow, at H.C. Oersted Institute, University of Copenhagen, Denmark; joint appointment, 1979, 1980

NASA/Goddard Institute for Space Studies, New York City, New York

NRC Resident Research Associate, 1981, 1982
Senior Staff Associate in Physics, Columbia University Radiation Laboratories, 1983, 1984

Research Associate Professor, Department of Electrical Engineering, School of Engineering and Applied Science, University of Virginia, Charlottesville, Virginia, 1985 --

Professional Societies:

The American Physical Society
The American Association for the Advancement of Science
The American Vacuum Society
Sigma Xi

Marc J. Feldman **January 1988**

Research: Prof. Feldman has specialized in device-oriented theoretical research related to high frequency applications of superconductivity since 1972. Since 1979 he has worked with groups researching superconductor quasiparticle (SIS) mixers for radio astronomy applications, contributing to the successful development of SIS receivers for the Onsala Space Observatory, the NASA/Columbia Sky Survey, the airborne observatories on NASA's C-141 and Convair-990 aircraft, and NRAO's 12-M Kitt Peak telescope. In this work Prof. Feldman has predicted, delineated, and explained many of the phenomena important to SIS mixers. He wrote (with J.R. Tucker) the definitive review on this subject.

In earlier work, Prof. Feldman was co-originator of the four-photon Josephson junction parametric amplifier, and he created the theory of this device. He identified and explained the gain-proportional noise of Josephson parametric amplifiers, still a topic of active controversy. This work entailed the experimental developmental of Josephson microbridges, semi-metal barrier junctions, and oxide-barrier junctions, and practical expertise in vacuum techniques, thin film deposition, materials research, cryogenics, and microwave technology.

He was co-inventor of the inverse ac Josephson effect voltage standard, which now defines the standard volt at the National Bureau of Standards.

All of the above emphasized noise mechanisms and the properties of arrays of devices. Other research has included: optical parametric interactions, electron acceleration by lasers, interstellar extinction, and astronomical observations of interstellar CN at 113 GHz.

Significant Publications:

1. M.J. Feldman, P.T. Parrish, and R.Y. Chiao, "Parametric Amplification by Unbiased Josephson Junctions," J. Appl. Phys. 46, 4031 (1975).
2. M.T. Levinsen, R.Y. Chiao, M.J. Feldman, and B.A. Tucker, "An Inverse AC Josephson Effect Voltage Standard," Appl. Phys. Lett. 31, 776 (1977).
3. M.J. Feldman and M.T. Levinsen, "Gain-Dependent Noise Temperature of Josephson Parametric Amplifiers," Appl. Phys. Lett. 36, 854 (1980).
4. M.J. Feldman, "Some Analytical and Intuitive Results in the Quantum Theory of Mixing," J. Appl. Phys. 53, 584 (1982).
5. M.J. Feldman, S. Rudner, "Mixing with SIS Arrays," in Reviews of Infrared and Millimeter-Waves, Volume 1, edited by K.J. Button (Plenum, New York, 1983) p. 47.
6. S.-K. Pan, M.J. Feldman, A.R. Kerr, and P. Timbie, "Low-Noise 115-GHz Receiver Using Superconducting Tunnel Junctions," Appl. Phys. Lett., 43, 786 (1983).
7. J.R. Tucker and M.J. Feldman, "Quantum Detection at Millimeter Wavelengths," Rev. Mod. Phys. 57, 1055 (1985).
8. M.J. Feldman, "Quantum Noise in the Quantum Theory of Mixing," IEEE Trans. Magnetics MAG-23, 1054 (1987).
9. M.J. Feldman and D.W. Face, "Image Frequency Termination of the Superconducting Quasiparticle Mixer," Jpn. J. Appl. Phys. 26, 1633 (1987).
10. M.J. Feldman, "Theoretical Considerations for THz SIS Mixers," invited, to appear in Int. J. Infrared Millimeter Waves.

APPENDIX D. Technical Data Sheets

(see attached)

Announcement of Opportunity

SPACE STATION ATTACHED PAYLOADS

TECHNICAL DATA SHEETS

In accordance with the Announcement of Opportunity for Space Station Attached Payloads, Section VIII.B.1., the following contains Technical Data Sheets (also refered to as Announcement of Opportunity Fact Sheets) to be completed and submitted with your flight proposal. It is also requested that Technical Data sheets be completed for concept proposals.

In completing all Technical Data Sheet questions regarding use of Space Station accommodations refer to the Attached Payload Users Guide as a point of departure for Space Station accommodation capabilities.

It is understood that not all investigations are at a sufficient level of maturity to permit full completion of the Technical Data Sheets. However it is requested that all applicants answer as many questions as possible, consistant with the level of detail in the proposal. It is recognized that concept proposal Technical Data Sheets will not be completed to the same level of detail as those for the flight proposals. Wherever data is unknown or unavailable at the time, so indicate on the Technical Data Sheets.

It is also recognized that completing this Technical Data Sheet will include duplication of some information in the proposal required by Appendix E .

The completed Technical Data Sheets are to be submitted with each proposal.

ATTACHED PAYLOAD FACT SHEET

Proposal Title: High-Resolution Imaging Spectroscopy at Terahertz Frequencies

Proposer's Name (Organization, Contact): National Radio Astronomy Observatory

Proposal No. (for NASA use):

Payload Discipline: Astrophysics

Payload Objective(s): To provide spectroscopic images at high resolution of [CI], [OI], [CII] lines at terahertz frequencies.

Present State of Development: Hardware and software concepts well understood. Adaptation to space environment needs further development.

Hardware Design Inheritance --> % New: 25 % Modified: 50

% Off-the-shelf: 25

Supporting Investigations Required : None

Anticipated On-Orbit Stay Time (yrs) : Indefinite - no limited life components

PHYSICAL ATTRIBUTES

1a. Experiment Hardware - Identify equipment at the major component level (do not include rack or carrier requirements).

Attached Payload	Width (m)	Depth (m)	Height (m)	Volume (m^3)	Mass (Kg)	* Mass of Electronics	Total Mass (Kg)
1. Ant./receiver 1	2.0	1	2.5	4	200		200
2. Ant./receiver 2					200		200
3. Ant./receiver 3					200		200
4.							
5.							
TOTAL							

Pressurized Rack Mounted Equipment	Width (m)	Depth (m)	Height (m)	Volume (m^3)	Mass(Kg)	* Mass of Electronics	Total Mass (Kg)
1. IF electronics	0.5	0.5	2	0.5		150	150
2. Correlator	0.5	0.5	2	0.5		150	150
3.							
4.							
5.							
TOTAL							

b. Describe launch carrier(s) for attached equipment (i.e., pallet mounted, MPESS, payload unique).

Is NASA expected to provide this carrier? (NOTE: Racks for pressurized equipment will be NASA provided)

* Mass of Electronics is defined as mass of PC cards and electronic components (not cables, boxes, etc.)

c. Storage Hardware - Identify spares at the major component level (do not include rack or carrier requirements). N/A

Unpressurized Stored Eqpt	Width (m)	Depth (m)	Height (m)	Volume (m^3)	Mass(Kg)
1. 2. 3.					
TOTAL					
Pressurized Stored Eqpt	Width (m)	Depth (m)	Height (m)	Volume (m^3)	Mass(Kg)
1. 2. 3.					
TOTAL					

Is this stored equipment dormant, or do any unique cooling, data, etc. requirements exist? ______________________________

____

Provide any schematics, drawings or dimensional sketches which would be illustrative of the above requirements.

d. Initial experiment launch configuration. Re-identify components from 1a, 1b, and 1c above that are required for the initial experimental launch such that totals reflect launch configuration totals.

To be determined (TBD)

If a weight constrained operational scenerio is planned during Space Station Assembly, identify nominal and mininum requirements.

Unpressurized Eqpt	Width (m)	Depth (m)	Height (m)	Volume (m^3)	Mass(Kg)
1. 2. 3.					
TOTAL					
Pressurized Eqpt	Width (m)	Depth (m)	Height (m)	Volume (m^3)	Mass(Kg)
1. 2. 3.					
TOTAL					

e. 90 day Payload resupply- Re-identify components from 1a, 1b, 1c, and 1d that are required for a 90 day Payload resupply such that totals reflect launch configuration totals.

N/A

If a weight constrained operational scenerio is planned during Space Station Assembly, identify nominal and mininum requirements.

Unpressurized Eqpt	Width (m)	Depth (m)	Height (m)	Volume (m^3)	Mass(Kg)
1. 2. 3.					
TOTAL					
Pressurized Eqpt	**Width (m)**	**Depth (m)**	**Height (m)**	**Volume (m^3)**	**Mass(Kg)**
1. 2. 3.					
TOTAL					

ATTACHED PAYLOAD ACCOMMODATION EQUIPMENT (APAE)

2a. Identify quantities of the following Space Station provided items which will be utilized for attached payload mounting or command/control support ?

SIA/[redacted]: 3 Payload Pointing System (PPS): ____________

Deck Carrier: ____________ Multiple Payload Adapter: ____________

Crew Support Station: ____________ Attitude Determination System : ____________

Other: ____________ Contamination Monitoring System: ____________

b. Describe any unique mounting requirements.

1 or 2 of the SIA should be reconfigurable.

c. Specify payload pointing requirements:

Pointing Accuracy: 3 arc sec rms (Deg, ArcSec)

Stabilization: TBD (Deg, ArcSec/Sec)

Field of View : 90% hemisphere

Viewing Direction: $-Z_{SB} \pm 90°$ in X and Y

d. If the Space Station PPS capability does not meet your requirements, specify how you will meet your unique pointing requirements (include sketches, drawings, etc.)

Probably use own mount/star tracker.

FUNCTIONAL DESCRIPTION

3. Identify pressurized rack equipment at the major component level and its function(s).

Pressurized Equipment	Function
IF Processor	converts IF signals to baseband digital form
Correlator	correlation of digitized signals from antennas

Please provide any instrument or functional block diagrams which are available.

RESOURCE REQUIREMENTS

4. Power - Complete the following table at the major component level (specify in kW):

	Hardware Components	Average Pwr (while operating)	Peak Power	Standby Power	Prelaunch Power	Ascent Power	Descent Power
Attached payload	1. Antenna 1	approx. 0.2 KW					
	2. Antenna 2	approx. 0.2 KW					
	3. Antenna 3	approx. 0.2 KW					
	4.						
	5.						
	6.						
Pressurized Equipment	1. IF Processor	approx. 1.0 KW					
	2.	(to be determined)					
	3. Correlator	approx. 1.0 KW					
	4.	(to be determined)					
	5.						
	6.						

a. Indicate the type of power required - - > Frequency (hz): ________ ~~ac~~/dc: 28

b. Complete the attached power profile timeline chart for 1 cycle of payload activity.

c. How many cycles do you expect to run per 90 day mission? continuous

d. Are there any significant power requirement differences between the unmanned, man-tended, or permanently manned capability timeframes? Please explain. No

e. Is a secondary power source required to safe the payload in the event of power interrupt?
No

POWER PROFILE DIAGRAM - Complete for one cycle of payload operations.

ATTACHED PAYLOAD

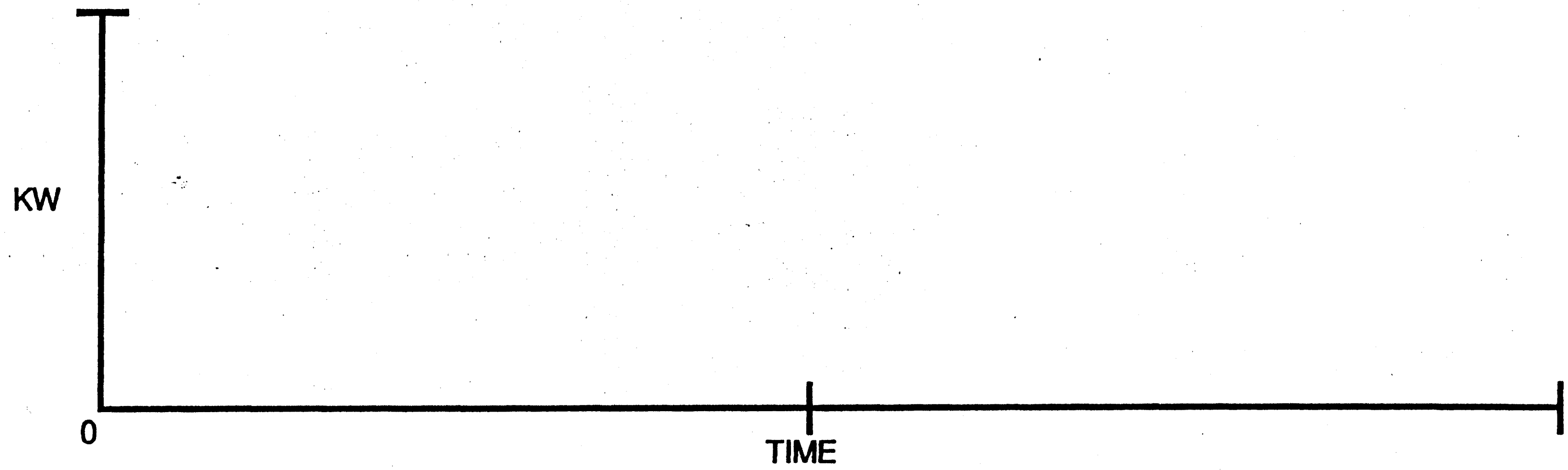

PRESSURIZED EQUIPMENT

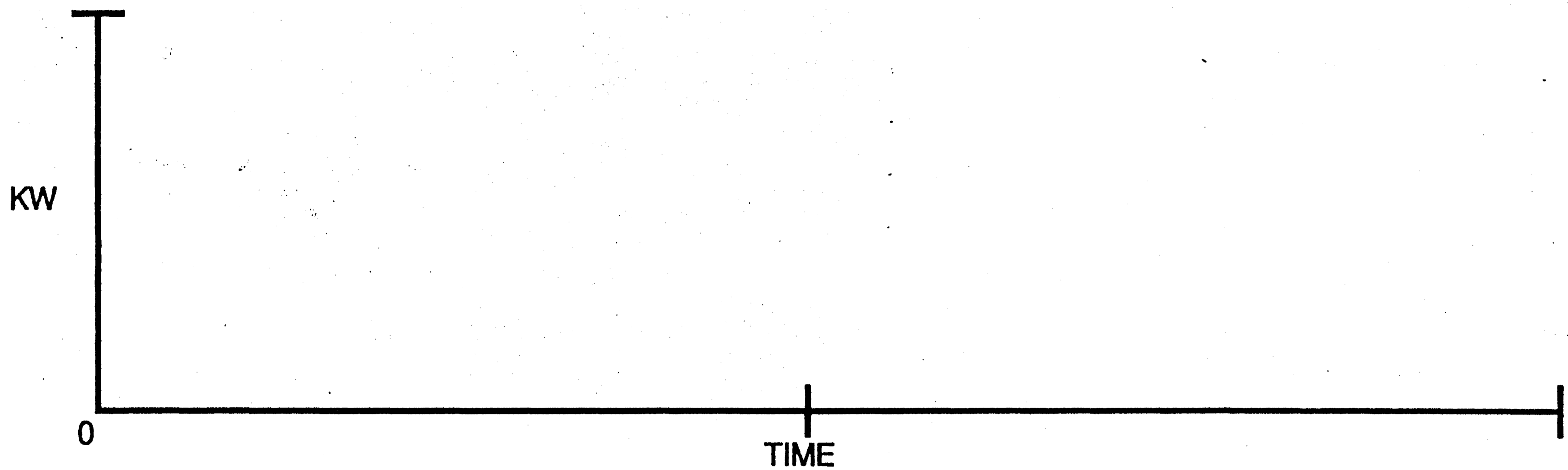

5. Thermal Control: TBD

Type - - -> Active:__________ Passive: __________

a. Is active thermal control Station or PI provided? __________

b. Total Heat Dissipated (kw-hr) - - - > Attached Payload: __________

Pressurized Equipment: __________

c. Describe any unique thermal control requirements.

Receivers mounted in L^4He dewars.

d. Complete for the attached payload equipment:

- Operating Temperature Range: 20 ° C to 30°C
- Preferred Operating Temperature: 25 °C
- Non Operating min/max Temperature with no damage to payload: -40 °C (min) to 40 °C (max)

6. Data

a. Complete the following table

		Ground to Station (Uplink)	Station to Ground (Downlink)	Station to Station
DIGITAL	• Dump Rate (kbps during run)			
	• # Transmissions per day	3		
	• Transfer Time (hrs)	0.1 Hr.		
	• Realtime Rate (kbps during run)	1 kbps	100 kbps	
VIDEO	• Dump Rate (kbps during run)	None		
	• # Transmissions per day	None		
	• Transfer Time (hrs)	None		
	• Realtime Rate (kbps during run)	None		
AUDIO	• Rate (HZ)	None		
	• # Transmissions per day	None		
	• Transfer Time (min)	None		

b. What is the on-orbit temporary data storage per payload run (MB): 20 Mega Bytes

c. Will data buffering be required? ________ If so, indicate (MB): 20 Mega Bytes

d. Is video in analog or digital form when it reaches the Station interface? N/A

e. Will the payload generate analog data other than audio or video? No If so, what rate per payload cycle (kbps)? ________

f. Will you use direct data transmission to the ground assuming Station interference specifications are met? No

g. Do you plan to use computational resources from the DMS? No State type of applications below.

h. What type of data interface to the station will your hardware incorporate?

Standard interface

i. Are there any significant data requirement differences between unmanned, man-tended, or permanenetly manned capability timeframes?

No

7. Process Fluids/ Consummables - Specify consummable requirements per payload cycle.

Consummable	Mass (kg)	Vol (m^3)	Storage Press (kpa)	Storage Temp (°C)	Station Provided?
1.					
2.					
3.					
4.					
5.					
6.					
7.					

Describe or provide scenario for resupply of payload consummables.

OPERATIONS

8a. How many payload runs per 90 days are acceptable for achieving scientific return?
Continuous

b. What IVA crewtime (hrs) per run is required? None

c. What EVA crew time (hrs) per run is required? 4 hrs./90 days - helium transfer
6 hrs./60 days - move antennas

d. Are there any significant crew requirement differences between unmanned, man-tended, or permanently manned capability timeframe? If so, explain.

No

e. Describe typical resupply operations.

Refill L^4He dewars every 90 days.

f. Describe typical maintenance operations.

Antennas need to be moved periodically (greater than 50 days).

g. Complete the attached experiment timeline form and crew profile timeline for one payload cycle.

TBD

COMMAND AND DISPLAY

9a. Describe the types of pressurized controls and displays which will be required for your payload.

All control and monitor from ground.

b. What type of commands do you anticipate the IVA crewman issuing? (The data format for these commands should be reflected in the Section 6 Station to Station requirements.)

None

c. What type of commands will be issued directly from the ground? (The data format for these command should be reflected in the Section 6 Ground to Station requirements.)

All experiment control data through standard channels.

EXPERIMENT TIMELINE

Provide timeline of operations for one experiment cycle (include assembly and normal operations).

EXPERIMENT STEP	DURATION (HRS)	EVA TIME (HRS)	IVA TIME (HRS)	EQUIPMENT REQUIRED
Assembly TBD				
Normal Operations TBD				

EXPERIMENT TIMELINE

Provide timeline of operations for one experiment cycle (include resupply and maintenance).

EXPERIMENT STEP	DURATION (HRS)	EVA TIME (HRS)	IVA TIME (HRS)	EQUIPMENT REQUIRED
Resupply TBD				
Maintenance TBD				

CREW TIME PROFILE DIAGRAM - Complete for one cycle of payload operations.

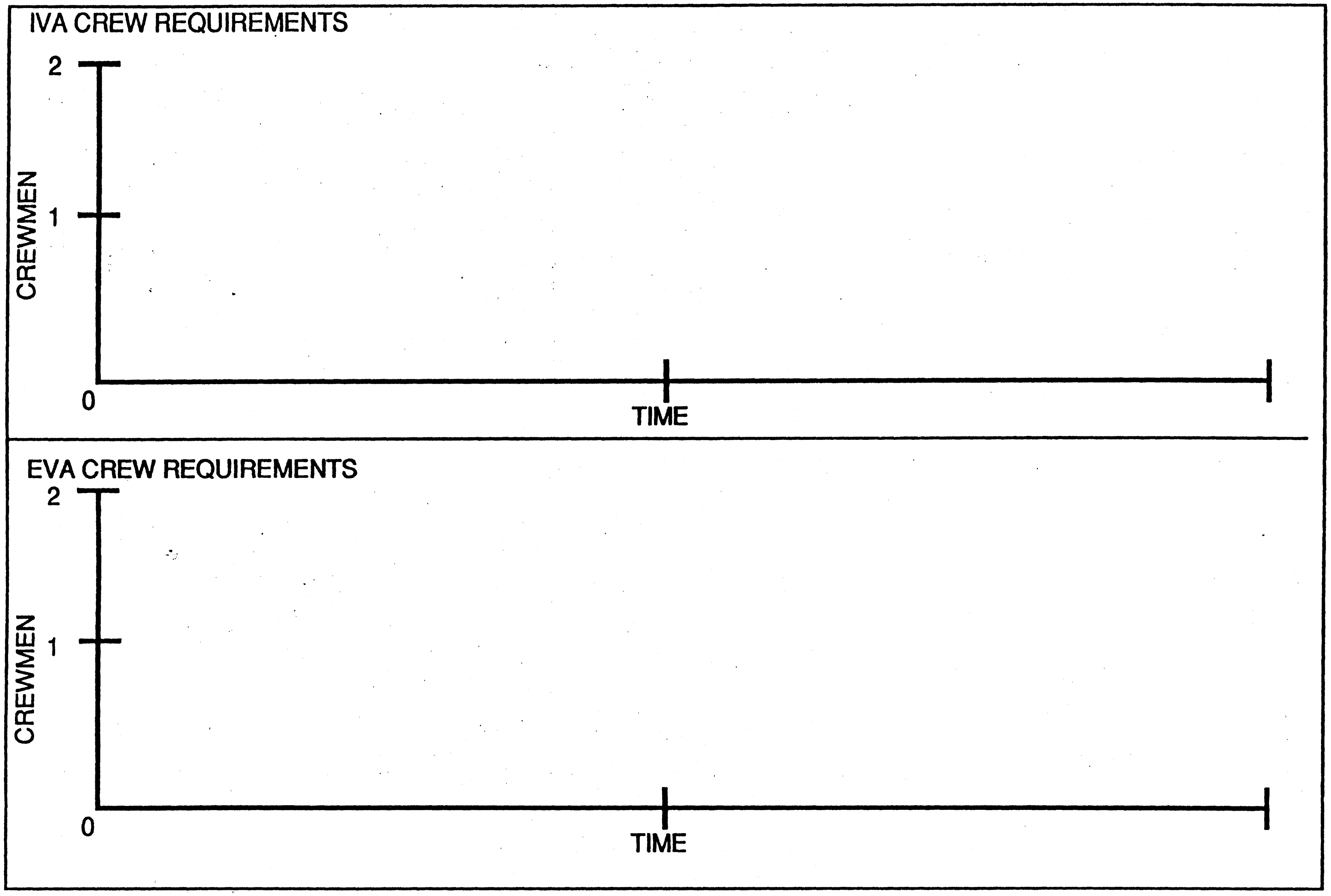

ENVIRONMENTAL LIMITS

10 a. Humidity

Will humidity levels impact payload equipment? __No__ If so, please specify acceptable humidity ranges.

Attached (prior to & during launch)- - -> ________% to ________ %

Pressurized - - -> ________% to ________ %

b. Acoustics

Will acoustic levels impact payload equipment? __No__ If so, please specify acceptable acoustic ranges.

Attached - - -> _____dB to _____dB

Pressurized- - -> _____dB to _____dB

c. Acceleration

Compatible with shuttle launch

What acceleration force and frequency range can equipment withstand during launch? __________ g; ____________hz to _____________hz

What acceleration force and frequency ranges are required for on-orbit operations? _________g to __________g; __________hz to __________hz

d. Contamination

List sources of contamination which the payload is susceptible to:

EMI: Not critical

RFI: Need to look out for IF passband

Radiation: No

Other: None

Specify maximum column densities (molecules/cm^2) acceptable to the payload:

H_2O: ____________ N_2 : ____________

CO_2 : ____________ H_2 : ____________

O_2 : ____________ Other: ____________

Will the payload equipment be adversely affected by molecular depostion? No

If so, identify maximum acceptable depostition rate: -------- (g/cm^2 yr)

Is the payload equipment, as a result of its design or operation, a contamination source in itself? No If so, please specify the sources created (EMI, RFI, particulates, etc.)

PHOTOGRAPHY

11a. Will the attached equipment utilize an externally mounted camera? No
b. Will the camera be Station or PI provided? ____________

c. Identify the type of camera and video format required. (An estimate of film volume and mass per payload cycle should be reflected in Section 7- Consummables.)

SAFETY, RELIABILITY, AND MAINTAINABILITY

12a. Describe reliability goals and objectives and maintainability philosophies.

Use of three antennas allows interferometry to continue even if performance of antenna becomes temporarily degraded.

b. Identify and discuss any potential hazardous materials, features, or operations of this proposed payload.

None

GROUND SUPPORT EQUIPMENT AND OPERATIONS

13a. Identify special ground support service requirements

	YES	NO	Comment
Cryogenic loading? Identify cryogens, when to be loaded, etc.	X		L^4He loaded in orbit
Fluid or gas services required ?		X	
Calibration? Specify equipment		X	Built into instrument
Checkout? Specify equipment		X	Built into instrument
Radioactive material storage? Identify isotope.		X	
Hazardous chemical storage? Identify chemicals		X	
Special ground transportation or handling?		X	

b. Is late access to the instrument required prior to launch? No
Please describe the time of access and activities required.

c. Is early access to the instrument required following landing? No
Please describe time of access and activities required.

INTEGRATION REQUIREMENTS/ACTIVITIES

14. Describe or provide a functional flow block diagram of the major activities and sequence of events necessary for the integration of the payload components (including integration onto its carrier).

TBD